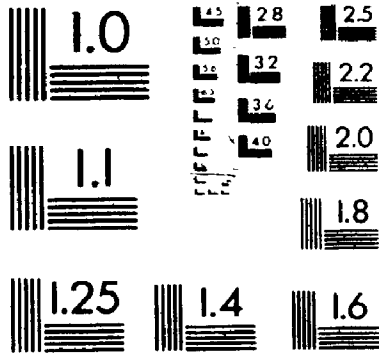


1





National Library
of Canada

Bibliothèque nationale
du Canada

Canadian Theses Service Service des thèses canadiennes

Ottawa, Canada
K1A 0N4

NOTICE

The quality of this microform is heavily dependent upon the quality of the original thesis submitted for microfilming. Every effort has been made to ensure the highest quality of reproduction possible.

If pages are missing, contact the university which granted the degree.

Some pages may have indistinct print especially if the original pages were typed with a poor typewriter ribbon or if the university sent us an inferior photocopy.

Previously copyrighted materials (journal articles, published tests, etc.) are not filmed.

Reproduction in full or in part of this microform is governed by the Canadian Copyright Act, R.S.C. 1970, c. C-30.

AVIS

La qualité de cette microforme dépend grandement de la qualité de la thèse soumise au microfilmage. Nous avons tout fait pour assurer une qualité supérieure de reproduction.

S'il manque des pages, veuillez communiquer avec l'université qui a conféré le grade.

La qualité d'impression de certaines pages peut laisser à désirer, surtout si les pages originales ont été dactylographiées à l'aide d'un ruban usé ou si l'université nous a fait parvenir une photocopie de qualité inférieure.

Les documents qui font déjà l'objet d'un droit d'auteur (articles de revue, tests publiés, etc.) ne sont pas microfilmés.

La reproduction, même partielle, de cette microforme est soumise à la Loi canadienne sur le droit d'auteur, SRC 1970, c. C-30.

A WIDEBAND MICROWAVE SURVEILLANCE RECEIVER

by

Andre Varin

A thesis submitted to the
Faculty of Graduate Studies and Research
in partial fulfilment of the requirements
for the degree of

Master of Engineering

Ottawa-Carleton Institute for Electrical Engineering

Faculty of Engineering

Department of Electronics

Carleton University

August, 1987

© copyright Andre Varin

Permission has been granted to the National Library of Canada to microfilm this thesis and to lend or sell copies of the film.

The author (copyright owner) has reserved other publication rights, and neither the thesis nor extensive extracts from it may be printed or otherwise reproduced without his/her written permission.

L'autorisation a été accordée à la Bibliothèque nationale du Canada de microfilmer cette thèse et de prêter ou de vendre des exemplaires du film.

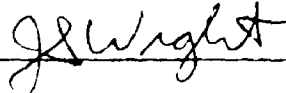
L'auteur (titulaire du droit d'auteur) se réserve les autres droits de publication; ni la thèse ni de longs extraits de celle-ci ne doivent être imprimés ou autrement reproduits sans son autorisation écrite.

ISBN 0-315-39431-5

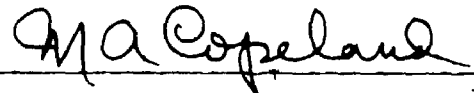
The undersigned hereby recommends to the Faculty of Graduate Studies and
Research acceptance of the thesis,

A WIDEBAND MICROWAVE SURVEILLANCE RECEIVER

submitted by Andre Varin, in partial fulfilment of the requirements for
the degree of Master of Engineering



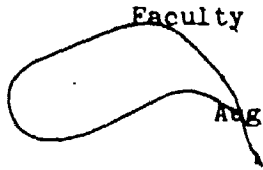
Thesis Supervisor



Chairman
Department of Electronics

Department of Electronics

Faculty of Engineering



August 1987

ABSTRACT

A wideband microwave surveillance receiver has been proposed, assembled, and demonstrated. The receiver system consists of a hybrid approach which combines a front-end stepping receiver with a microscan intercept receiver to monitor the frequency bandwidth extending from 3.2 to 4.2 GHz. This spectral analysis system is designed to determine and identify the presence of low level amplitude pulse or CW signals. Real-time analog processing on signal levels as low as -123 dBm for a frequency resolution capability of 40 KHz and an accuracy of ± 26 KHz across the 1 GHz bandwidth is demonstrated.

ACKNOWLEDGEMENTS

I wish to express my sincere gratitude to my supervisor Professor J.S. Wight for his valuable support and friendly discussions. His drive and persistence gave me the courage to complete this thesis in the short period of time I was allotted.

I am also truly indebted to Mr. Simon Gauthier, Engineering Unit Head of the Communications Research Establishment, where this research work was carried out. His invaluable aid in providing the necessary resources throughout the course of this work cannot be given justice in such a small space. His comradeship was also much appreciated throughout this endeavor.

Special thanks are also extended to Mr. Art Sharp, Mr. Ray Molyneaux, and the members of the S2b section for their inestimable aid in the procurement of vital components and measurement systems for this research. I am also grateful for their numerous practical suggestions and the many fruitful discussions.

Finally, I would like to dedicate this work to my parents, for all their years of inspiration, support and continual encouragement.

TABLE OF CONTENTS

	<u>Page</u>
Abstract	111
Acknowledgements	iv
Table of Contents	v
List of Tables	viii
List of Figures	ix
List of Symbols and Abbreviations	xi
Chapter 1 INTRODUCTION	1-1
1.1 Introduction	1-1
1.2 Background and Objective	1-2
1.3 Thesis Organization	1-5
Chapter 2 MICROSCAN RECEIVER AND SYSTEM DESIGN PARAMETERS	2-1
2.1 Introduction	2-1
2.2 Receiver Characteristics	2-1
2.2.1 Thermal Noise	2-2
2.2.2 Noise Figure	2-4
2.2.3 Operational Sensitivity	2-5
2.2.4 Dynamic Range	2-9
2.2.5 Probability of Intercept (POI)	2-15
2.3 Microscan Receiver	2-19
2.3.1 Introduction	2-19
2.3.2 Principles of Operation	2-19
2.3.3 Signal Interception	2-23
2.3.4 Probability of Intercept	2-27
2.3.5 M-C Receiver Configurations	2-33
2.3.6 SAW Receiver Components	2-39
2.3.6.1 SAW Compression Filter	2-41
2.3.6.2 LO Chirp Waveform	2-42
2.3.6.3 Logarithmic Amplifier and Video Detector	2-48
2.3.7 Summary	2-51

Chapter 3	A WIDEBAND MICROWAVE SURVEILLANCE SYSTEM	3-1
3.1	Introduction	3-1
3.2	Environmental Scenario and General System Description	3-1
3.3	Subsystem Level Description and Design Considerations	3-6
3.3.1	Microscan Receiver	3-6
3.3.1.1	Principles of Operation	3-11
3.3.1.2	Sweeping-Local Oscillator	3-15
3.3.1.3	Timing	3-15
3.3.1.4	Dynamic Range	3-15
3.3.1.5	Detection and Thresholding	3-17
3.3.2	Downconversion	3-19
3.3.2.1	Front-End Design	3-23
3.3.2.2	LO Synthesizer	3-26
3.3.2.3	Noise Figure and Dynamic Range Calculations	3-32
3.3.3	Controller	3-35
3.4	Summary	3-39
Chapter 4	EXPERIMENTAL RESULTS	4-1
4.1	Introduction	4-1
4.2	AS-520 Microscan Receiver Measurements	4-1
4.3	Receiver System Evaluation	4-7
4.3.1	Introduction	4-7
4.3.2	Basic Measurement Set-Up	4-7
4.3.3	Sensitivity	4-9
4.3.4	Frequency Accuracy	4-11
4.3.5	Frequency Resolution	4-13
4.3.6	Dynamic Range	4-17
4.3.6.1	Linear Dynamic Range	4-17
4.3.6.2	Instantaneous Dynamic Range	4-19
4.3.6.3	Two-Tone Spur-Free Dynamic Range	4-21
4.3.7	Pulse Width	4-24
4.3.8	Summary of Results	4-30
Chapter 5	CONCLUSIONS	5-1
5.1	System Evaluation	5-1
5.2	Future Studies	5-2

LIST OF TABLES

<u>Table</u>	<u>Description</u>	<u>Page</u>
4.1	Values of sidelobe suppression and 3 dB width for the output pulses of the AS-520 receiver at different IF frequencies.	4-4
4.2	Frequency resolution measurement of the 150-170 MHz IF input band.	4-14
4.3	Linear dynamic range of the receiving system taken at selected frequencies in the 3200 to 3220 MHz band.	4-18
4.4	Linear dynamic range of the receiving system taken at frequencies spaced 100 MHz from each other in the frequency range between 3.2 to 4.2 GHz.	4-18
4.5	Summary of results	4-30

LIST OF FIGURES

<u>Figure</u>	<u>Description</u>	<u>Page</u>
1.1	Comparison of intercept receivers.	1-4
2.1	Equivalent noise bandwidth.	2-3
2.2	Envelope detection circuit.	2-6
2.3	P_d for a sine wave in noise as a function of SNR and P_{fa} .	2-10
2.4	Receiver linear dynamic range.	2-11
2.5	Two-tone spur-free dynamic range.	2-12
2.6	Second and third order intercept points.	2-14
2.7	Time-bandwidth window functions. (a) Activity of an emitter, and (b) Activity of a scanning receiver.	2-16
2.8	PDF in terms of the variable z .	2-18
2.9	Block diagram of a microscan receiver.	2-21
2.10	(a) Frequency versus time of the IF signal. (b) Frequency versus time of the matched PCF.	2-22
2.11	Microscan receiver architectures. (a) Multiply-convolve, (b) Multiply-convolve-multiply, (c) Convolve-multiply-convolve.	2-24
2.12	Time and frequency relation of an M-C microscan receiver.	2-25
2.13	Signal interception for non-interlaced scan.	2-29
2.14	Degradation loss for pulses narrower than the filter integration time.	2-31
2.15	Improvement of PGI with interlaced scan.	2-32
2.16	The M(1)-C(s) microscan receiver.	2-35
2.17	Outputs from a PCF. (a) Without a weighting filter, and (b) With a weighting filter.	2-40
2.18	SAW filter technologies.	2-42
2.19	IDT SAW filter. (a) A typical interdigital transducer. (b) A dispersive IDT filter with apodization.	2-43
2.20	The reflective array compressor (RAC).	2-45
2.21	Amplitude and phase ripples in SAW filters.	2-46
2.22	Methods of increasing the TBP of chirp filters. (a) Cascaded filters for increased integration time. (b) X_2 multiplication for increased bandwidth.	2-47
2.23	Interleaving chirp signals in neighboring frequency bands for increased chirp TBP.	2-49
2.24	Pulse detection circuit. (a) With a single comparator, and (b) With an array of comparators.	2-50

3.1	Block diagram of wideband fast scanning receiver.	3-3
3.2	Complete receiver system realization.	3-5
3.3	Front view photograph of AS-520.	3-7
3.4	Rear view photograph of AS-520.	3-8
3.5	Simplified block diagram of AS-520 microscan receiver.	3-9
3.6	IF block diagram of AS-520 microscan receiver.	3-12
3.7	Timing illustration of 20 MHz scan with CW signals at 170, 165, 160, 155, and 150 MHz.	3-14
3.8	20 MHz coverage control signals.	3-16
3.9	AS-520 receiver dynamic range.	3-18
3.10	Basic superheterodyne receiver conversion stage.	3-20
3.11	Desired signal competing with interfering image at IF frequency.	3-22
3.12	Front-end downconversion block diagram and signal flow budget.	3-24
3.13	Front-end downconversion stage.	3-27
3.14	LO tone allocation.	3-28
3.15	Basic phaselock synthesizer.	3-30
3.16	Timing sequence for the AS-520 trigger pulse, HP-8672A synthesizer, and LO single tone output.	3-36
3.17	Cable connection between the HP microprocessor and the AS-520 receiver.	3-38
4.1	Output voltage versus input RF power for the AS-520 microscan receiver.	4-3
4.2	(a) Output pulse spectrum of a CW tone. (b) An expanded view of (a) at the 3 dB pulse width.	4-6
4.3	Basic experimental set-up.	
4.4	(a) System noise figure, and (b) Gain versus frequency.	4-10
4.5	Error frequency versus input frequency.	4-12
4.6	Simultaneous signal resolution at (a) 100 KHz separation, (b) 60 KHz separation, and (c) 50 KHz minimum separation.	4-16
4.7	Downconversion stage linear dynamic range for CW tone at 3210 MHz.	4-20
4.8	Instantaneous dynamic range for a strong CW tone at 3212 MHz with -20 dBm input power. (a) Weak signal 30 dB down at 355 KHz offset. (b) Maximum amplitude separation of 30 dB at 80 KHz offset.	4-22
4.9	Two-tone 3rd order suppression of downconversion stage inside the 3200 to 3220 MHz band for CW inputs of -43 dBm. (a) $f_1 = 3208.068$ MHz, $f_2 = 3211.320$ MHz, 3rd order suppression = 53.40 dB; (b) $f_1 = 3208.380$ MHz, $f_2 = 3205.068$ MHz, 3rd order suppression = 51.90 dB; (c) $f_1 = 3207.067$ MHz, $f_2 = 3212.340$ MHz, 3rd order suppression = 52.80 dB.	4-25

- 4.10 Two-tone 3rd order suppression of system inside the 3200 to 3220 MHz band for CW inputs of -43 dBm.
- (a) $f_1 = 3208.068$ MHz, $f_2 = 3211.320$ MHz, suppression = 38 dB;
 - (b) $f_1 = 3205.068$ MHz, $f_2 = 3208.380$ MHz, suppression = 37 dB;
 - (c) $f_1 = 3207.068$ MHz, $f_2 = 3212.340$ MHz, suppression = 38 dB.
- 4.11 Relative sensitivity degradation of receiver for gated CW pulse at 160 MHz with -36 dBm input power and pulse width of (a) 200 μ sec, (b) 20 μ sec, (c) 2 μ sec, and (d) 0.2 μ sec.
- 4.12 Pulse width versus relative sensitivity degradation.

26

4-28

4-29

LIST OF SYMBOLS AND ABBREVIATIONS

$A(t)$	Signal amplitude
B	Dispersive filter input bandwidth
BER	Bit error rate
B_{if}	IF bandwidth
B_n	Noise equivalent bandwidth
B_s	Signal bandwidth
B_v	Video bandwidth
$C_1(t)$	Impulse response function of chirp filter and convolution filter
C-M-C	Convolve-multiply-convolve
CW	Continuous wave
DAV	Data available line
f_c	Carrier frequency
f_0	Frequency of maximum response
f_R	Frequency at RF
F	Noise figure
F_t	Overall noise figure of cascaded network
GaAsFET	Gallium arsenide field effect transistor
G_T	Overall system gain
GHz	Gigahertz
GPIOB	General Purpose Interface Bus
$I_0(z)$	Bessel function of zero order
IDT	Interdigital transducer
IF	Intermediate frequency
K	Boltzmann's constant equal to 1.38×10^{-23} J/°K

log amp	Logarithmic amplifier
m	Slope of output voltage versus input power of log amp
M-C	Multiply-convolve
M-C-M	Multiply-convolve-multiply
N	Thermal noise power
N_0	Available noise output from receiver
P_d	Probability of detection
P_{fa}	Probability of false alarm
PCF	Pulse compression filter
PDF(z)	Probability density function for the time coincidence of two independent window functions
PLL	Phase lock loop
POI	Probability of intercept
$P_{12}(T)$	Probability of having an intercept during a period of time T
$P_{31,T}$	Overall third order intercept point for n components in cascade
rect(τ)	$\begin{cases} 1 & \tau \leq 1/2 \\ 0 & \text{otherwise} \end{cases}$
RAC	Reflective array compressor
RF	Radio frequency
S(t)	Real bandpass signal
$\hat{S}(t)$	Baseband complex envelope of the real bandpass signal
SAW	Surface acoustic wave
SFDR	Spur-free dynamic range
SLO	Sweeping local oscillator
SNR	Signal-to-noise ratio
T	SAW filter integration time
T_{fa}	Time between false alarms
T_M	LO chirp duration (multiplier time)

TBP	Time-bandwidth product
V_T	Threshold voltage
VCO	Voltage controlled oscillator
$w(t)$	Weighting filter function
$x(t)$	Input signal
$X(\tau)$	Fourier transform of input signal $x(t)$
$Y(t)$	Envelope detector output
$Y'(t)$	Envelope detector output after filtering
YIG	Yttrium iron garnet
ΔF	Frequency resolution of receiver
$\theta(t)$	Signal phase
ψ_0	Mean square of the noise voltage
μ	Chirp slope
τ	Time variable

Chapter 1

INTRODUCTION

1:1 INTRODUCTION

In modern applications requiring surveillance, spectral analysis systems must cope with the difficult task of intercepting signals over a wide frequency bandwidth and collecting information from exotic emitters. Signals must be sorted on a pulse-by-pulse basis for they can potentially provide vital information about the emitter such as [8]:

- . Frequency
- . Received power
- . Pulse duration
- . Polarization
- . Time of arrival
- . Angle of arrival
- . Characteristic of intrapulse modulation

While several types of receivers can fulfill present-day surveillance roles, each has their own advantages and limitations. The demands for better performance in particular applications have even lead to the hybridization of certain receiver types. In this thesis, the performance characteristics of a wideband microwave surveillance receiver combining a microscan receiver and a superheterodyne receiver are investigated for the purpose of identifying long duration noise disturbances occurring over a wide frequency bandwidth.

In section 1.2, the background and objectives of the thesis are presented in greater detail, while the thesis organization is presented in section 1.3.

1.2 BACKGROUND AND OBJECTIVE

In recent years, extensive efforts have been undertaken to design surveillance receivers capable of operating in an increasingly dense and complex signal environment while maintaining high fidelity on all measured signal parameters. In applications requiring the collection of information from exotic emitters such as frequency hopping signals, spread spectrum signals, multi-beam radars, jammers, weapon guidance signals, etc., a reconnaissance receiver must exhibit wide instantaneous RF bandwidth consistent with the requirement for high probability of intercept on all incoming signals. It should also provide high sensitivity for the detection of low level amplitude signals, offer simultaneous signal handling capability for the occurrence of multiple signal events, and have a high dynamic range to avoid analyzing spurious products unintentionally [9].

Conventional receiver technology such as superheterodyne, crystal video, or tuned radio frequency fail to meet the requirements set by a high-density environment, rapid acquisition, and high probability of intercept (POI). However, with advances made with surface acoustic wave (SAW) devices and microwave integrated circuits (MIC) a new breed of intercept receivers have surfaced to meet the challenge. These include the instantaneous frequency measurement (IFM), channelized, microscan, and Bragg cell receivers [2,8,9]. Of these, only the latter three can provide simultaneous signal capability. Of the latter three, only the

microscan receiver technology combines low complexity and high sensitivity in a package of small size [14]. A more meaningful comparison is presented in Figure 1.1 which lists the performance parameters for high-probability of intercept receivers. An excellent overview of these receivers is addressed by Tsui [2].

In a microscan receiver, the incoming signals are mixed with a linear chirp waveform and the result is convolved in a matched chirp filter to produce the Fourier transform of the input signals. In spite of its many attributes as a high speed signal processor, the microscan receiver does present certain shortcomings. In particular, its usefulness in processing a wide frequency bandwidth with fine frequency resolution cells is still presently limited by SAW technology. In addition, the relatively large amount of insertion loss found in SAWs limits the attainable system noise figure. While it is clear that a single receiver cannot simultaneously meet all system requirements, it is possible to achieve the demands of a wideband surveillance system with fine-frequency resolution capability by combining certain receiver types. The hybridization of a stepping superheterodyne receiver with a microscan receiver offers a promising solution for wideband spectral analysis. While the microscan performs fine resolution high-speed signal processing, the superheterodyne receiver offers excellent selectivity of the RF region to be processed and very high sensitivity for the detection of low level input signals.

The objective of this thesis is to demonstrate the performance of a hybrid technique combining an ARGOS microscan receiver with a front-end stepping receiver to rapidly scan a 1 GHz communication bandwidth

System Parameter	IFM	Channelized	Microscan	Bragg Cells
Sensitivity	Low	High	High	High
Resolution	Moderate	High	High	High
Intercept Probability	High	High	High	High
Simultaneous Signal Performance	Very Low	Moderate	High	Moderate
Dynamic Range	50-60 dB	40-50 dB	40-50 dB	25-35 dB
Signal Analysis Capability	Moderate	High	High	High
Output Format	Single Channel	Parallel Channels	Single Channel	Parallel Channels
System Complexity	Moderate	High	Low	Low
Size	Moderate	Large	Small	Small

Figure 1.1: Comparison of intercept receivers.

between 3.2 to 4.2 GHz. This approach is designed to determine and identify, to within a channel spacing of 30 KHz, the presence of low level amplitude, long duration noise disturbances in the vicinity of Ottawa, Ontario.

1.3 THESIS ORGANIZATION

Chapter 2 is divided into two parts. The first part reviews some of the practical design considerations which must be applied when designing receiving systems. Receiver sensitivity, receiver noise figure, third-order intercept level, and dynamic range are some of the factors which are highlighted. The most important part of this spectral analysis system is the microscan receiver and thus a good understanding of its characteristics is essential. Consequently, the second part of Chapter 2 is devoted to the basic theory of the microscan receiver. The microscan receiver is also referred in the open literature as the compressive receiver; both terms are used interchangeably in this text.

In Chapter 3, the system requirements and the proposed design solution for the wideband surveillance receiver are assessed in detail. Areas of interest include the ARGOS microscan receiver, the front-end downconversion stage, and the microprocessor controller.

In Chapter 4, the experimental results obtained from the receiver are presented. The performance of the surveillance system is examined and compared with theoretical predictions.

In Chapter 5, conclusions and recommendations for future work are presented.

Chapter 2

MICROSCAN RECEIVER AND SYSTEM DESIGN PARAMETERS

2.1 INTRODUCTION

The many important concepts of a wideband spectral analysis system using a microscan receiver are considered in this chapter. The chapter is divided into two parts with emphasis placed on both a sound understanding of the theoretical aspects of a microscan intercept receiver, and the many practical design considerations which must be applied when designing a receiving system.

The first portion of the chapter reviews some of the important concepts involved in receiver design. These include thermal noise, noise figure, operational sensitivity, dynamic range, and probability of intercept. The second part of the chapter focuses its attention more specifically on the microscan receiver. Here, the theoretical and analytical foundations of the microscan receiver are established. Moreover, a brief overview on some of the practical components which make up the receiver is also presented. Finally, this chapter concludes with a brief summary.

2.2 RECEIVER CHARACTERISTICS

The most significant characteristics and parameters used in describing receiver performance are discussed in the following subsections.

2.2.1 Thermal Noise

The chief limiting factor in receiver sensitivity is noise. Noise is unwanted electromagnetic energy which prevents the receiver from properly detecting the desired signal energy. It originates within the receiver itself or it may enter via the receiving antenna along with the desired signal. There is always noise present due to the thermal agitation of electrons in the ohmic portions of the receiver. This is known as thermal noise and is directly proportional to temperature and bandwidth of the receiver [1]. The available thermal noise power generated by a receiver of bandwidth B_n (Hz) at a temperature T ($^{\circ}\text{K}$) is equal to:

$$N = KT B_n \quad (2.1)$$

where K is Boltzmann's constant equal to 1.38×10^{-23} J/deg.

T is the equivalent noise temperature in Kelvin (290°K =room temperature).

The bandwidth B_n is the noise equivalent bandwidth and is given by:

$$B_n = \frac{\int_{-\infty}^{+\infty} |H(f)|^2 df}{|H(f_0)|} \quad (2.2)$$

where $H(f)$ is the frequency response characteristic of the IF filter and f_0 is the frequency of maximum response (usually specified at midband). This is an integrated bandwidth of an equivalent rectangular filter whose noise power output is the same as the filter with characteristic $H(f)$ as shown in Figure 2.1.

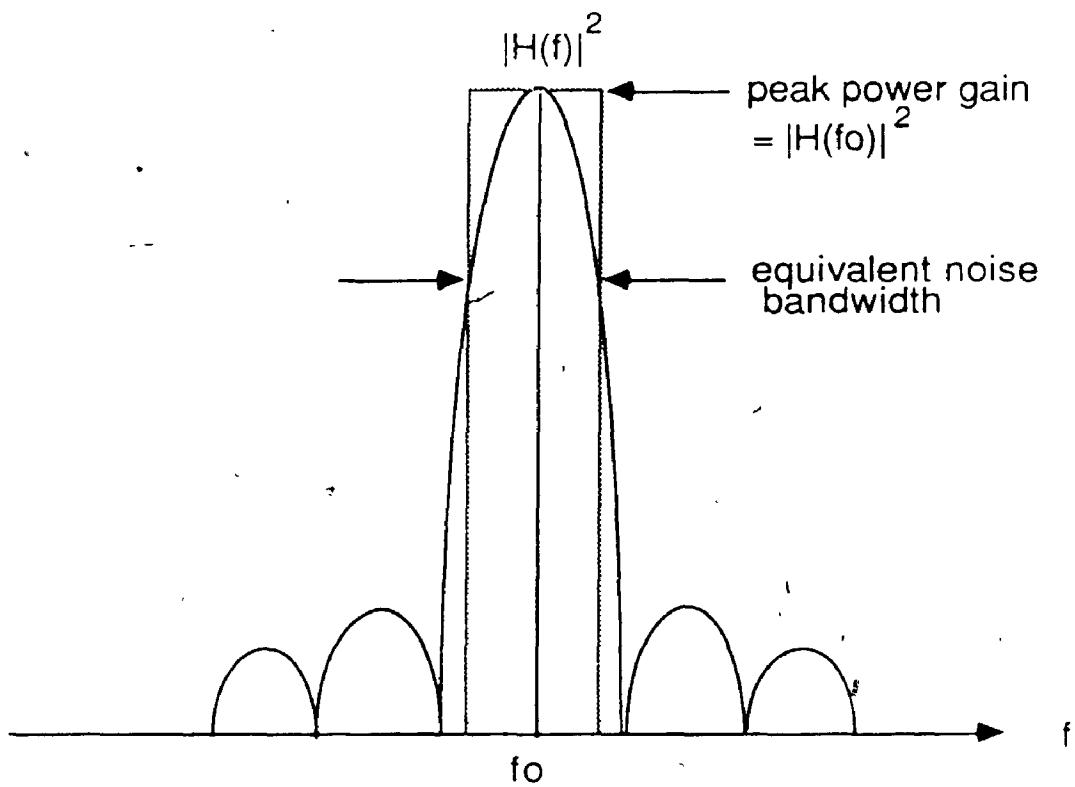


Figure 2.1: Equivalent noise bandwidth.

2.2.2 Noise Figure

The noise power of a practical receiver is always greater than thermal noise because noise is added by every component in the receiver. The noise figure F of a receiver is defined as:

$$F = \frac{N_o}{KT_o BnG} = \frac{\text{noise out of practical receiver}}{\text{noise out of ideal receiver at std temperature}} \quad (2.3)$$

where N_o is the noise output from the receiver and G is the available gain. The standard temperature T_o is 290°K . Since the output signal is related to the input signal through:

$$S_o = G S_i \quad (2.4)$$

equation (2.3) can be rewritten as:

$$F = \frac{S_i/N_i}{S_o/N_o} = \frac{\text{SNR}_i}{\text{SNR}_o} \quad (2.5)$$

where SNR_i is the signal-to-noise ratio at the input of the receiver and SNR_o is the signal-to-noise ratio at the output. Equation (2.5) can be interpreted as a measure of the degradation of signal-to-noise ratio as the signal passes through the receiver. Therefore F is always greater than unity. Noise figure is often expressed in dB as:

$$\text{NF(dB)} = 10 \log F \quad (2.6)$$

For n components connected in cascade, the overall noise figure F_T may be shown to be equal to:

$$F_T = F_1 + \frac{F_{2-1}}{G_1} + \frac{F_{3-1}}{G_1 G_2} + \dots + \frac{F_{n-1}}{G_1 G_2 \dots G_{n-1}} \quad (2.7)$$

where F_1 and G_1 are the noise figure and gain of the i th network respectively. If the gain of the first stage is high and its noise figure is low, the noise contribution of the following stages can be rendered negligible. This is an important concept in receiver design [1-7].

2.2.3 Operational Sensitivity

The detection of weak signals is limited by noise energy occupying the same portion of the band as the signal. The operational sensitivity of a receiver is usually expressed as the minimum signal strength required to provide a specified probability of detection without exceeding a specified probability of false alarm [2].

Consider the envelope detector circuit shown in Figure 2.2. It consists of an IF filter of bandwidth B_{IF} followed by a linear or square law detector with a video amplifier of bandwidth B_v . By rearranging equation (2.5), the input signal may be expressed as:

$$S_1 = KT B_n F \frac{S_o}{N_o} \quad (2.8)$$

If the minimum detectable signal S_{min} is that value of S_1 corresponding to the minimum ratio of output (IF) signal-to-noise ratio $(S_o/N_o)_{min}$ necessary for detection, then:

$$S_{min} = KT B_n F \left(\frac{S_o}{N_o}\right)_{min} \quad (2.9)$$

Equation (2.9) can also be expressed in dBm as:

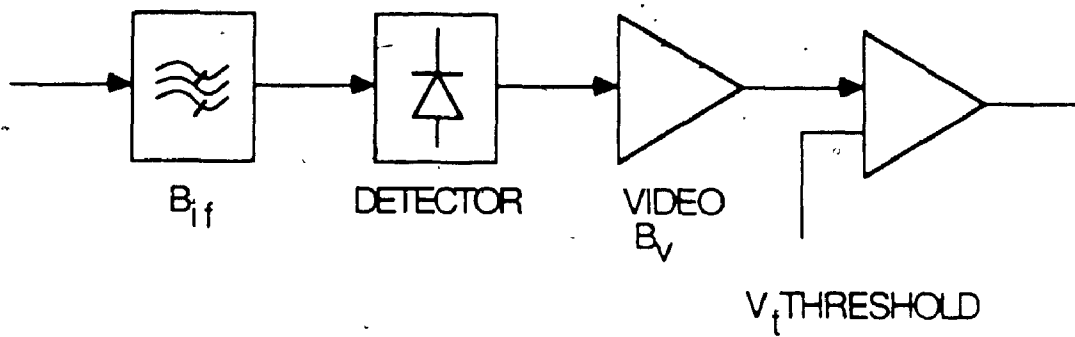


Figure 2.2: Envelope detection circuit.

$$S_{\min}(\text{dBm}) = 10 \log_{10}(1000KT) + \text{NF}(\text{dB}) + 10 \log_{10} B_n + \text{desired S/N}(\text{dB}) \quad (2.10)$$

Often a 0 dB S/N ratio is used to express receiver sensitivity and is referred to as the minimum discernible signal (MDS) level. This means the signal power is equal to the noise power at the output of the IF filter. At this level the false alarm rate is high and it is, therefore, a common practice to threshold the output of the envelope detector to keep the false alarm rate at a desirable level.

The required threshold setting to get a specified probability of detection without exceeding a specified probability of false alarm is known as the Neyman-Pearson criterion and has been addressed by Skolnik [1]. Only the results are presented here. The instantaneous noise voltage V entering the IF filter is assumed Gaussian with mean equal to 0 and variance ψ_0 . Let the threshold voltage be V_T . Then the average time interval between crossings of the threshold by noise alone is defined as the false-alarm time T_{fa} :

$$T_{fa} = \frac{1}{B_{IF}} \exp \frac{V_T^2}{2\psi_0} \text{ (sec)} \quad (2.11)$$

The ratio of the time the noise is above a certain threshold to the overall observation time is defined as the probability of false alarm. It is expressed as:

$$P_{fa} = \frac{1}{T_{fa} \cdot B_{IF}} \quad (2.12)$$

By substituting equation (2.12) into (2.11) the result may be manipulated to give the required threshold voltage in terms of the noise variance and false alarm probability:

$$V_T = \sqrt{2\psi_0 \ln(1/P_{fa})} \quad (2.13)$$

If a sine wave signal of amplitude A is present along with the noise in the IF bandpass filter, then the probability of detection Pd is given by:

$$P_d = \int_{V_T}^{\infty} \frac{R}{\psi_0} \exp\left(\frac{-R^2 + A^2}{2\psi_0}\right) I_0\left(\frac{RA}{\psi_0}\right) dR \quad (2.14)$$

where R is the amplitude of the envelope of the filter output. Here, $I_0(z)$ is the modified Bessel function of zero order and argument Z given by:

$$I_0(z) = \frac{e^z}{\sqrt{2\pi z}} \left(1 + \frac{1}{8z} + \dots\right) \quad (2.15)$$

Equation (2.14) can only be evaluated by numerical techniques or by some form of approximation [1,2]. The signal amplitude A and noise variance ψ_0 can be related to the signal-to-noise ratio as:

$$\frac{A}{\sqrt{\psi_0}} = \sqrt{\frac{2S}{N}} \quad (2.16)$$

The probability of detection Pd as a function of signal-to-noise ratio at the input of the detector and probability of false alarm P_{fa} is illustrated in Figure 2.3. By determining B_{IF} and T_{fa} , the false alarm probability P_{fa} can be calculated from equation (2.12). Then, for a desired probability of detection Pd, the SNR required at the output of

the filter can be read directly from Figure 2.3. In the above discussion the video bandwidth B_V is assumed to be greater than $B_{IF}/2$ but less than B_{IF} .

2.2.4 Dynamic Range

The dynamic range of a receiver is the input RF power a receiver can process correctly. It is defined as the ratio of the maximum signal handled by a receiver to the smallest signal capable of being detected [1,6]. The smallest signal is the MDS or a specified threshold level and the maximum signal is that which causes a specified degree of intermodulation or a specified deviation from linearity (usually 1 dB) of the output-vs-input curve as shown in Figure 2.4.

The dynamic range of a receiver is often determined by its simultaneous signal handling capability. It refers to the range of RF input power over which two signals can be free from noise, harmonics, or intermodulation products. The instantaneous dynamic range defines the maximum amplitude separation between a strong signal and a weak one (separated in frequency by more than the frequency resolution of the receiver) such that the receiver can measure both of them correctly [2]. The spurious free dynamic range (SFDR) also indicates the receiver's ability to handle two simultaneous signals [2]. As shown in Figure 2.5, this range is bounded in the lower limit by a specified threshold and at the upper limit by the input power level at which two signals F_1 and F_2 produce third order intermodulation products F_3 and F_4 equivalent to the MDS. Third order spurious products are of greatest concern because they appear inband.

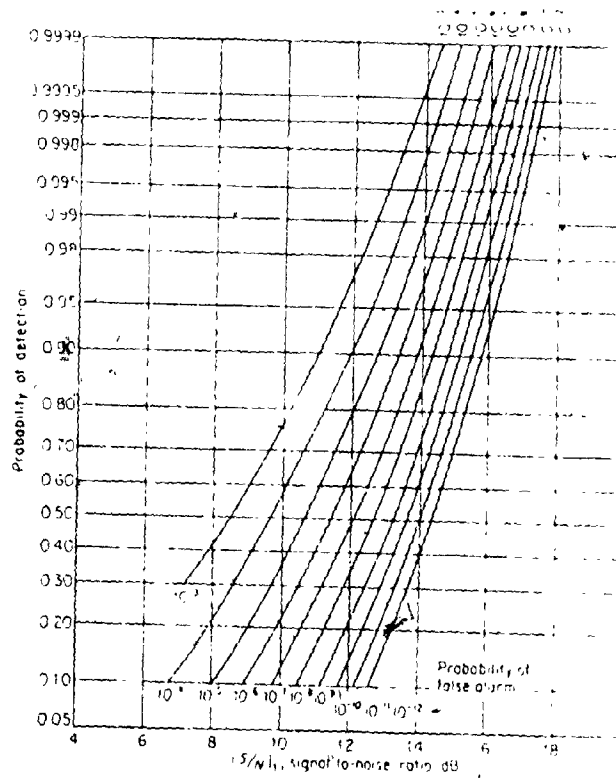


Figure 2.3: Probability of detection for a sine wave in noise, as a function of the signal-to-noise (power) ratio and the probability of false alarm (copied from [1]).

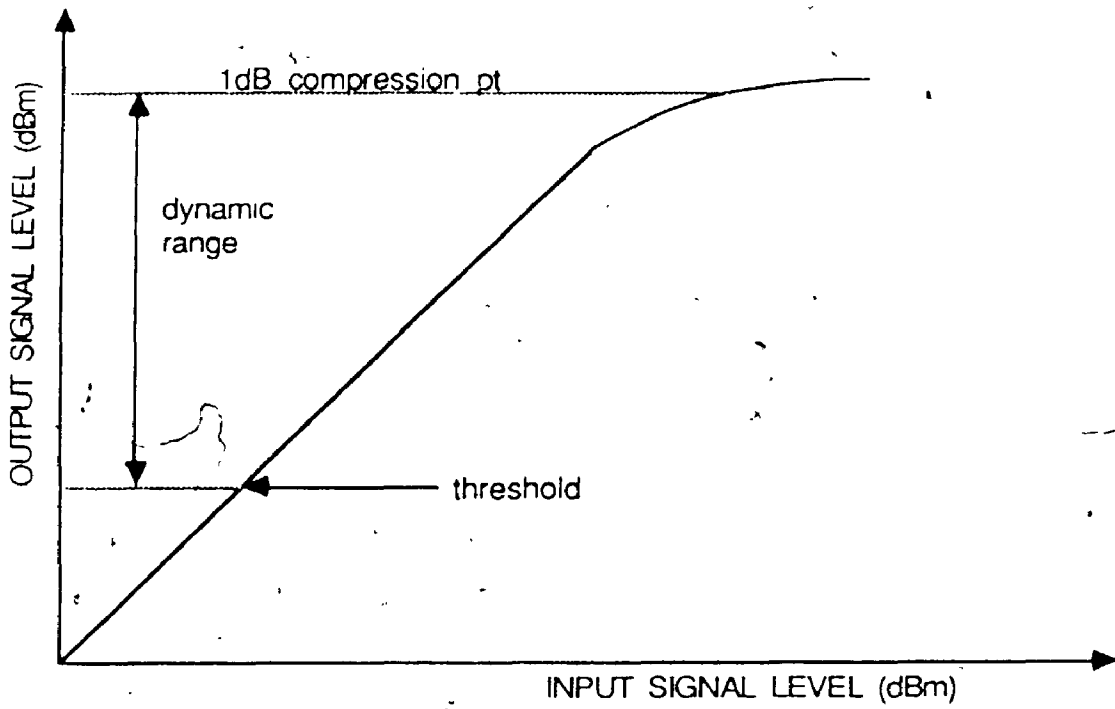


Figure 2.4: Receiver linear dynamic range.

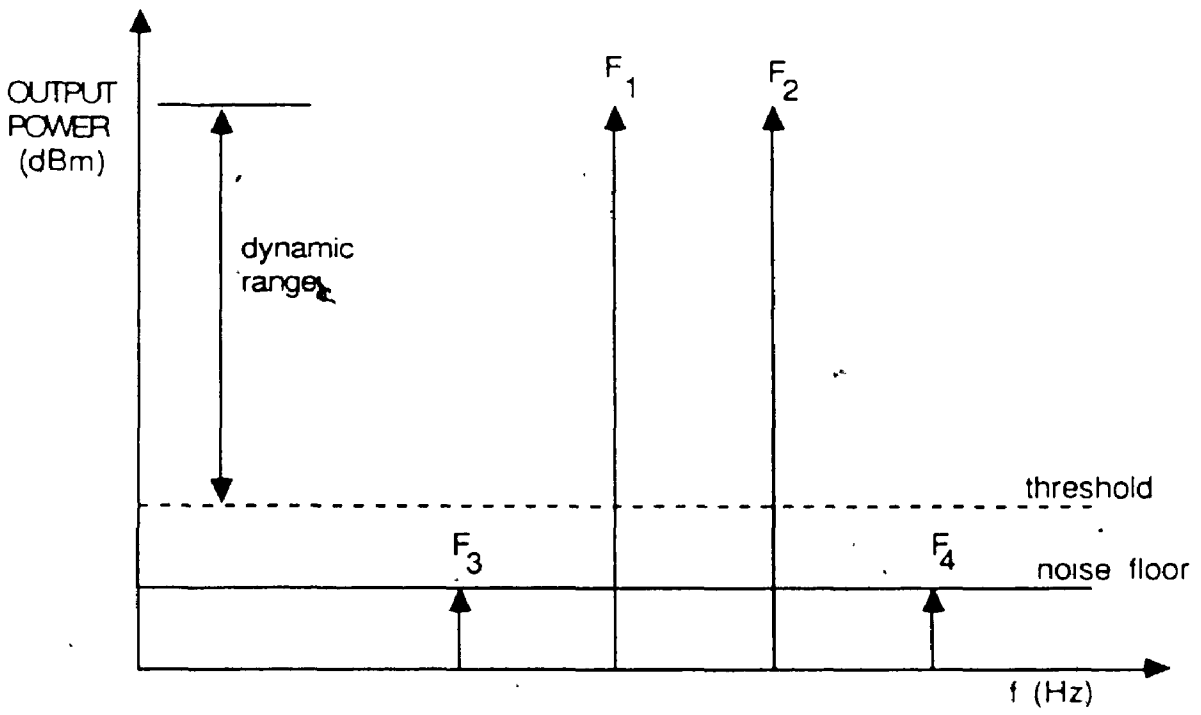


Figure 2.5: Two-tone spur-free dynamic range .

It is possible to calculate the level of third order intermodulation products given the third order intercept point P_{31} , the total gain of the receiver G_T , and the input power P_I . The third order intercept point P_{31} is the intercept point of the gain curve of slope 1 and the third order product curve of slope 3 as shown in Figure 2.6. The amplitude F_3 and F_4 in Figure 2.5 can be evaluated as [6]:

$$I_{m_3} = 3(P_I + G_T) - 2 P_{31} \quad (2.17)$$

The input level at which the intermodulation products are equivalent to the noise floor is given by:

$$P_I = \frac{\text{Noise floor}}{3} - \frac{2G_T}{3} + 2 \frac{P_{31}}{3} \text{ dBm} \quad (2.18)$$

The spurious free dynamic range is often defined from this input power level to the threshold level for a specified P_{fa} . This is stated as:

$$\text{SFDR} = P_I - \text{threshold} = \frac{2}{3} (P_{31} - G - \text{threshold}) \quad (2.19)$$

The spurious free dynamic range of a receiver can be evaluated if the third order intercept point of each component in the receiver is known. The overall third order intercept point $P_{31,T}$ can be written as [7]:

$$\frac{1}{P_{31,T}} = \sum_{i=1}^n (P_{31,i} G_{(i+1,n)})^{-1} \quad (2.20)$$

where $P_{31,i}$ and G_i are the third order intercept point and gain of element i respectively.

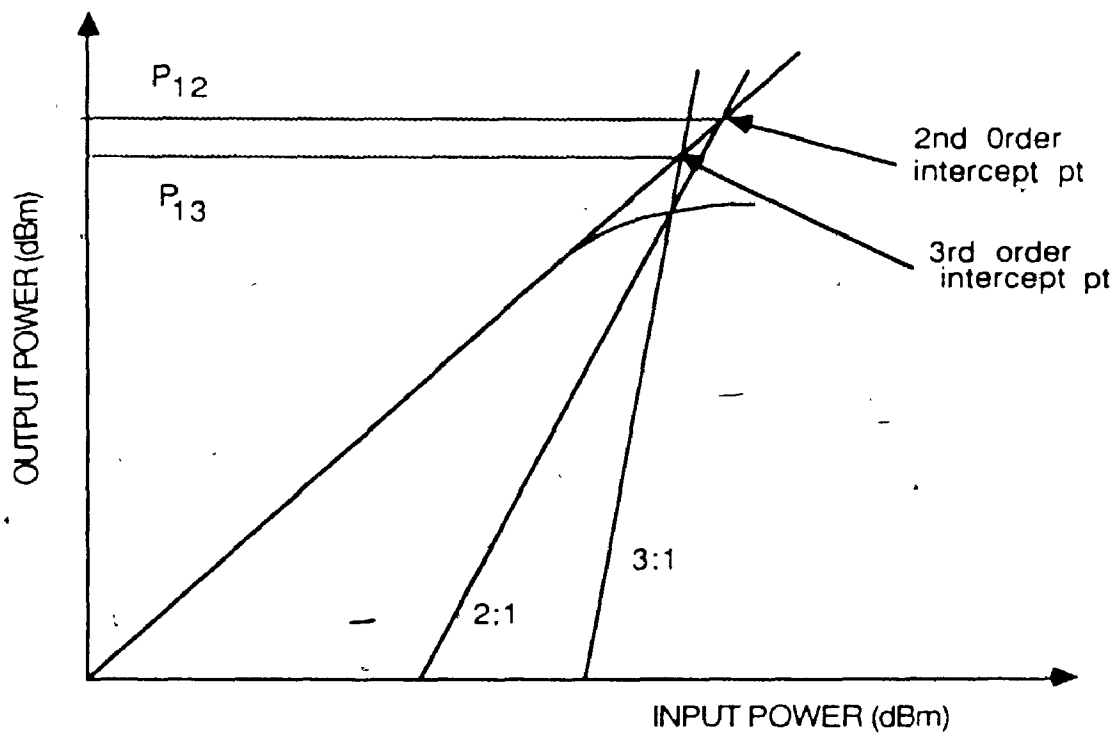


Figure 2.6: Second and third order intercept points (copied from [2]).

2.2.5 Probability of Intercept

The probability of intercept (POI) plays an important role in surveillance systems. The POI gives an indication of the likelihood of acquiring signals which are radiated by an emitter within a given frequency band of interest and within a specified amount of time after the start of a particular activity. Interception should not be mistaken for detection. Detection, as explained in Section 2.2.3, is related to the signal level, noise level, and threshold of a previously acquired activity, whereas interception dictates the time coincidence of two or more activities [38].

Determining the POI is often a difficult task. It depends on the signal environment as well as on the different system parameters which influence the time required to achieve an intercept. Consider the two independent window functions illustrated in Figure 2.7. Figure 2.7(a) represents the activity of an emitter while Figure 2.7(b) represents the activity of a scanning receiver. Each window function is characterized by a width τ , a period T , and a starting time t . For the scanning receiver, T represents the total time required to scan a bandwidth of B_{tot} and the time that the receiver dwells at a particular frequency is given by:

$$\tau = \frac{BT}{B_{tot}} \quad (2.21)$$

where B is the instantaneous bandwidth of the receiver. An intercept will occur when the window functions overlap. The condition required to have an intercept in the first period is expressed as:

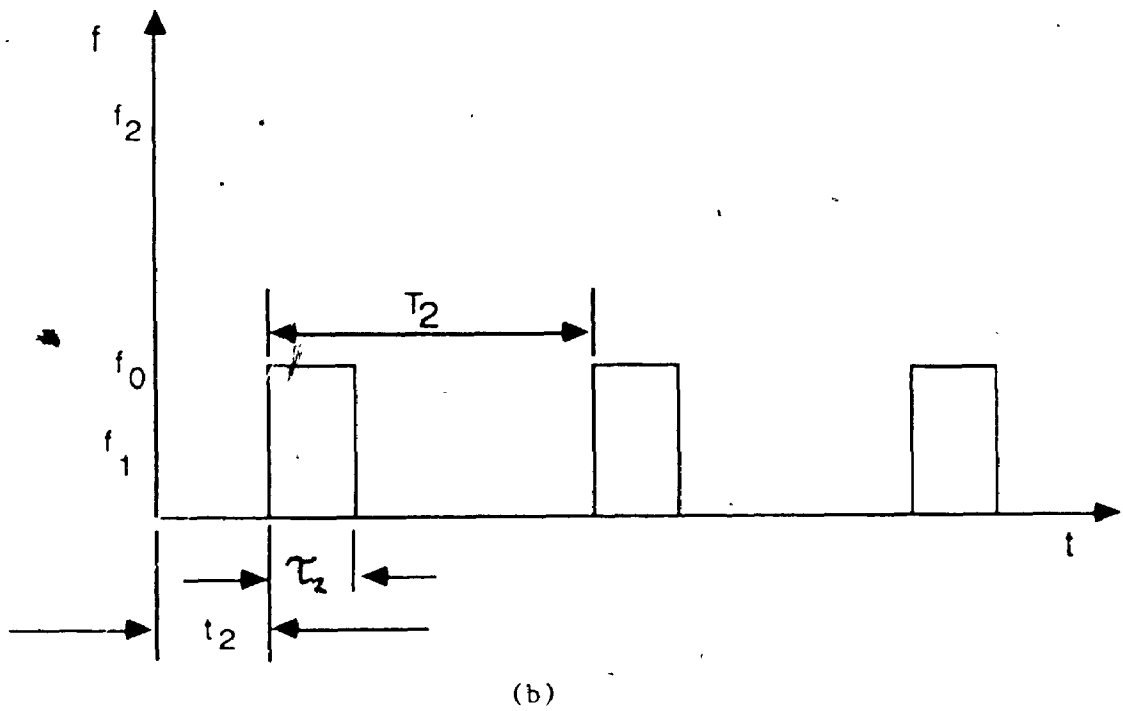
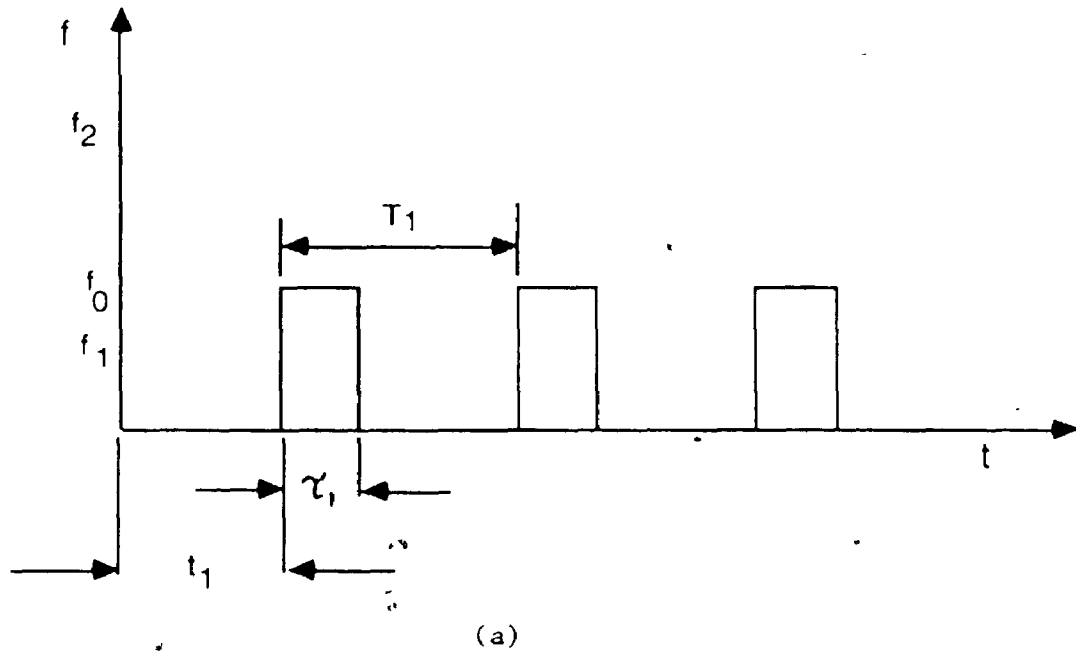


Figure 2.7: Two independent time-bandwidth window functions.
 (a) Activity of an emitter and
 (b) Activity of a scanning receiver.

$$-t_1 \leq t_1 - t_2 \leq t_2 \quad (2.22)$$

Assuming the start times are independent of one another, the probability of the two windows coinciding during the first period of the window function with the shorter period can be shown to be equal to:

$$P_{12}(T_i) = \int_{-T_i}^{T_i} \text{PDF}(z) dz, \quad T_i \quad (i=1,2) \quad (2.23)$$

where PDF is the probability distribution function for the independent random variable z illustrated in Figure 2.8.

Once $P_{12}(T_i)$ is determined, the probability of having an intercept during a period of time T is given by the equation:

$$P_{12}(T_i) = 1 - [1 - P_{12}(T_i)]^{T/T_i} \quad (2.24)$$

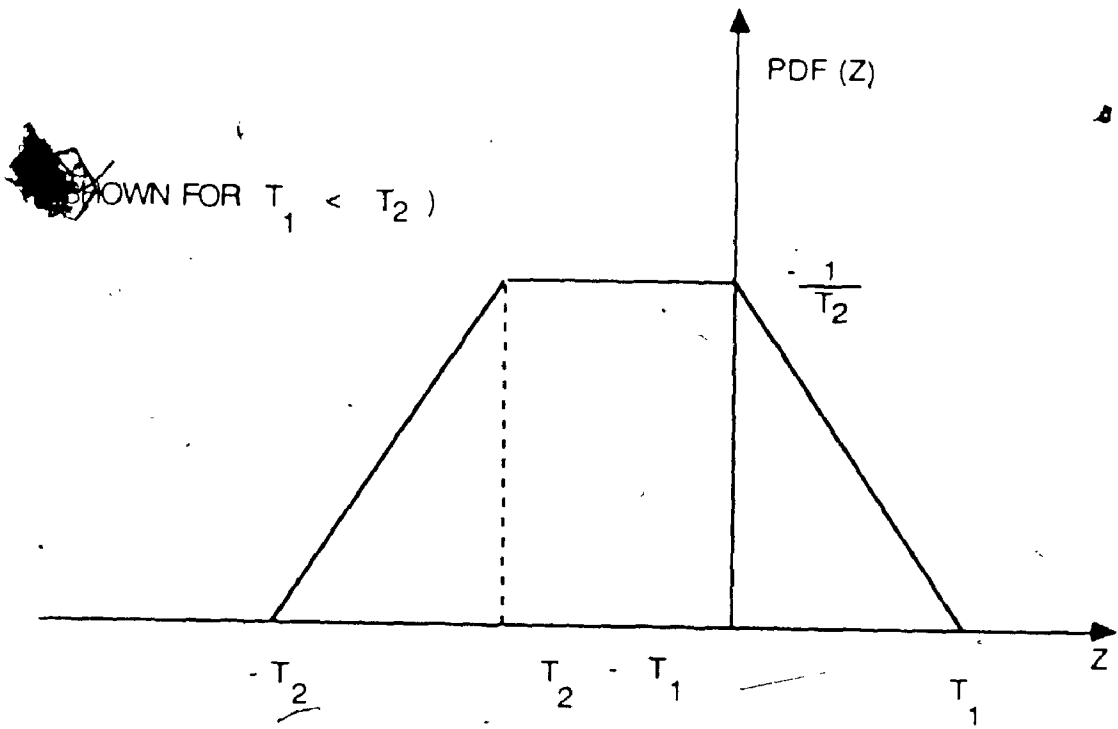


Figure 2.8: PDF in terms of the variable z (copied from [38]).

2.3 MICROSCAN RECEIVER

2.3.1 Introduction

The microscan receiver is an analog processor which extracts the spectral contents of an incoming signal by performing a real-time continuous Fourier transform. Its name derives from the fact that it can scan a large bandwidth in a period of time shorter than the duration of the shortest pulse expected. This has the added advantage over conventional scanning receivers to achieve a higher probability of intercept (POI) on both CW and pulsed signals.

The following sections will examine in closer detail the theoretical and analytical operation of the microscan receiver. First, the basic principles of operation of the receiver are presented followed by a section on signal interception and probability of intercept. An analytical description of the receiver operation immediately follows in order to give a more in depth understanding on how signals are being processed. Furthermore, an overview on some of the key components which make up the receiver such as the pulse compression filter, the sweeping local oscillator, and the logarithmic amplifier and detector is addressed.

2.3.2 Principles of Operation

A microscan receiver obtains spectral information by performing a continuous Fourier transform on every signal entering its bandwidth. It overcomes the sweep rate versus resolution constraint found in superheterodyne scanning receivers by using a pulse compression

technique. A block diagram of a microscan receiver is illustrated in Figure 2.9. The incoming signal is mixed with a linear chirp local oscillator (LO) signal of constant signal strength to produce a frequency modulated signal at an intermediate frequency (IF). This IF signal can either chirp up or down depending on the direction of the LO sweep. Chirp is the general term used to describe a signal having a quadratic phase variation. If the LO chirps up then the IF signal's instantaneous frequency increases linearly with time with a slope of $+m$ as shown in Figure 2.10(a). The IF signal is then convolved in a pulse compression filter (PCF) which has a frequency versus time delay of $-m$ as shown in Figure 2.10(b). This has the effect of speeding up the higher frequencies at the trailing edge with respect to the lower frequencies at the leading edge of the pulse. The outcome results in collapsing (in time) all the energy of the incoming signal to produce a pulse at the output of the PCF. By conservation of energy, if the signal duration is compressed then its amplitude must increase proportionately [15,24]. Consequently, the spectral content of this signal is embedded in the time function coming out of the PCF. By carefully measuring the onset time at which this time function emerges from the filter, the desired information is obtained. Noise is unaffected by the PCF since different noise frequency components are uncorrelated; delaying some more than others will have no effect on the noise output [24]. Because of its compression effects, the microscan receiver is often referred to in the open literature as a compressive receiver.

The arrangement shown in Figure 2.9 is known as the M-C configuration which stands for multiply-convolve and it is the most

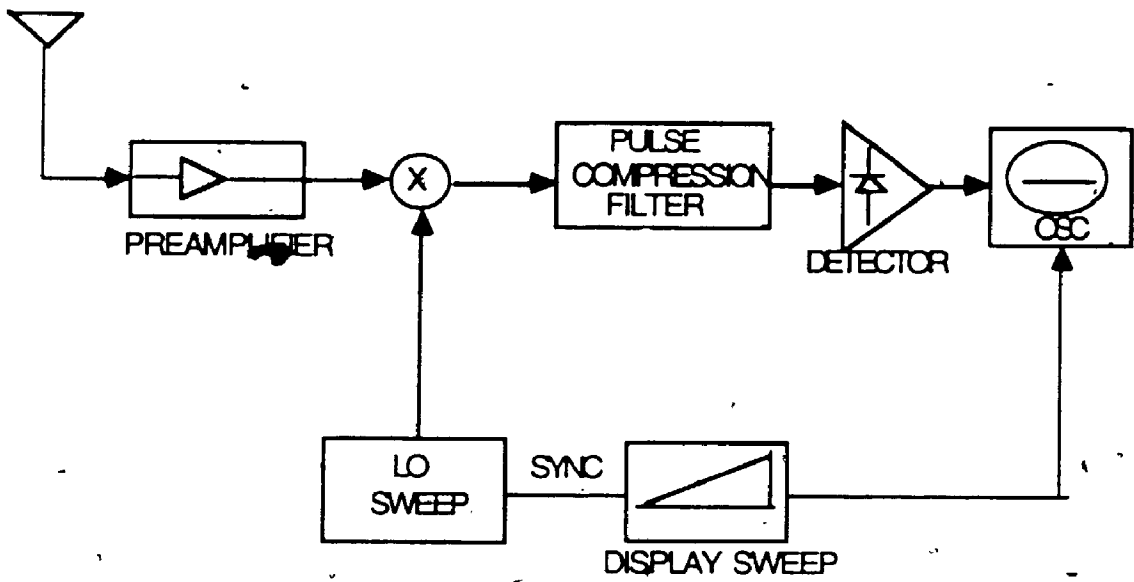
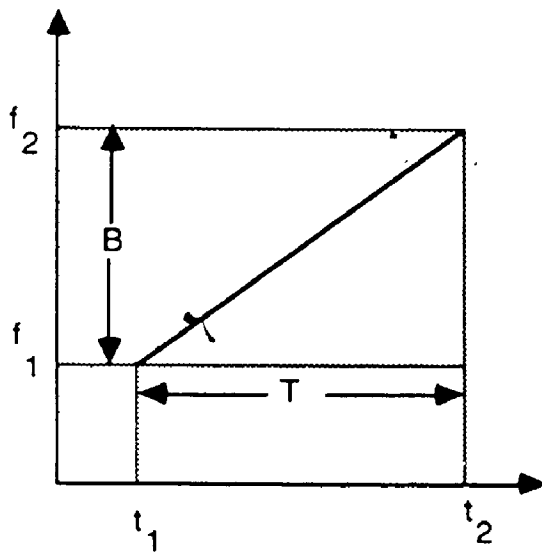
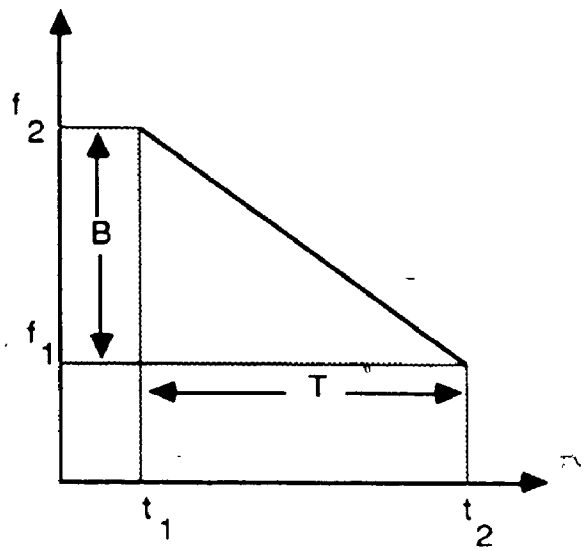


Figure 2.9: Block diagram of a microscan receiver.



(a)



(b)

Figure 2.10: (a) Frequency vs time of the IF signal and
 (b) Frequency vs time of the matched PCF.

basic of three possible architectures. The two others being the multiply-convolve-multiply and the convolve-multiply-convolve (C-M-C), a dual of each other as shown in Figure 2.11. In fact, the M-C configuration is derived from the M-C-M configuration and has use only in the power spectrum analysis of signals [10,11,18,19] (see Section 2.3.5). Our attention will be primarily focused on the M-C configuration. In the M-C configuration the difference in time between the longest delay t_2 and the shortest delay t_1 of the PCF is referred to as the integration time T . The range of frequencies which experiences the delay is known as the filter bandwidth B [2,14]. The integration time of the filter determines the sensitivity and the frequency resolution (ΔF) of the system and is given by $1/T$. Frequency resolution refers to the ability to distinguish between neighboring frequency signals close-in. The filter bandwidth determines the pulse width at the output of the filter and the probability of intercept of the system. The product of these two parameters gives the time-bandwidth product (TBP) of the compression filter. The TBP is a figure of merit for the compressive receiver which determines its overall processing gain. For a fixed resolution, the larger the TBP the faster the LO can scan and, thus, a wider band can be monitored [10,13,14,15].

2.3.3 Signal Interception

To further understand how signals are intercepted and passed through the compressive receiver, a simplified graphical approach is presented. Figure 2.12 represents the time and frequency relation of a M-C microscan receiver. In Figure 2.12(a) three frequency tones f_{\min} , f_c , and f_{\max} where appropriately chosen so that f_{\max} and f_{\min} are both

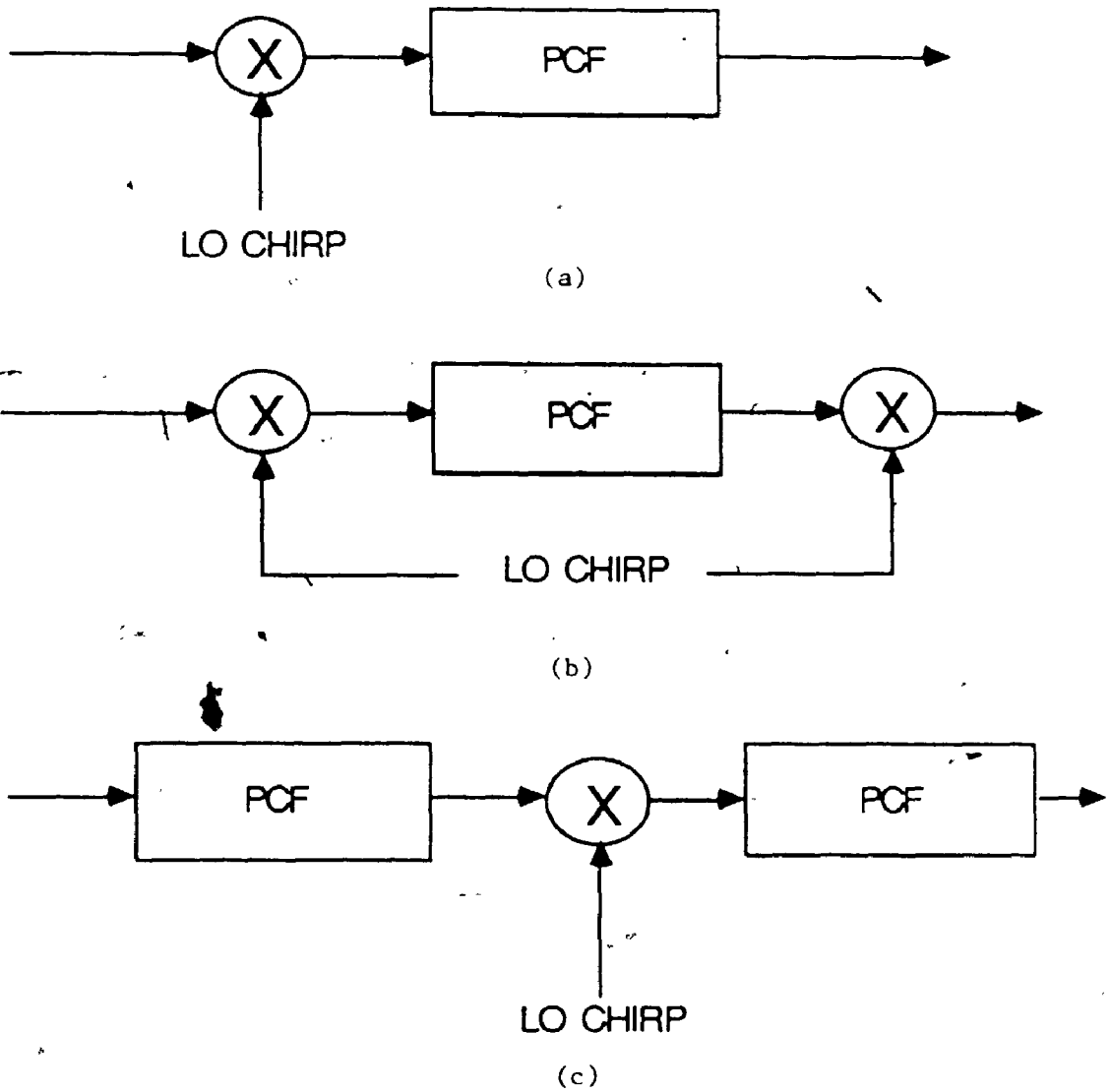


Figure 2.11: Microscan receiver architectures
 (a) Multiple-convolve,
 (b) Multiply-convolve-multiply, and
 (c) Convolve-multiply-convolve (copied from [35])

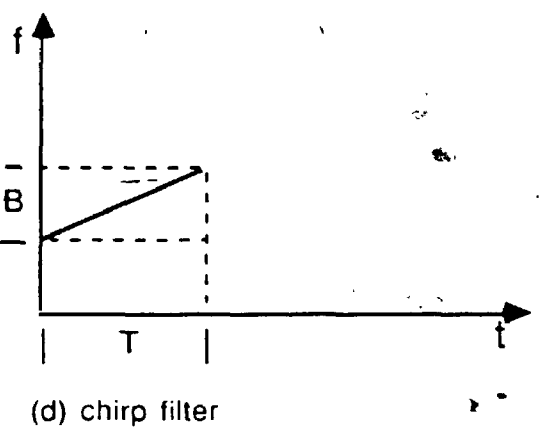
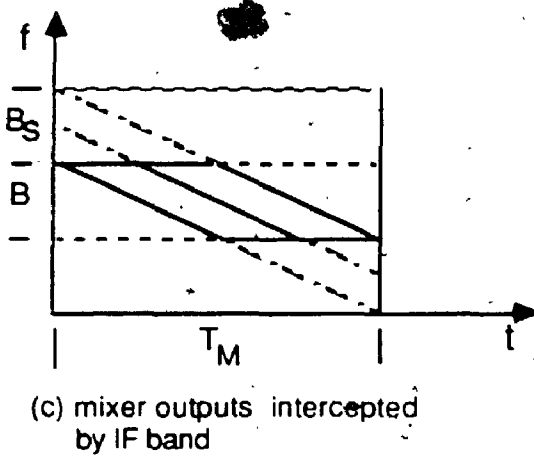
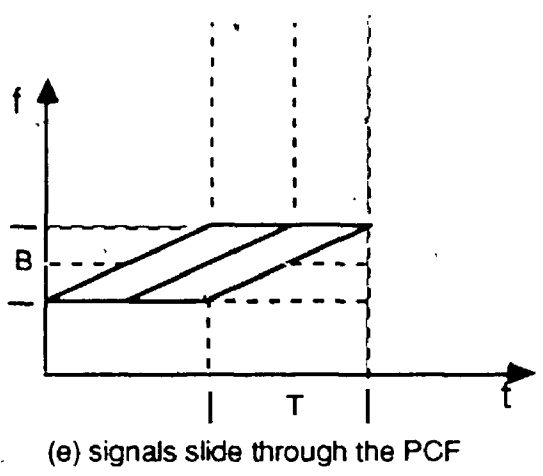
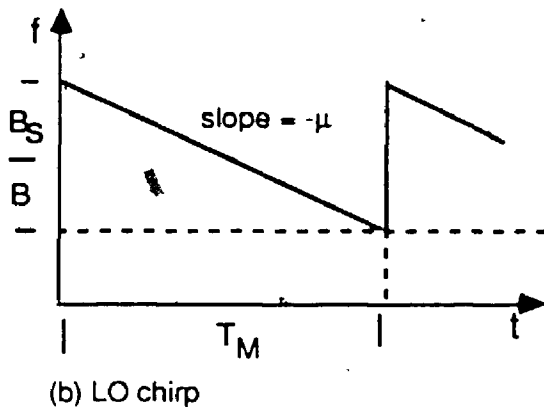
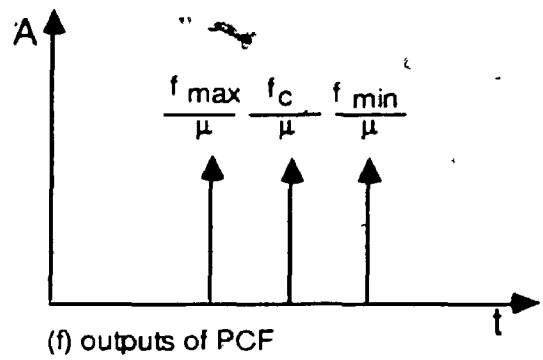
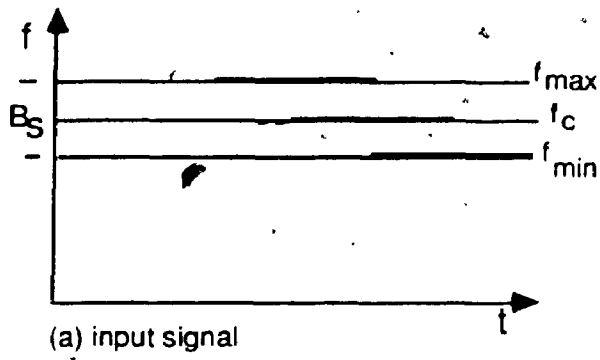


Figure 2.12: Time and frequency relation of a M-C microscan receiver

at the edge of the RF band while f_c is located in the center of the receiver band. It is assumed that the RF bandwidth B_s is equal to the input filter bandwidth B with the phase response of the convolver matched to the phase response of the LO.

In Figure 2.12(b) the LO must scan a band consisting of $B_s + B$ in a time T_m in order to ensure that all three tones in the signal bandwidth fill up the input filter bandwidth B completely in order to be intercepted with full sensitivity at the output. T_M is twice as long as the filter integration time T .

Figure 2.12(c) shows the mixer outputs being intercepted by the input bandwidth B . The output of the multiplier is a windowed version of the input superimposed with frequency modulation.

Figure 2.12(d) illustrates the signals entering the PCF with a frequency versus delay slope matched to the LO. Both the bandwidth and the filter response time of the convolver are only half that of the LO in order to keep the sweep rate constant.

In Figure 2.12(e) f_{\min} enters the PCF first followed by f_c and f_{\max} a short time later. The windowed chirps produced by the mixer "slide" through the PCF until their centre frequency corresponds to the centre frequency of the PCF.

Finally, Figure 2.12(f) illustrates the three time shifted pulses at the output of the PCF. Frequency information can be derived through a scaling factor [2,12] as:

$$f = \mu t \quad (2.25)$$

where μ is the chirp slope.

For the practical case when $B_s = B$, the IF signal enters the PCF during the first half of the LO chirp duration T_M and emerges from the PCF during the second half. In other words the PCF has a valid output only during the second half of the multiplier chirp (i.e. $T_M/2$ to T_M , $3/2 T_M$ to $2T_M$, etc.). Therefore the POI cannot be 100% [2,14]. This suggests that if a short pulse arrives at a time when the LO has passed through a certain portion of its band, it could be missed entirely as shown by the heavy lines in Figure 2.12(a). The POI of the system determines the likelihood of intercepting each and every pulse received. Because of its importance in fast sweeping receivers like the compressive receiver the POI is reviewed more thoroughly in the following section.

2.3.4 Probability of Intercept (POI)

Given the same resolution bandwidth, a compressive receiver can intercept a signal faster than a conventional scanning receiver by an amount equal to the time-bandwidth product (TBP) of the pulse compression filter. This is expected, simply because the scan rate ($\mu = B/T$) of the compressive receiver is $B F$ times faster than that of a conventional superheterodyne scanning receiver [2]. Unfortunately, the POI of a compressive receiver is not easily defined. Its measure depends largely upon the complex effects of three parameters [15]:

1. energy of the signal
2. pulse duration versus start of LO sweep
3. center frequency of signal versus LO center frequency

To simplify the definition, it is assumed that the energy of the incoming signal is sufficiently strong during a time equal to the filter

integration period T in order to cause a detection when intercepted by the receiver. Full interception means that the signal must fill the entire integration time period of the pulse compression filter in order to guarantee a detection at full sensitivity. When the signal is not present for the entire duration of T , in the filter, the output signal energy is decreased and, thus, degradation in receiver sensitivity and resolution occurs. This can be seen when both the time duration and/or the center frequency of an incoming signal do not coincide with the start time and/or the center frequency of the sweeping local oscillator respectively. The graphical representation in Figure 2.13 will help clarify these points.

Three different pulse durations are illustrated, each being at a different center frequency. If the signal duration is very long like the case for the CW tone, the signal will be intercepted in the filter integration time window at every scan of the LO. The compression filter will have outputs at $1/T_M$ repetition rate with full sensitivity.

If the pulse duration is equal to the sum of the scan period plus integration period ($T_M + T$) this will guarantee at least one full integration at full sensitivity for any input time of arrival with respect to the LO scan and for any frequency within the filter bandwidth as shown.

Finally, the case when the signal duration is equal to the filter integration time. Three things might occur. In the best case possible, the pulse completely fills the receiver integration period and is fully intercepted resulting in full receiver sensitivity. In the worst case, the pulse falls between two adjacent scans and is completely missed and therefore no interception occurs. Anywhere between these two extremes,

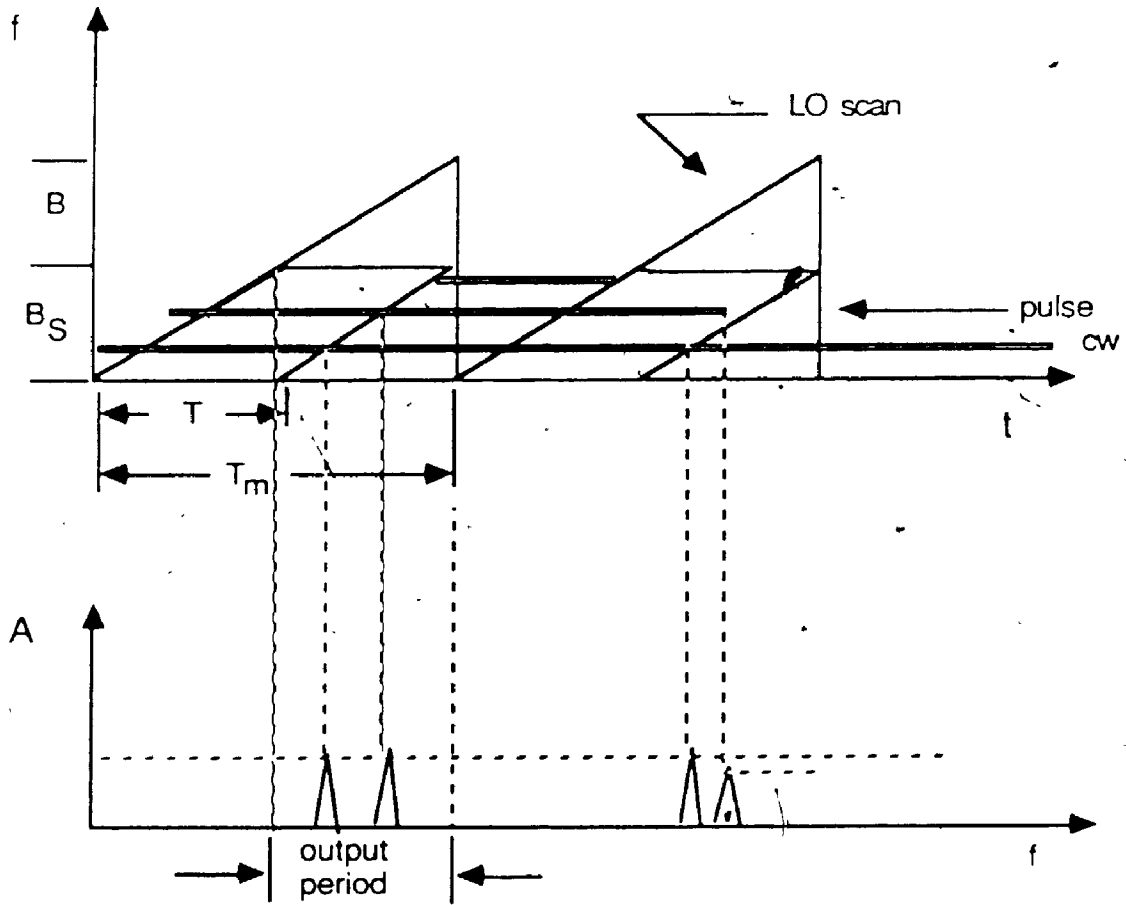


Figure 2.13: Signal interception for non-interlaced scan.

partial overlap of the pulse and integration time occurs which results in reduced sensitivity and resolution [14].

The effects of partial interception is analogous to the interception of pulses narrower than the filter integration time as shown in Figure 2.14. Since full interception cannot be achieved, a receiver sensitivity degradation results from a combination of:

1. variable compression ratio loss
2. conservation of energy

Since the detection process is one of peak detection and not energy a sensitivity loss occurs. To have 100% POI requires that the signal duration must be greater or equal than $T_M + T$. For pulses narrower than this and which decreases towards zero the POI is given by the following equation:

$$POI = \frac{T}{T_M} = \frac{B}{B + BS} \quad (2.26)$$

$$\frac{1}{2} = 50\%$$

In other words pulse widths narrower than the filter integration time arriving at random would be intercepted by the receiver with a probability of 50 percent. A method of improving the POI to 100% is by interlacing a second LO scan between the adjacent scan period of the existing LO as illustrated in Figure 2.15. This method suggests that any pulse width can be intercepted and that in the worst case scenario the pulse would be split equally by adjacent integration period for reduced sensitivity of 4-5 dB [2,14].

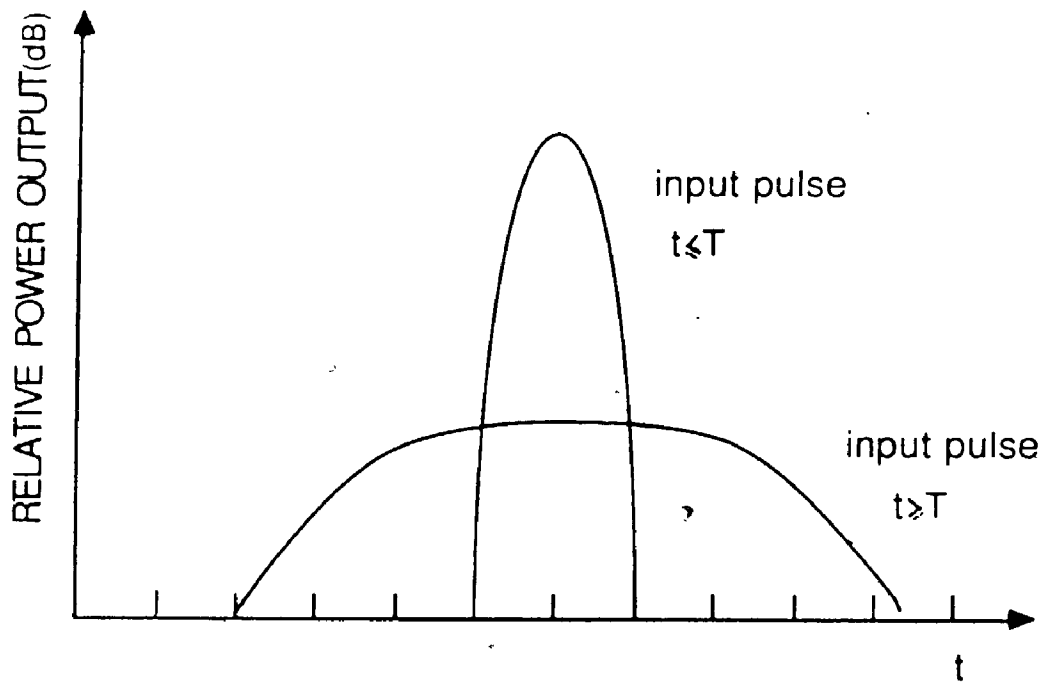


Figure 2.14: Degradation loss for pulses narrower than filter integration time.

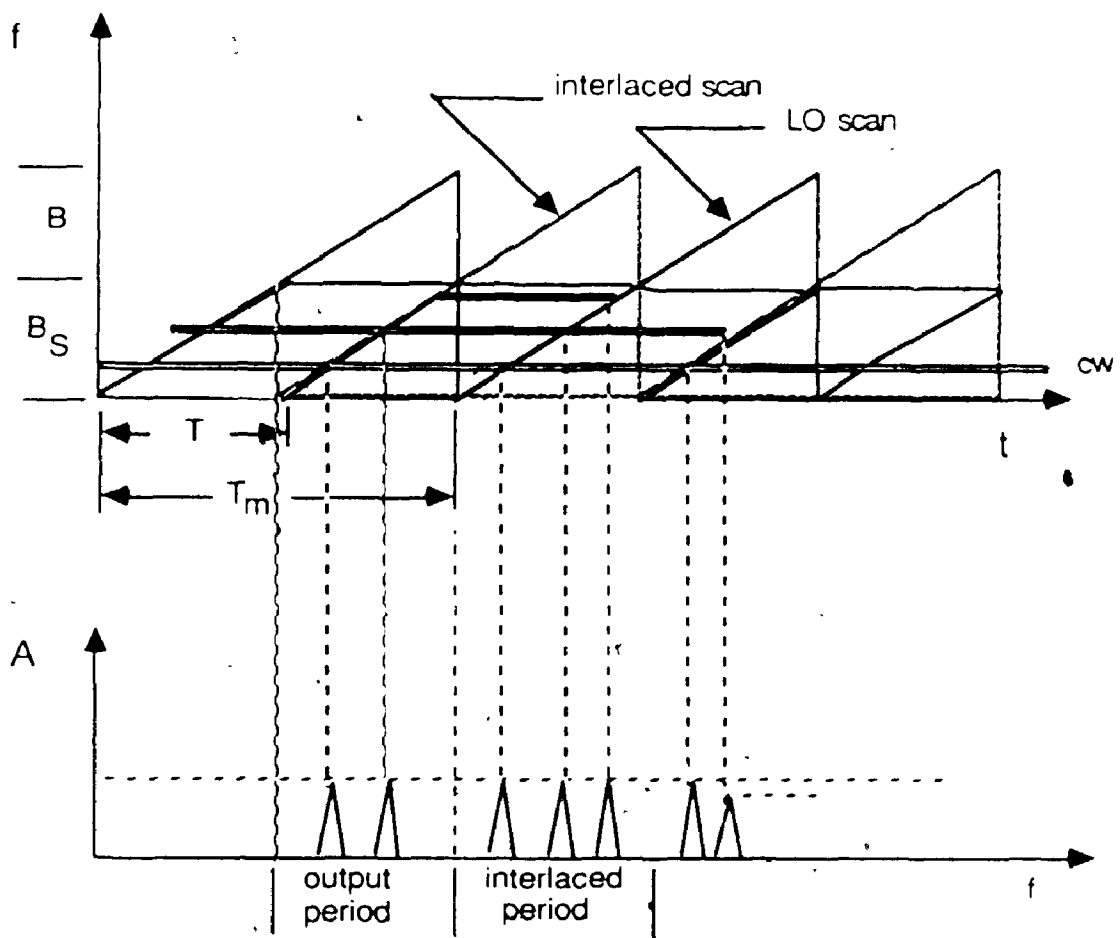


Figure 2.15: Improvement of POI with interlaced scan.

In summary, the POI is a measure of the percentage of pulses which will be intercepted by a receiver. This measurement depends greatly on the duration of incoming pulses and where they are located within the filter bandwidth with respect to the LO scan. The shorter the pulse the lower is the POI. A 100% POI will occur only if the pulse width is greater or equal than the LO scan period and filter integration time ($T_M + T$). Pulse duration shorter than this will result in reduced receiver sensitivity and resolution. Interlaced scanning can also improve the POI to 100%.

Thus far, a general description of the microscan receiver has been presented along with a simplified discussion on how signals are intercepted and passed through the receiver. The following section is a more analytical description on the operation of the receiver.

2.3.5 The M-C Receiver Configuration

The M-C (multiply-convolve) receiver configuration is suitable only for signal processing schemes which require the amplitude information and not the phase. It is a simplification of the M-C-M (multiply-convolve-multiply) arrangement. The last multiplier in the M-C-M scheme strictly provides the phase information of the input signal and therefore is often not required for spectral analysis. There are two generic forms for the M-C configuration. They are:

1. $M(s)-C(l)$
2. $M(l)-C(s)$

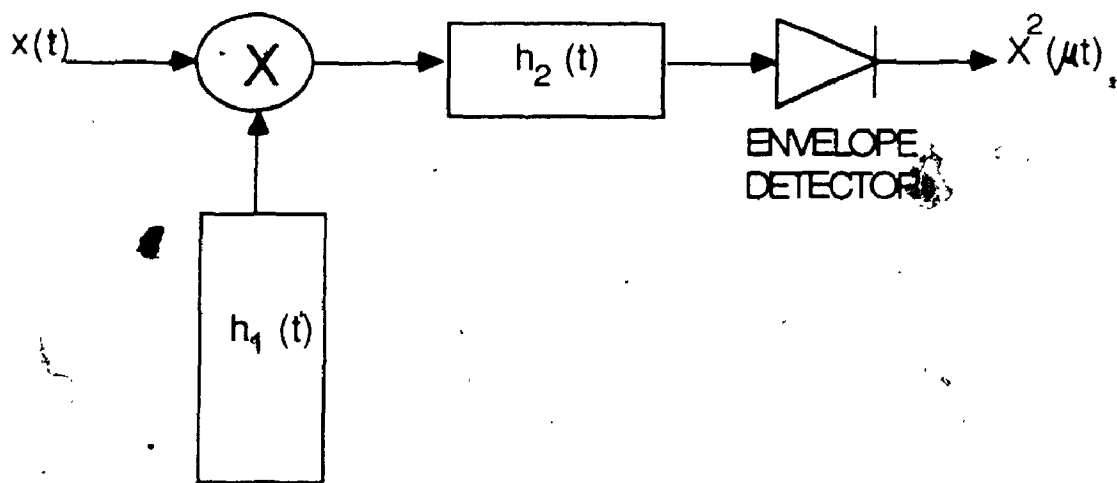
The notation used for (l) and (s) denotes a long duration chirp and a short duration chirp respectively. The $M(l)-C(s)$ scheme is also known

as the "sliding" transform processor which can be used only in the power spectrum analysis of signals whose spectral components remain unchanged for the duration of the multiplier interval T_M as shown in Figure 2.16 [10]. Further theoretical analysis will be focused on the $M(1)-C(s)$ scheme since a receiver with this configuration is employed in this thesis. The analysis is based on a similar analysis performed by Bridle [19] for the $M(s)-C(1)$ spectrum analyser. The theoretical aspects describing this bandpass system will be based on complex signal analysis. This is a consequence of the assumed linearity of the system. The advantage of using this approach is that the carrier can be removed from the information signal and that an equivalent baseband model can be established to simplify the analysis. A basic review of complex signal analysis is presented in Bridle [19].

The $M(1)-C(s)$ is implemented via surface acoustic wave (SAW) chirp filters. The chirp waveform used for signal multiplication is assumed to be generated by impulsing a physically realizable SAW chirp filter. The impulse response of the premultiplier chirp $C_1(t)$ and the convolution filter $C_2(t)$ are given by the real function:

$$\begin{aligned}
 C_1(t) &= \text{Re} [w_1(t) \cdot \exp(-j\pi\mu t^2) \cdot \exp(j2\pi f_1 t)] \\
 &= w_1(t) \cos(2\pi f_1 t - \pi\mu t^2), \quad i=1,2 \quad (2.27)
 \end{aligned}$$

where $w_1(t)$ is an arbitrary weighting function to be determined. Frequency f_1 represents the carrier frequency of the bandpass signal $C_1(t)$. The factor μ is the rate of change of the instantaneous angular frequency and corresponds to the dispersive slope of the chirp filter and is expressed in Hz/s^2 .



$$h_1(t) = \exp(-j\pi\mu t^2)$$

$$h_2(t) = \exp(j\pi\mu t^2)$$

Figure 2.16: The M(1)-C(s) microscan receiver

Complete system characterization can be achieved by removing the carrier and use only complex envelope analysis. The complex envelope signal $s(t)$ at the output of the convolution filter is written as:

$$\hat{s}(t) = [\hat{x}(t) \cdot \hat{C}_1(t)] \cdot \hat{C}_2(t) \quad (2.28)$$

where

$$\begin{aligned} \hat{C}_1(t) &= w_1(t) \exp(-j\pi ut^2) \\ \hat{C}_2(t) &= w_2(t) \exp(j\pi ut^2) \end{aligned} \quad (2.29)$$

are the complex envelope of the real-analog impulse response of the SAW chirp filters. The set of window functions may be given by:

$$\begin{aligned} w_1(t) &= \text{rect} \frac{[t-T_1/2]}{T_1} \\ w_2(t) &= \text{rect} \frac{[t-T_2/2]}{T_2} \end{aligned} \quad (2.30)$$

where the rect function is defined as:

$$\text{rect}(t) = \begin{cases} 1 & t \leq 1/2 \\ 0 & \text{otherwise} \end{cases} \quad (2.31)$$

By expanding the convolution sign in its integral form gives:

$$s(t) = \int_{-\infty}^{+\infty} x(\tau) w_2(t-\tau) \exp(-j\pi u\tau^2) \exp(j\pi u(t-\tau)^2) dt \quad (2.32)$$

$$\text{for } T_2 \leq t \leq T_1$$

where T_1 and T_2 are the multiplier interval and dispersive delay of the SAW filters respectively.

Using Bluestein's relation [19]:

$$-2t\tau + t^2 = (t-\tau)^2 - \tau^2 \quad (2.31)$$

the expression in equation (2.32) can be written as:

$$\begin{aligned} \hat{s}(t) &= \int_{-\infty}^{+\infty} \tilde{X}(\tau) w_2(t-\tau) \exp(-j2\pi\tau t) \exp(j\pi\tau t^2) d\tau, \\ &= \exp(j\pi\tau t^2) F(x(\tau) \cdot w_2(t-\tau)) \end{aligned} \quad (2.33)$$

$F(\bullet)$ denotes the Fourier transform of the function $x(\tau) \cdot w_2(t-\tau)$. An interesting point to note here is that the gating function $w_2(t-\tau)$ varies with time and thus "slides" across $x(\tau)$ embracing different sections of this function. This results in a Fourier transform which also varies with time. Now, by applying the well known property of the Fourier transform which states that multiplication in the time domain results in convolution in the frequency domain equation (2.33) can be rewritten as:

$$\hat{s}(t) = \exp(j\pi\tau t^2) [F(x(\tau)) * F(w_2(t-\tau))] \quad (2.34)$$

With subsequent manipulation, the complex envelope of the output signal can be written in its final form as:

$$\begin{aligned} \hat{s}(t) &= \exp(j\pi\tau t^2) \{X(\omega t) * \exp(-j2\pi\tau t^2) T_2 \text{sinc}(\omega t \frac{T_2}{2})\} \\ &= \exp(j\pi\tau t^2) \cdot X_{SW}(\omega t) \quad \text{for } T_2 \leq t \leq T_1 \end{aligned} \quad (2.36)$$

where, for simplicity, $X_{SW}(\omega t)$ denotes the sliding weighted Fourier transform of $x(t)$. It is possible to remove the phase modulation by passing the signal through an envelope detector. This in turn will result in the amplitude of the Fourier transform being squared to give the power spectrum of the input signal. When analyzing a signal going through an envelope detector it is more convenient to use the real signal as opposed to the complex envelope. Assuming a real signal $s(t)$ has a carrier frequency f_c , then:

$$\begin{aligned}
s(t) &= \text{Re} [\hat{s}(t) \exp(j2\pi f_c t)] \\
&= \text{Re} [A(t) \exp(j2\pi f_c t + \theta(t))] \\
&= A(t) \cos(2\pi f_c t + \theta(t)) \quad \text{for } T_2 \leq t \leq T_1 \quad (2.37)
\end{aligned}$$

From equations (2.36) and (2.37) the magnitude and phase components of $s(t)$ can be determined and thus are given as:

$$\begin{aligned}
A(t) &= |X_{SW}(\mu t)| \\
\theta(t) &= \phi X_{SW}(\mu t) + \pi \mu t^2 \quad (2.38)
\end{aligned}$$

The output of the envelope detector is given by:

$$Y(t) = S^2(t) \quad (2.39)$$

Substitution of equation (2.37) into equation (2.39) gives:

$$\begin{aligned}
Y(t) &= A^2(t) \left(\frac{1 + \cos 2[2\pi f_c t + \theta(t)]}{2} \right) \\
&= |X_{SW}(\mu t)|^2 \left(\frac{1 + \cos[4\pi f_c t + 2\theta(t)]}{2} \right) \quad \text{for } T_2 \leq t \leq T_1 \quad (2.40)
\end{aligned}$$

By passing this signal through a low pass filter with cut-off frequency below f_c it is possible to separate the weighted amplitude spectra from the carrier frequency. The output of the filtering gives:

$$Y'(t) = \frac{|X_{SW}(\mu t)|^2}{2} \quad (2.41)$$

This expression turns out to be the weighted amplitude spectra of the input signal.

Due to harmonic windowing, the compressed pulse shape contains a $\frac{\sin \pi Bt}{\pi Bt}$ term which produces sidelobes at 13 dB below the main lobe. The sidelobes of one signal tend to mask the peak of other close-in signals which are relatively weaker by 13 dB. These time sidelobes can be reduced by choosing a proper windowing function for $w_2(t)$ as shown in Figure 2.17. The effect of weighting the received signal to suppress the sidelobes also widens the mainlobe which, in turn, decreases the frequency accuracy measurement in the time domain. Therefore, a careful tradeoff must be made when choosing a proper windowing function. The Kaiser-Bessel weighting filter as well as the Hamming filter have been preferred choices. An excellent overview on weighting filters is given in a paper written by Harris [26].

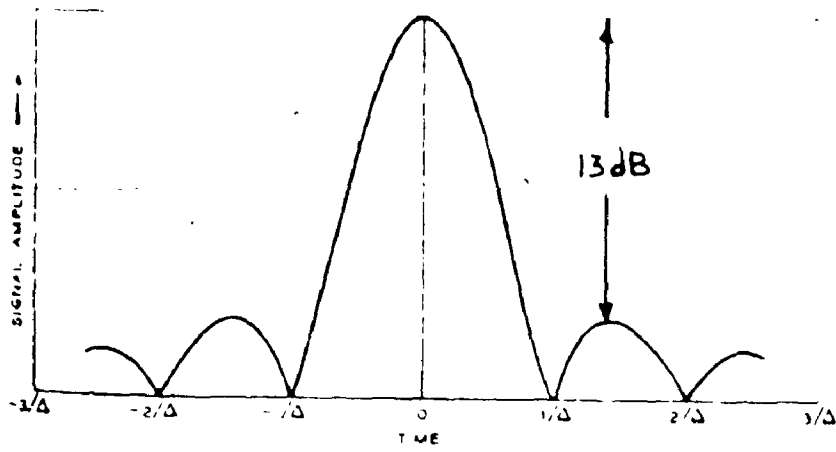
In summary, the mathematical groundwork necessary for describing how a compressive receiver performs spectral analysis has been established with an emphasis placed on complex envelope signal analysis. The next topic is an overview of the key components which make-up a compressive receiver.

2.3.6 SAW Receiver Components

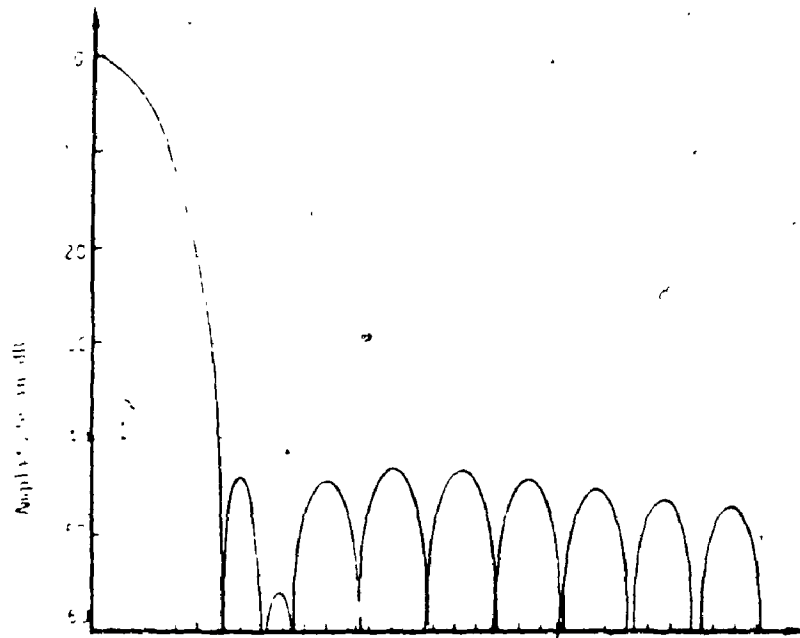
A compressive receiver implements the chirp transform, hence spectral analysis, via three important components. They are:

1. the SAW compression filter
2. the sweeping local oscillator, and
3. the logarithmic amplifier and detector circuitry

A brief overview on each of the three components is presented to provide more insight on some of the design considerations involved.



(a)



(b)

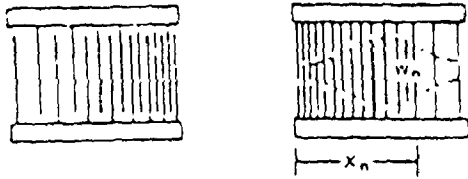
Figure 2.17: Outputs from PCF (a) without a weighting filter and (b) with a weighting filter.

2.3.6.1 SAW Compression Filter

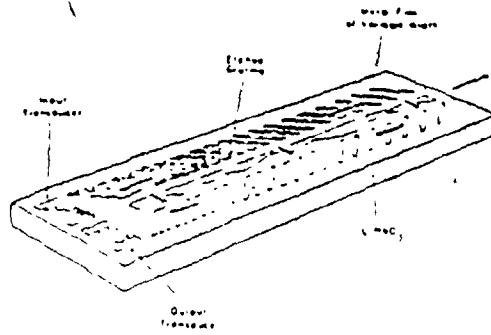
There are several techniques capable of creating a dispersive delay using a surface acoustic wave (SAW) device. These include: (1) the interdigital transducer (IDT), (2) the reflective array compressor (RAC), (3) the reflective dot array (RDA), (4) the slanted reflective array (SRAC), and (5) the in-line reflective array (ILRA) which are illustrated in Figure 2.18. Of the various device type listed only the IDT and the RAC are presently commercially available.

The interdigital transducer (IDT) is by far the simplest structure but has the lowest performance in terms of time-bandwidth product (TBP). It consists of metal electrodes spaced one-half of the acoustic wavelength of the signal propagating along the surface of a piezoelectric substrate, as shown in Figure 2.19. The distance between the metallic fingers determine which frequency components will interact. Low frequency components interact with widely spaced electrodes while high frequency components interact with closely spaced electrodes. A dispersive delay is incorporated in a SAW device by varying the spacings between the electrodes. The impulse response of the filter can be shaped through apodization of the electrodes for better sidelobe suppression [18,19].

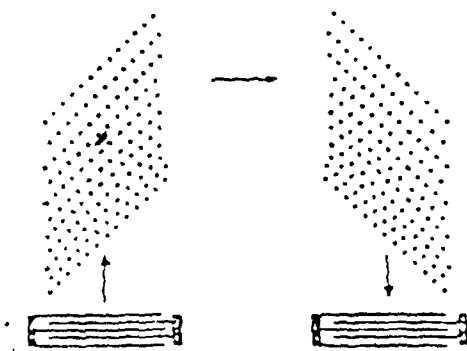
The reflective array compressor (RAC) is the most complex of the SAW compression filter technologies available, but has the highest performance in terms of TBP. It consists of shallow grooves etched in a substrate. The different frequency components in the incident wave reflect where the groove spacings are equal to the corresponding acoustic wavelength. By varying the groove spacings quadratically, it



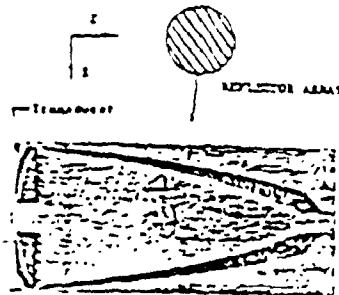
A dispersive IDT SAW filter with apodization



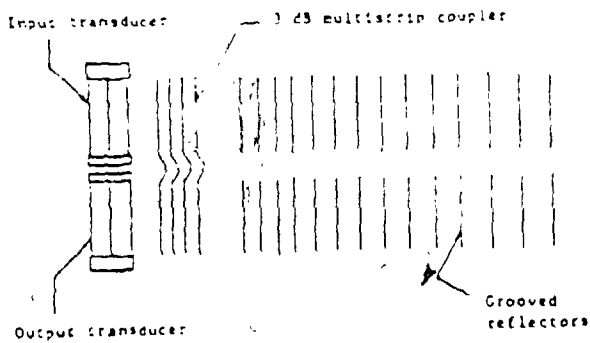
A 3D illustrating the metal phase compensating plate



A reflective dot array (RDA) dispersive filter

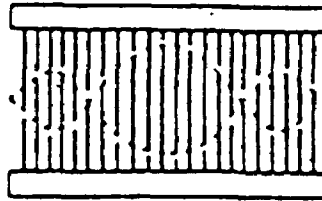
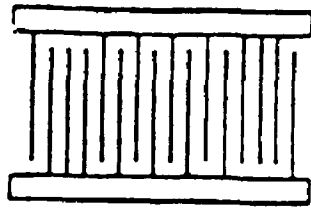


Slanted reflective array correlator (SRAC)

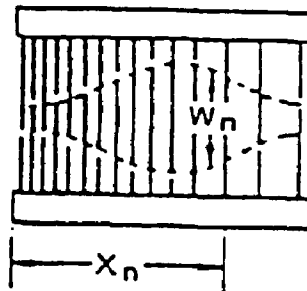
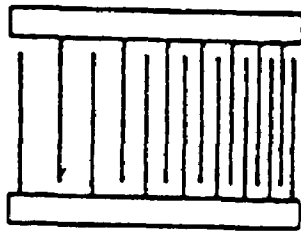


The 10-line reflective array correlator (ILRAC)

Figure 2.18: SAW filter technologies (copied from [18]).



(a)



(b)

Figure 2.19: IDT SAW filter (copied from [19]).
(a) A typical interdigital transducer (IDT).
(b) A dispersive IDT filter with apodization.

is possible to create the require dispersion delay as shown in Figure 2.20. Amplitude weighting for better sidelobe suppression can be achieved by varying the depth of the grooves.

A critical requirement in most SAW filters is to have an accurate phase and low amplitude ripple across the entire bandwidth, if better sidelobe suppression and, hence, better detection speed and accuracy are to be achieved. Figure 2.21 illustrates typical phase and amplitude ripples found in SAW filters.

2.3.6.2 LO Chirp Waveform

There are two methods of generating an LO chirp waveform:

1. fast turning of a voltage controlled oscillator (VCO) or
2. impulsing a SAW compression filter

The first method, which is becoming unpopular in compressive receiver design, consists of rapidly tuning a voltage controlled oscillator (VCO) to produce an FM signal. The biggest problem facing this technique is that the frequency versus tuning voltage curve of most commercial VCOs are not perfectly linear. This results in a poor scan linearity which must be compensated for, with some type of linearizing circuit. The second approach consists of impulsing a physically realizable SAW compression filter. Usually the filter used to generate the scan is a duplicate of the one used for pulse compression. Because the LO must cover a bandwidth of $B_s + B$, two RAC filters with parameters (T, B) are cascaded together to give $(2T, B)$ which can be further increased to $(2T, 2B)$ by using a X2 multiplier as shown in Figure 2.22.

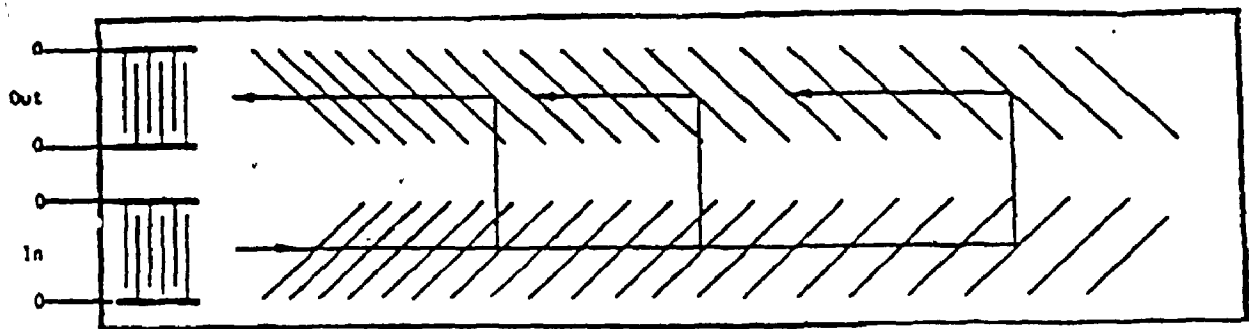


Figure 2.20: The reflective array compressor (RAC)
(copied from [19]).

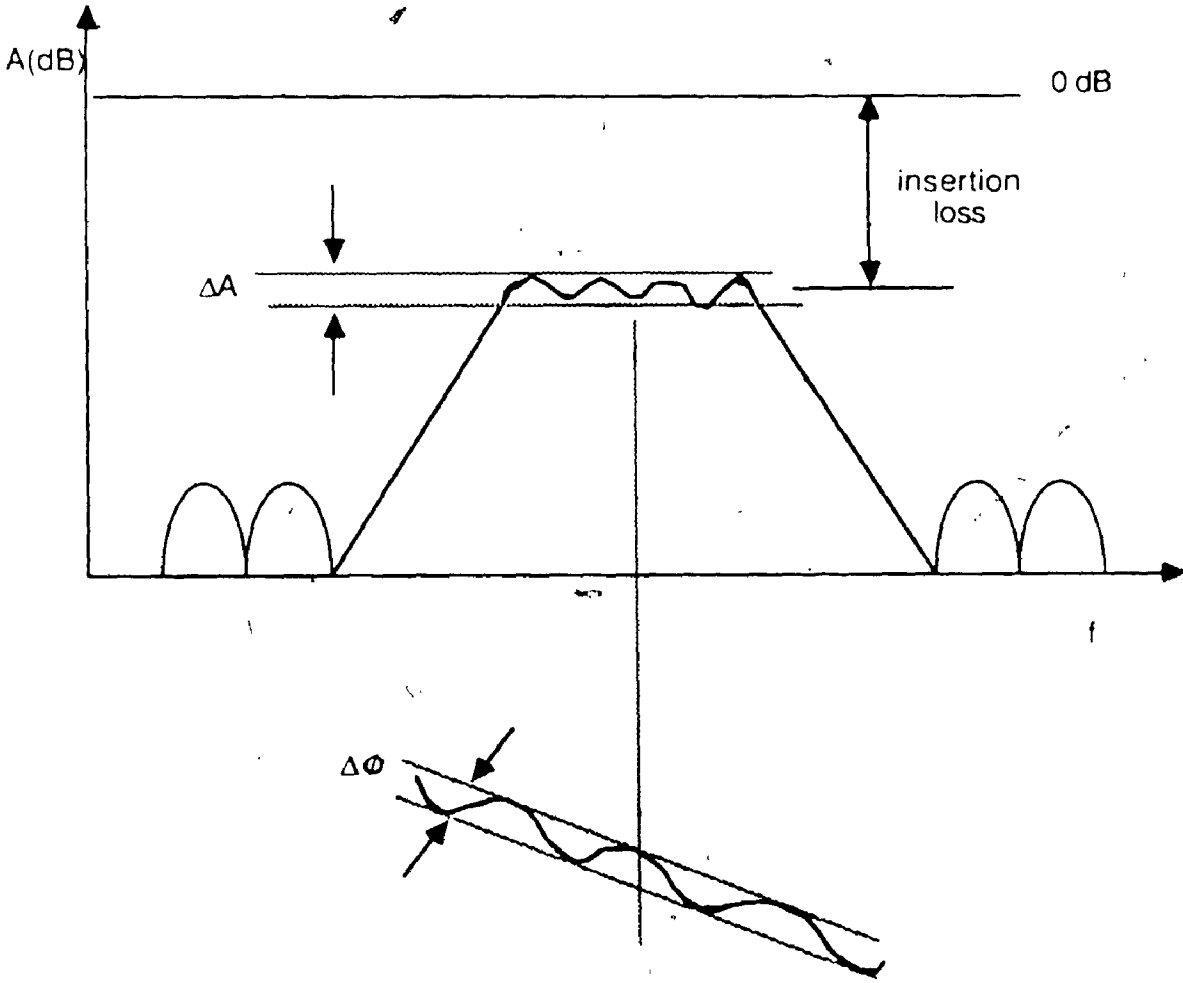


Figure 2.21: Amplitude and phase ripples in SAW filters.

Another approach to produce the sweeping frequency is to generate the long chirp waveform by interleaving two RAC filters with parameters (T,B). The RACs are shifted in neighboring frequency bands and then summed together to give a total bandwidth of 2B in time of 2T as illustrated in Figure 2.23. This method is feasible but tends to be rather complex as well as power consuming.

2.3.6.3 Logarithmic Amplifier and Video Detector

A method for measuring the input signal strength accurately is to use a log amplifier. In a log amplifier the output is proportional to the logarithm of the input power:

$$V = m \log P_i \quad (2.42)$$

where m is a constant and P_i is the input power. The log amplifier enables a video detector, which usually has a small dynamic range, to process the signals coming out of a receiver with a wide dynamic range (≈ 60 dB). Amplitude measurement of the output pulse is important because time measurement and, thus, frequency information is obtained from the pulse when it emerges from the compression filter.

A detection circuit consisting of comparators following the log amplifier is used to accurately measure the output time [2]. The comparators are used to locate the peak of the signal. One comparator is usually not sufficient to provide accurate information. If the output pulse amplitude is high the base of the pulse is wide and therefore time resolution is lower as shown in Figure 2.24. By setting an array of thresholds and using a logic circuit to detect the highest

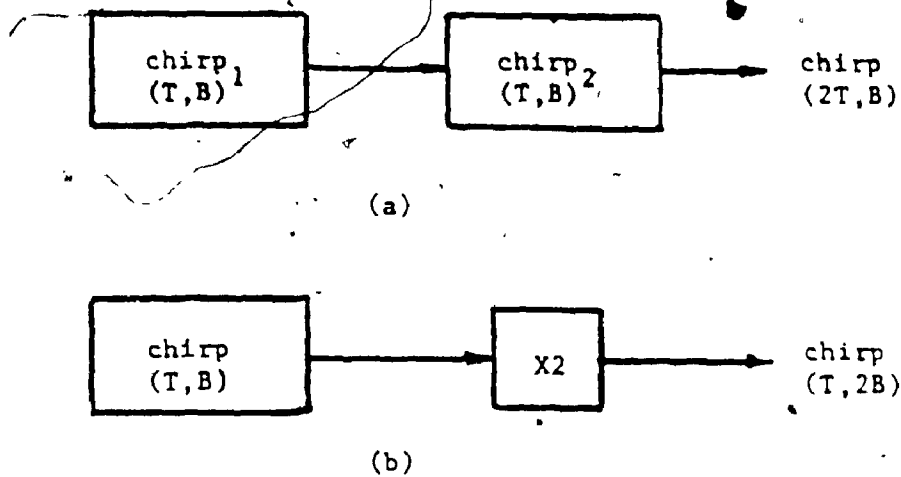
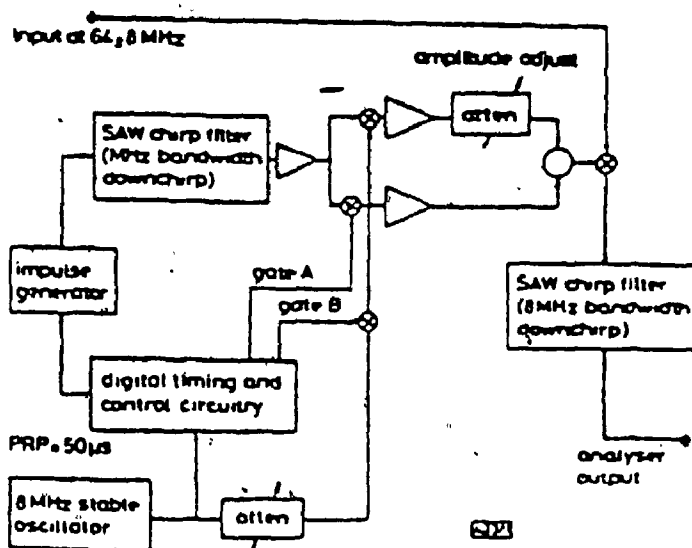


Figure 2.22: Methods of increasing the TBP of chirp filters.
 (a) Cascaded filters for increased integration time.
 (b) X2 multiplication for increased bandwidth (copied from [19]).



Schematic diagram for SAW spectrum analyzer employing coherent chirp multiplier waveform which sweeps from 44 MHz to 20 MHz in 150 µs

Figure 2.23: Interleaving chirp signals in neighbouring frequency bands for increased chirp TBP (copied from [19]).

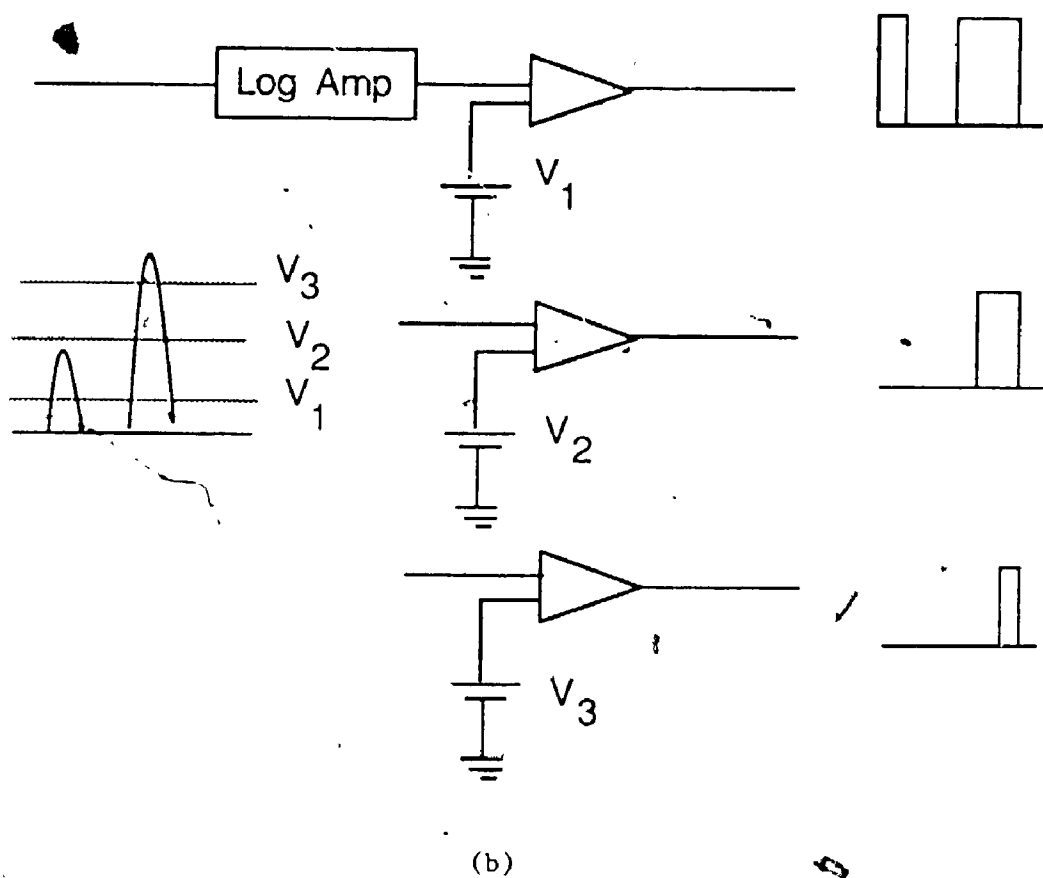
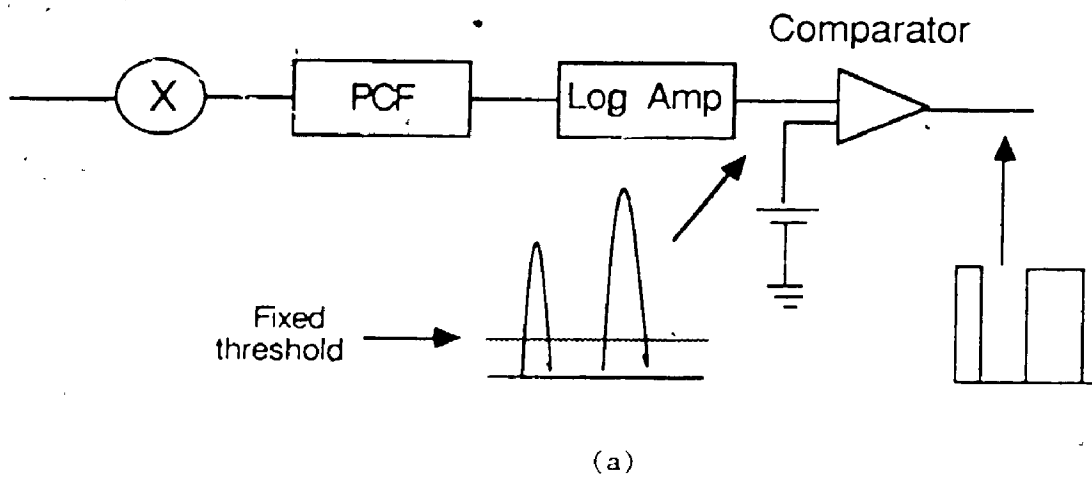


Figure 2.24: Pulse detection circuit (a) with a single comparator and (b) with an array of comparators.

threshold to be crossed provides better accuracy on the position of the pulse. Thus, input signal frequency can be measured with more precision.

It is usually required that log amplifiers have very fast response time in order to cope with short pulses at the output of the compressive line. For example, if the pulses coming out of the dispersive filter are 10 ns in width, then the log amplifier must have a video bandwidth of 100 MHz. Sometimes, very short pulses may cause a severe design problem on the log amplifiers.

2.3.7 Summary

In summary, we first discussed some important concepts regarding the design of receivers. Quantitative measures were established to determine the sensitivity, dynamic range and POI of acquisition systems. Secondly, we have introduced the microscan receiver. This intercept receiver has proven to be a valuable processing tool. It demonstrates superior characteristics over the laboratory type spectrum analyser. Its higher processing speed, reduced complexity, lower power consumption, and lower cost makes it a preferable choice over its counterpart. Some of the major features of the microscan receiver are:

1. The output signal represents the continuous Fourier transform of the input signal where the output time represents the input frequency.
2. The input signals are both time and bandwidth limited, producing a weighted Fourier transform output signal.

3. The system operates at 100% POI for signals of duration greater than or equal to the LO scan period plus the filter integration time ($T_M + T$).
4. The $M(l)-C(s)$ can provide amplitude spectrum (i.e. no phase information) by omitting the last multiplier. By replacing it by an envelope detector a simple and economical power spectrum analyser is realized.
5. Chirp transforms are implemented via SAW chirp filters with large time-bandwidth products.

Chapter 3

A WIDEBAND MICROWAVE SURVEILLANCE SYSTEM

3.1 INTRODUCTION

The previous chapter explored the theory of the microscan receiver and examined basic design considerations which apply to receivers in general. The thesis can now focus on the application of these concepts to the practical design of a wideband surveillance system. A general description of the spectral analysis system and the environmental scenario are first presented in the next section. The subsequent section examines the subsystem level design. The microscan receiver, the downconversion stage, and the controller are analyzed individually in order to meet the system requirements. Finally, the chapter concludes with a brief summary.

3.2 GENERAL SYSTEM DESCRIPTION AND ENVIRONMENTAL SCENARIO

Recently, unusual noise disturbances have been interfering with the bit error rate (BER) of a downlink satellite communication channel in the vicinity of Ottawa, Ontario. The disturbances are random, mostly narrowband, and tend to occur more often at certain times of the day. It has been reported that pulses as low as -126 dBm could interfere with the BER of 30 KHz channels spaced uniformly across the 3.2 to 4.2 GHz band. An attempt to characterize the frequency, the amplitude, and the time of the noise interference with a conventional laboratory type

spectrum analyzer was carried out unsuccessfully. The failure of this type of receiver in this particular application is attributed to the slow sweep rate of the local oscillator (which is limited to approximately B_{IF}^2 for a given resolution). This receiver must dwell for a relatively long time at each frequency in order to intercept a signal, thus resulting in a low probability of intercept on all incoming pulses. The demand for a frequency measurement system which exhibits high POI, high sensitivity, and good simultaneous signal handling capability has led to the design of a wideband microwave surveillance receiver. A simplified block diagram of the complete receiver system is shown in Figure 3.1. It is primarily divided into three sections: the front-end downconversion stage, the microscan receiver, and the controller.

The heart of the system is the microscan receiver. The model used is the AS-520 from ARGO System Inc., USA. It has an input bandwidth of 20 MHz centered at an IF of 160 MHz with a frequency resolution of 30 KHz. Its sweeping local oscillator can sweep at a rate of 0.1 MHz/ μ sec and therefore, can scan a bandwidth 250 times faster than an ordinary spectrum analyzer given the same resolution bandwidth. Consequently, the POI is improved by the same factor.

A front-end downconversion stage similar to that found in a superheterodyne receiver is placed in front of the AS-520 in order to extend its fine frequency measurement capability into the microwave region. A double-down conversion network consisting of mixers, amplifiers, and filters enable the microscan receiver to monitor an RF

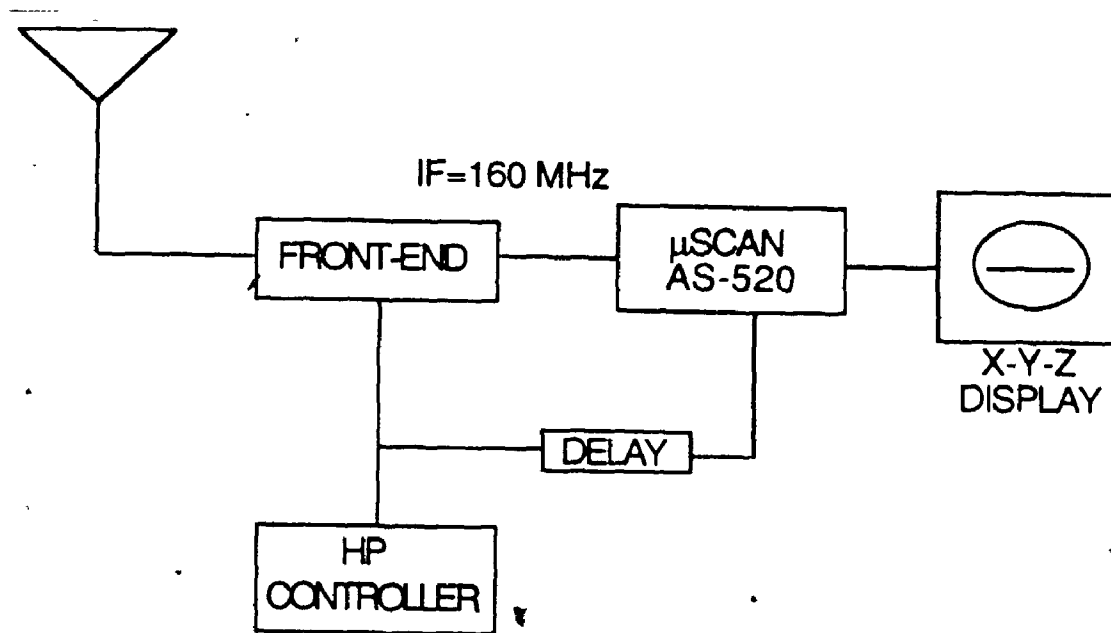


Figure 3.1: Block diagram of a wideband fast scanning receiver.

bandwidth between 3.2 to 4.2 GHz. The cascaded network offers simultaneously a low noise figure and a high dynamic range in order to meet the requirements for a high sensitivity receiving system. An HP8672A frequency synthesizer is used as a stepping local oscillator for the first stage downconversion process. The synthesizer generates a new tone of about 250 sec duration spaced 20 MHz from the previous one to cover the 1 GHz bandwidth. This effectively divides the RF spectrum into 20 MHz sub-bands for IF processing by the AS-520. A contiguous step scan across the 1 GHz bandwidth takes approximately 762 msec. This rather long duration is acceptable since the principle aim of the thesis is to demonstrate the performance of a wideband receiver.

A Hewlett-Packard microprocessor controller is used to automate the entire system. It serves to synchronize the AS-520 receiver to the front-end stepping receiver. The controller utilizes the HP-IB bus to command the frequency synthesizer to hop frequencies in predetermined steps. Once the hop is completed, it then sends a delayed time pulse to the external scan trigger of the AS-520 receiver. The hop cycle may be repeated as often as desired for continuous coverage.

The complete receiver system realization is shown in Figure 3.2. The following section will examine in greater detail the design and implementation of the receiving system.



Figure 3.2: Complete receiver system realization.

3.3 SUBSYSTEM LEVEL DESCRIPTION AND DESIGN CONSIDERATIONS

This section is concerned with the actual design and implementation of the three major subsystems discussed above. Each subsystem is important in the design of the receiver and must be given careful thought and consideration. The microscan receiver is described first due to its important role in signal processing. This will be subsequently followed by the downconversion stage and the controller.

3.3.1 Microscan Receiver

The microscan receiver is the key building block in the implementation of the wideband fast scanning receiver. The model used is the AS-520 from ARGO System Inc., USA. It employs a SAW dispersive filter to monitor a selectable band of 10 MHz or 20 MHz centered at an IF of 160 MHz with a frequency resolution of 30 KHz. Figures 3.3 and 3.4 are front and rear view photographs of the AS-520.

Figure 3.5 shows a simplified block diagram of the AS-520. It is configured with the M(1)-C(s) format discussed earlier in Chapter 2. The input signal $x(t)$ mixes with a sweeping local oscillator (SLO) and enters a SAW dispersive filter with a time lag linearly proportional to frequency. The overall bandwidth B of the SAW dispersive delay lines is 5 MHz and its integration time T is 50 μ sec. The AS-520 multiplexes two dispersive delay lines and two sweeping local oscillators to increase its overall IF input bandwidth to 10 MHz or 20 MHz centered at 160 MHz.

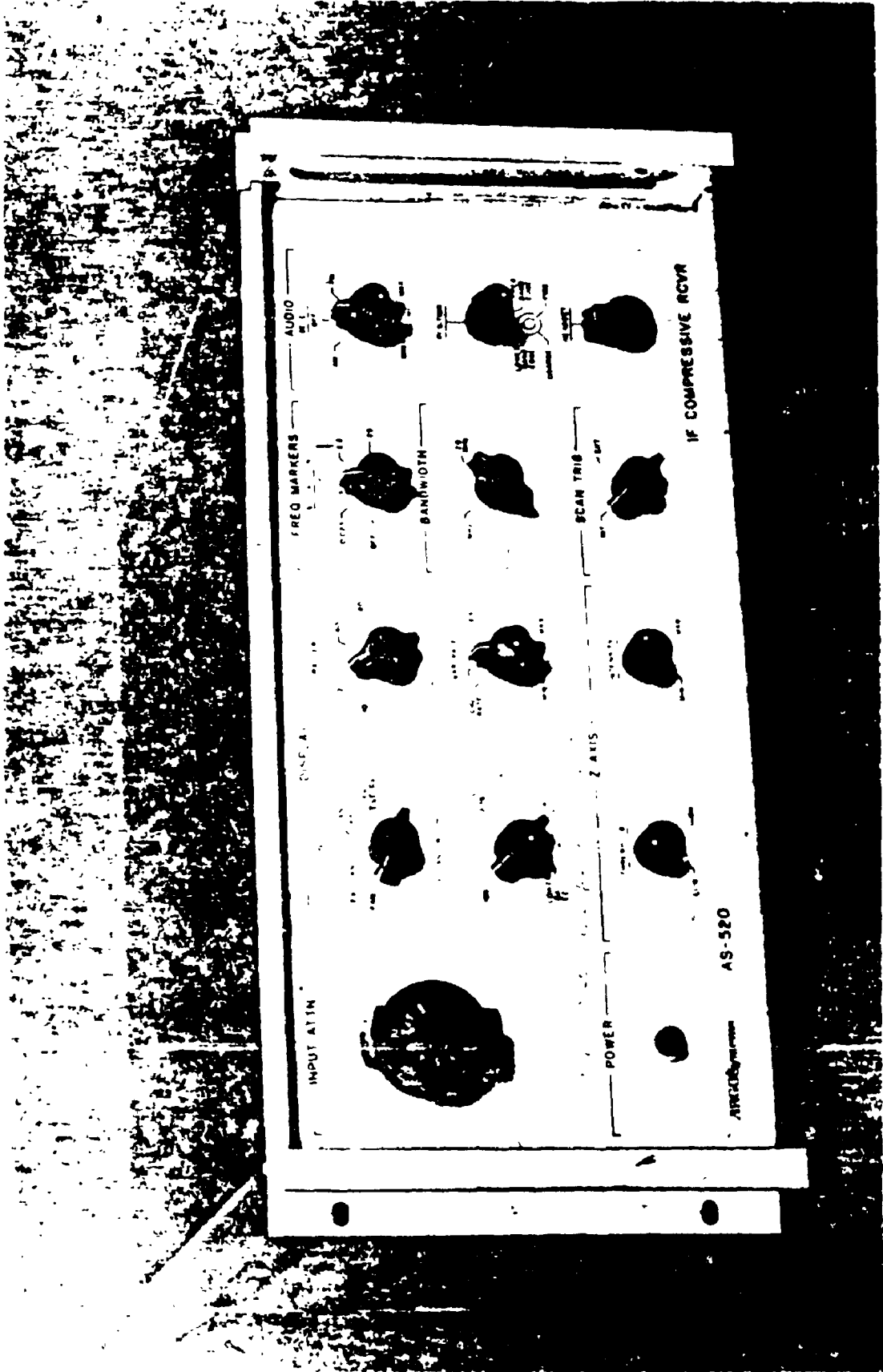


Figure 3.3: Front view photograph of AS-520 (copied from [33]).

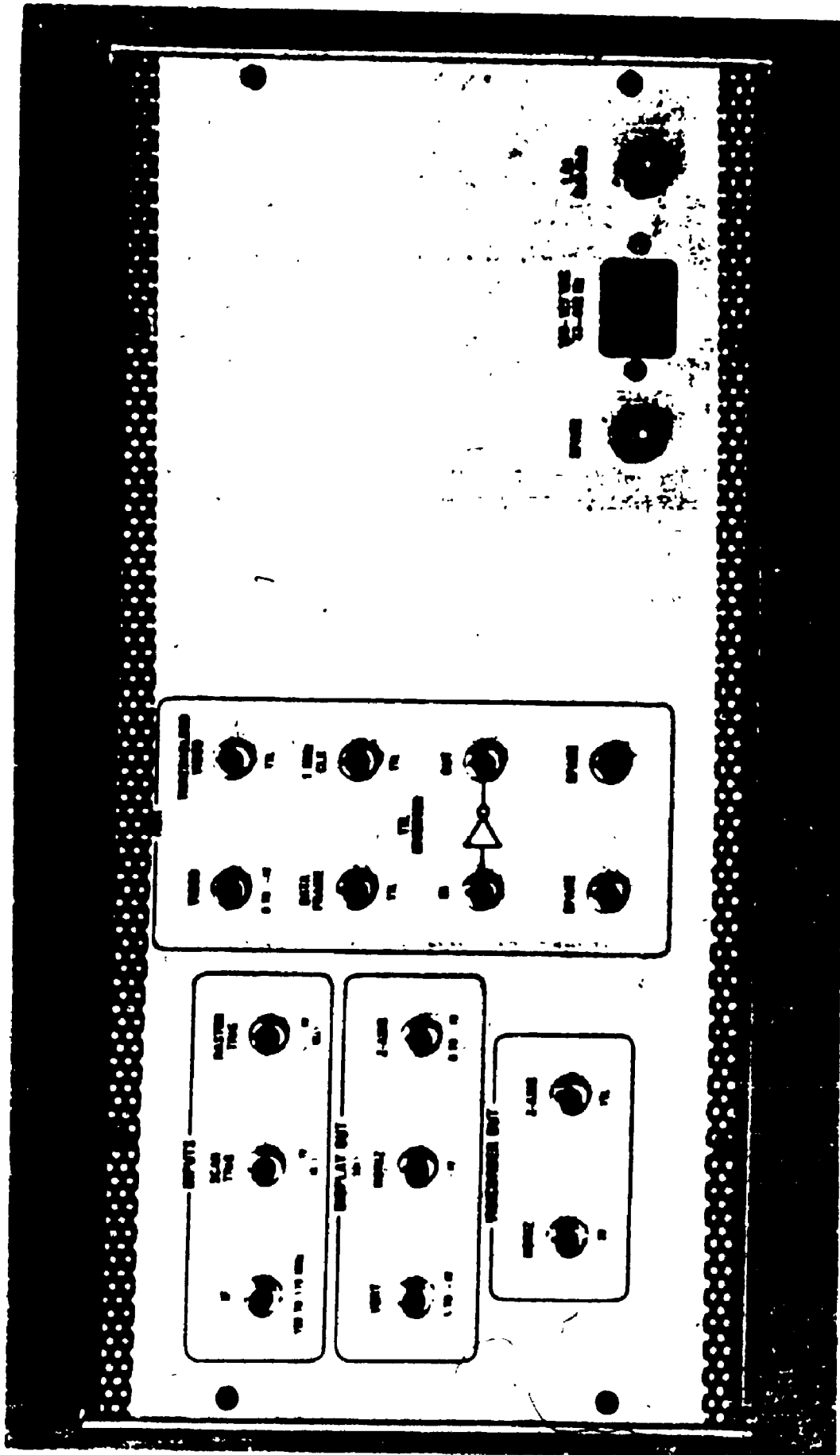


Figure 3.4: Rear view photograph of AS-520 (copied from [33]).

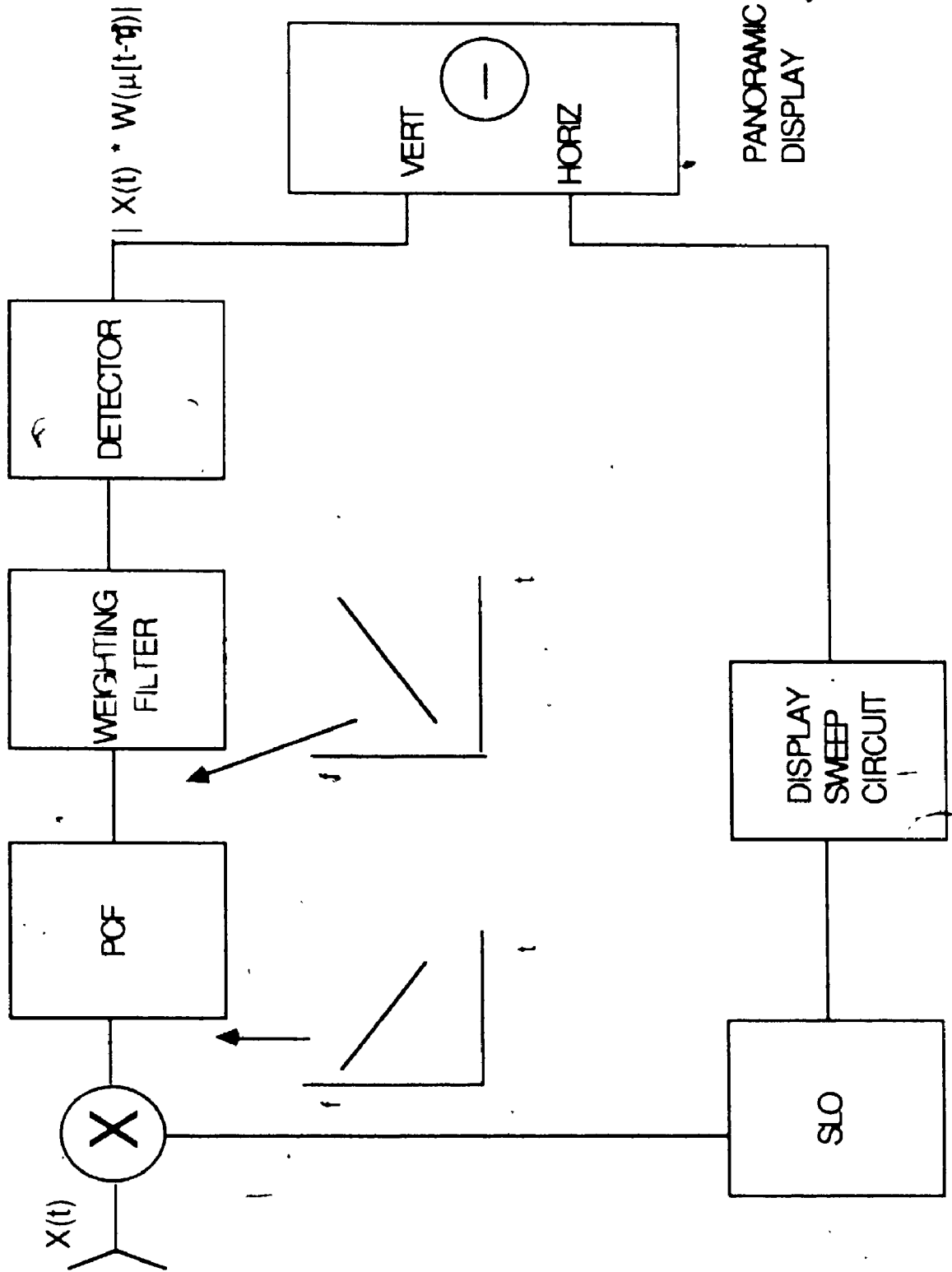


Figure 3.5: Simplified block diagram of AS-520 microscan receiver.

The output of the filter is a time compressed IF pulse with a sinc/x response. A weighting filter similar to the cosine squared window with $\mu = 2.0$ is used to taper the sidelobe levels. The compressed IF pulse is then detected in an envelope detector. The output of the envelope detector after filtering can be written as $|X(\mu t) * W(\mu [t - \tau])|$ which is equal to the sliding weighted Fourier transform of the input signal $x(t)$ where $X(\mu t)$ is the Fourier transform of $x(t)$, $W(\mu [t - \tau])$ is the transform of $w(t - \tau)$ and $*$ indicates a convolution operation. This receiver is an analog processor in which output time represents input frequency with a scaling factor. In particular, the output time t_{out} is related to the input frequency f_{in} by:

$$t_{\text{out}} - t_r = \frac{(f_{\text{in}} - f_r)}{\mu} \quad (3.1)$$

where μ is the chirp scale factor, t_r is the reference time, and f_r is a reference frequency. It is convenient to use offset time and frequency:

$$\begin{aligned} t &= t_{\text{out}} - t_r \\ f &= f_{\text{in}} - f_r \end{aligned} \quad (3.2)$$

as a result:

$$t = \frac{f}{\mu}$$

as stated previously by equation (2.25). For the ARGO system AS-520 analyzer:

$$\mu = \frac{B}{T} = \frac{5 \text{ MHz}}{50 \text{ sec}} = 0.1 \text{ MHz}/\mu \text{ sec}$$

Thus, the AS-520 microscan receiver provides an integration gain of TxB equal to 250. Therefore, as compared to an ordinary spectrum analyzer with the same resolution bandwidth the microscan receiver can scan the same bandwidth 250 times faster.

Because of its unusual design features, the following discussion describes in more detail the principles of operation of the AS-520 receiver. Furthermore, a complete table of specifications for the AS-520 microscan receiver can be found in Appendix A.

3.3.1.1 Principles of Operation

A block diagram of the IF assemblies of the Argos receiver is contained in Figure 3.6. The IF input passes through a directional coupler to the front panel 0-60 dB step attenuator and then, to a 24 MHz 1 dB bandwidth bandpass filter centered at 160 MHz. Frequency markers at 5 MHz spacings are switched into the IF path by a frequency marker generator when internal calibration is performed. The output of the filter is then split by a power divider and applied to A_3 and B_3 IF downconverters which result in chirp signals. These are then compressed by dispersive delay lines A_4 and B_4 at a center frequency of 30 MHz. The compressed IF pulses from the dispersive filters are amplified and applied to a RF switch. The switch selects which delay line will provide the compressed IF pulse for detection by a logarithmic amplifier. The output video is then processed digitally for display. The dispersive filters have bandwidths of only 5 MHz. Consequently, it is necessary to multiplex two compressive assemblies in order to obtain a 10 MHz or 20 MHz coverage.

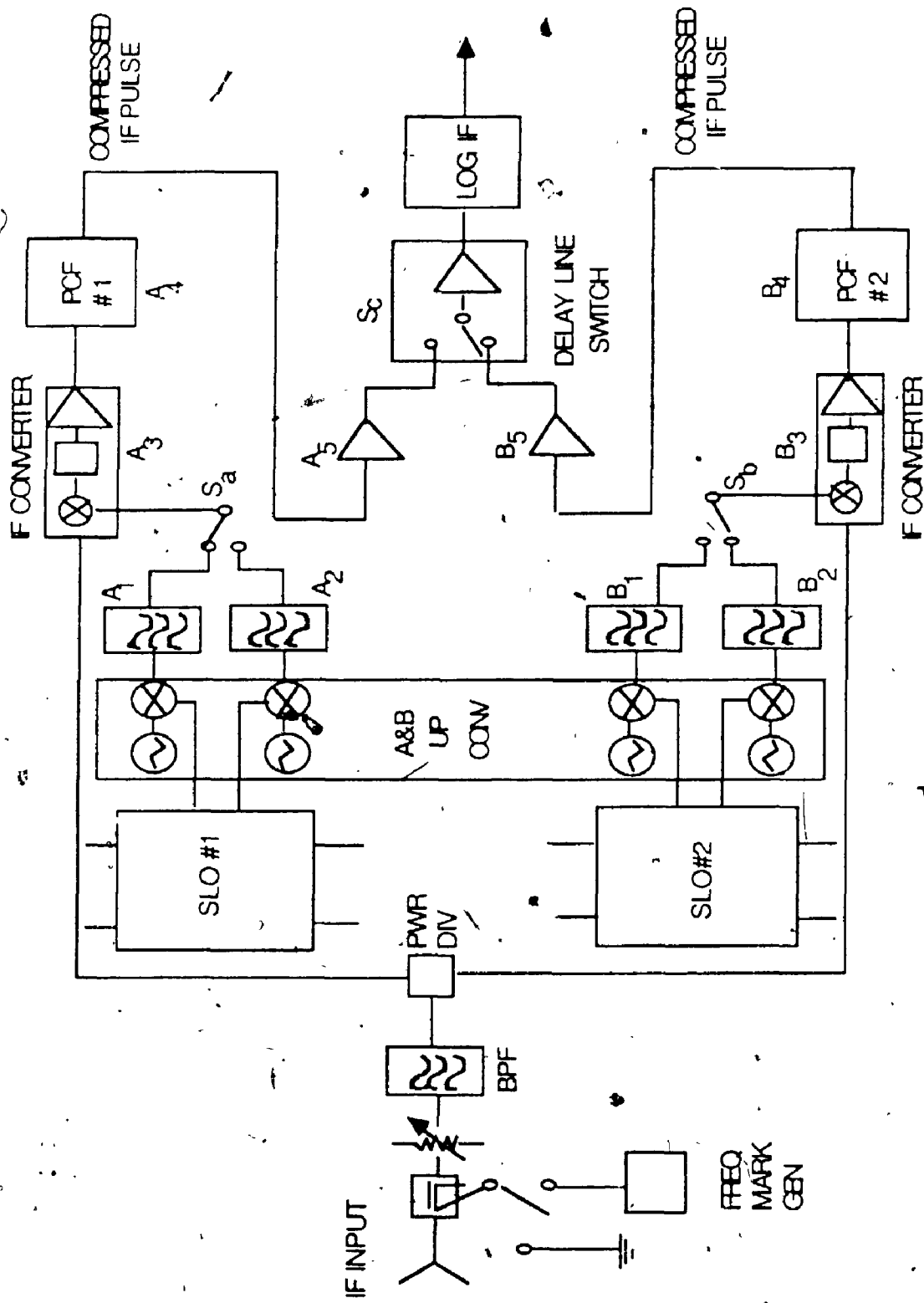


Figure 3.6: IF block diagram of AS-520 microscan receiver (copied from [33]).

Figure 3.7 shows a timing illustration of the 20 MHz multiplexing process. The SLOs are tuned by a ramp voltage and the output from each is a chirp from 5 MHz to 14 MHz in a time of 90 μ sec. This slope matches that of the dispersive filter slope of 5 MHz per 50 μ sec. To begin, the 5 MHz to 14 MHz chirp from SLO #2 is upconverted by assembly B and filter B₂ to a chirp starting at 202.5 MHz and stopping at 193.5 MHz. After conversion by assembly A and filter A₂, SLO #1 begins to sweep 50 μ sec later with a chirp starting at 197.5 MHz and finishing at 188.5 MHz. SLO #2 returns 50 μ sec after the start of SLO #1 to chirp from 192.5 MHz down to 183.5 MHz. Finally, SLO #1 completes the process 50 μ sec past the start of SLO #2 with a chirp starting at 187.5 MHz and ending at 178.5 MHz.

Switch S_A connects BPF A₁ and A₂ to the A₃ frequency converter while switch S_B connects BPF B₁ and B₂ to the B₃ frequency converter. At a time of 50 μ sec past the start of SLO #2, the compressed IF pulse (for a band edge signal of 170 MHz) is present at the S_C switch. A signal at 165 MHz would be present 50 μ sec later and so on. Switch S_C allows 5 MHz band from 170 MHz to 150 MHz to be detected successively by a logarithmic amplifier. The complete 20 MHz band is obtained by multiplexing four 5 MHz bands.

Due to high insertion loss in the SAW dispersive filters, a series of amplifiers in the RF, IF, and video paths are used to restore the signal level to approximately 0 dBm for a -20 dBm post-attenuator signal into the AS-520. The 0 dBm level is the rated input level for a maximum output video signal from the logarithmic amplifier. The transfer curve of the log amplifier of voltage out versus power input in dBm is linear to ± 1 dB from 0 dBm to -70 dBm.

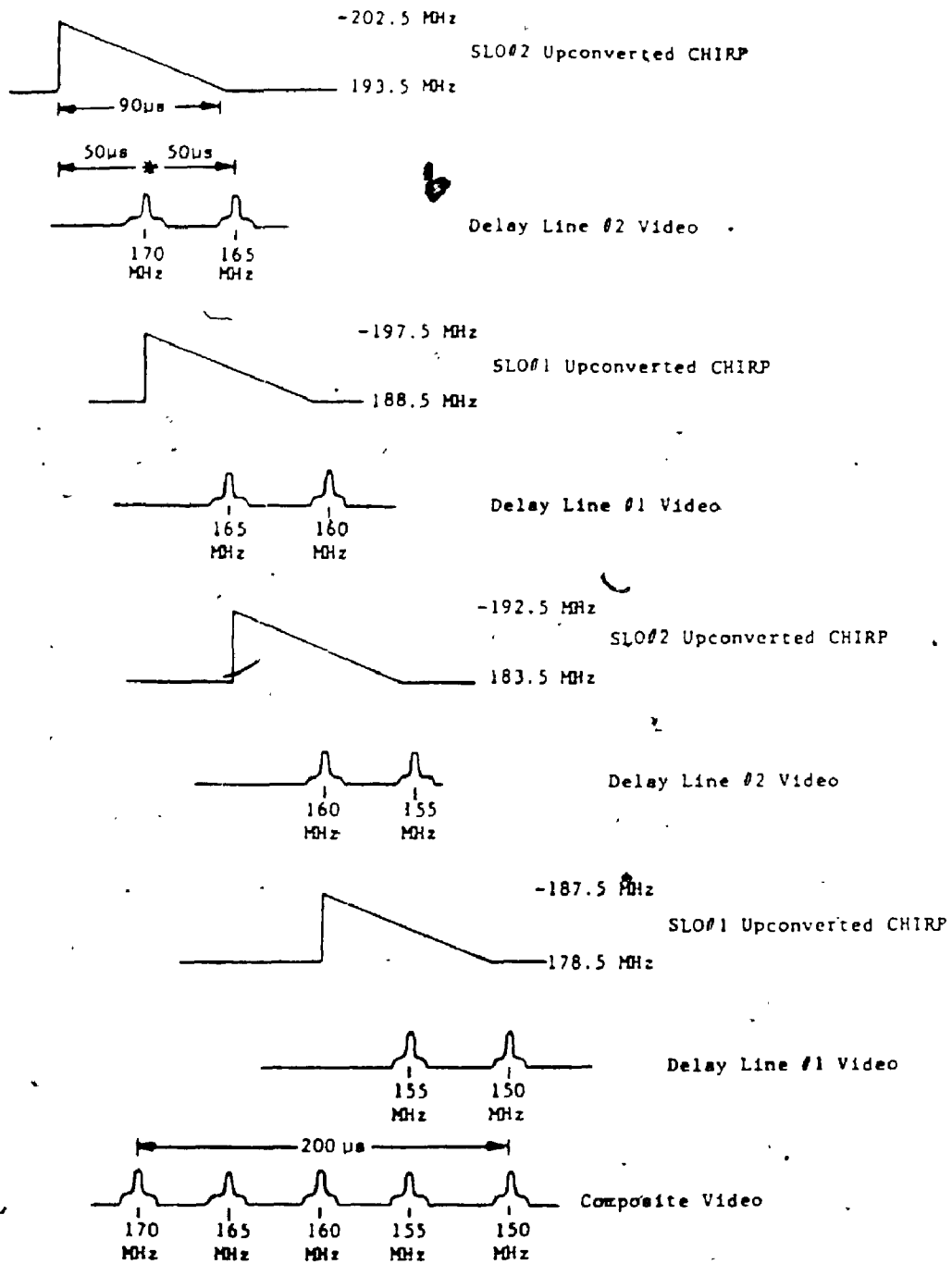


Figure 3.7: Timing illustration of 20 MHz scan with CW signals at 170, 165, 160, 155 and 150 MHz (copied from [33]).

3.3.1.2 Sweeping Local Oscillator (SLO)

The SLOs utilized in the AS-520 are very different from the more common SLO configuration listed in Chapter 2, in that they consist of capacitor coupled astable multivibrators which use constant current sources. Control voltages from logic circuits are used to control the amount of current provided by the current sources. The SLO frequency range is 5 MHz to 14 MHz.

3.3.1.3 Timing

A control circuitry card generates the primary timing signals for the AS-520. Figure 3.8 illustrates the internal timing sequence for some of the control signals which trigger the SLO's, bandswitches, delay line switches, generator display gates, and sweeps for the 20 MHz operation mode. The AS-520 may also be triggered externally with a pulse of amplitude greater than +1 volt and width greater than 1 μ sec. The maximum external trigger rates are equal to the internal trigger rates. External triggering will be used as a means for synchronizing the AS-520 to a front-end stepping receiver. This will be discussed further in the section on the downconversion stage.

3.3.1.4 Dynamic Range

The AS-520 has a linear dynamic range of 70 dB. The noise floor is at -90 dBm and the 1 dB compression point is at -20 dBm post-attenuation. The time sidelobes are 30 to 35 dB below the peak response

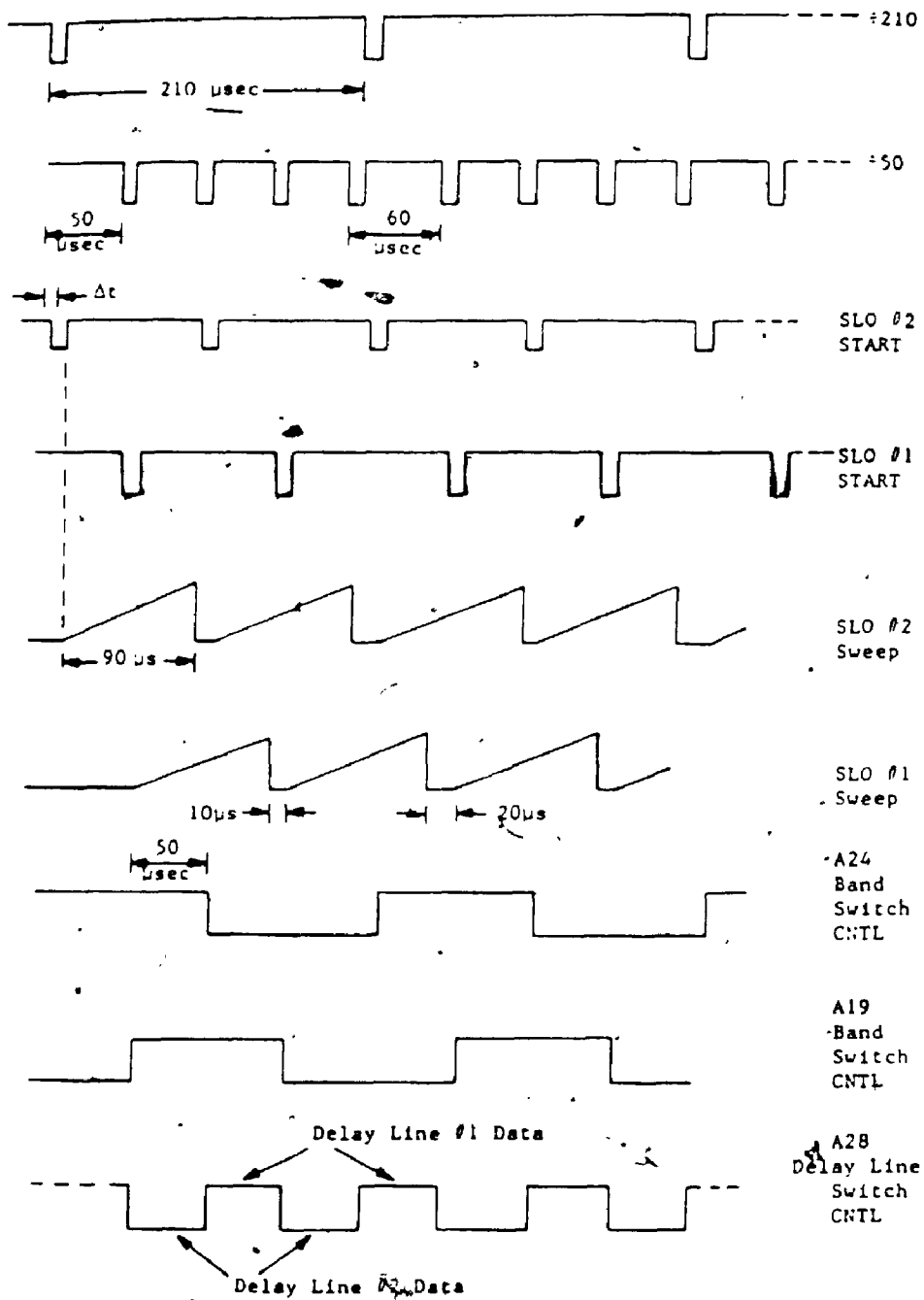


Figure 3.8: 20 MHz coverage control signals (copied from [33]).

of the output pulse while the clutter level (dynamic sidelobes) is typically 45 dB below. This, in fact, limits the instantaneous dynamic range of the receiver to approximately 30 dB at a frequency separation of 80 KHz. Therefore, an operating window of 30 dB which is free of spurs and sidelobes can be defined for any input signal strength within the 70 dB noise-limited dynamic range of the receiver. In practice, however, the lower limit of the linear dynamic range will be taken at the threshold level. An illustration of the receiver dynamic range is shown in Figure 3.9.

3.3.1.5 Detection and Thresholding

In order to operate the receiver satisfactorily a threshold level is set so as to observe the Neyman-Pearson detection criterion discussed in Section 2.2.3 of Chapter 2. The AS-520 microscan receiver can select the level at which thresholding occurs by a front panel Z-axis threshold control. It is desirable to set the threshold level such that a tolerable false-alarm time gives only one false-alarm every second ($T_{fa} = 1$ sec) at the lower end of the linear dynamic range. Therefore, the corresponding P_{fa} equals 3.33×10^{-5} for an IF bandwidth of 30 KHz (from equation (2.12)). This value is quite reasonable considering that for a 30 KHz bandwidth there are on the order of 30×10^3 noise pulses per second. Hence, the false-alarm probability of any one pulse must be small ($< 3.33 \times 10^{-5}$) if false-alarm times greater than seconds are to be obtained. The average noise power at the detector output is measured at -90 dBm. Consequently, the rms noise voltage at the detector is 1×10^{-6} V. The threshold voltage for an rms noise voltage of 1×10^{-6} V and a probability of false-alarm of 3.33×10^{-5} is

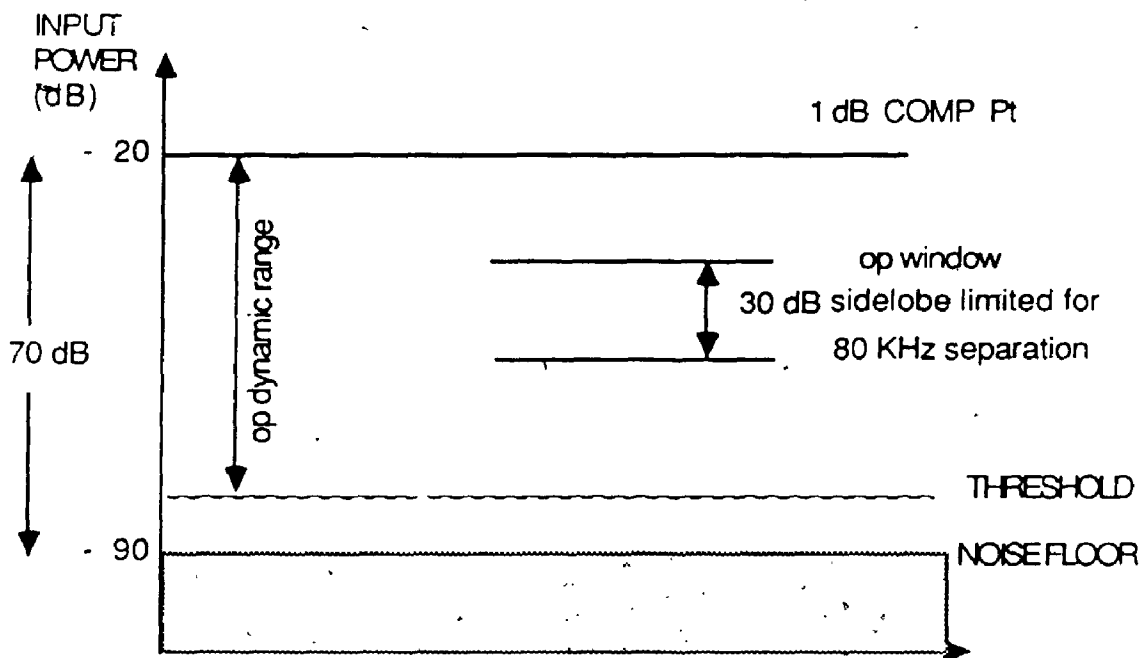


Figure 3.9: AS-520 receiver dynamic range.

calculated using equation (2.13) to be 4.54×10^{-6} V. This corresponds to a threshold level in dB above noise equal to 13.1 dB. Consequently, the probability of detection versus the signal-to-noise ratio can be read directly from Figure 2.3 for a fixed probability of false-alarm. For a desired P_d of 0.90, the SNR required at the input of the detector is 12.8 dB.

3.3.2 Downconversion

As mentioned earlier, the AS-520 microscan can only process an instantaneous RF input bandwidth of 10 MHz or 20 MHz. The only feasible way this microscan receiver can monitor a wide RF spectrum is by dividing the RF band into many sub-bands with bandwidth that matches that of the AS-520 receiver, and convert these sub-bands, one at a time, to the proper IF frequency for processing. This can be quite easily accomplished using a front-end downconversion stage similar to that found in a superheterodyne receiver as shown in Figure 3.10.

The basic superheterodyne receiver consists of a mixer that converts the input frequency to an intermediate frequency, and then passes it through a narrowband filter which determines the sensitivity and the resolution of the receiver. By utilizing a tunable local oscillator, the desired signal frequency can be placed at the center of the IF filter passband. Thus, the receiver is capable of scanning an entire RF bandwidth [2].

The front-end down conversion stage which precedes the AS-520 receiver performs similarly, but is slightly more complex than the one illustrated in Figure 3.10. Careful consideration has been given to

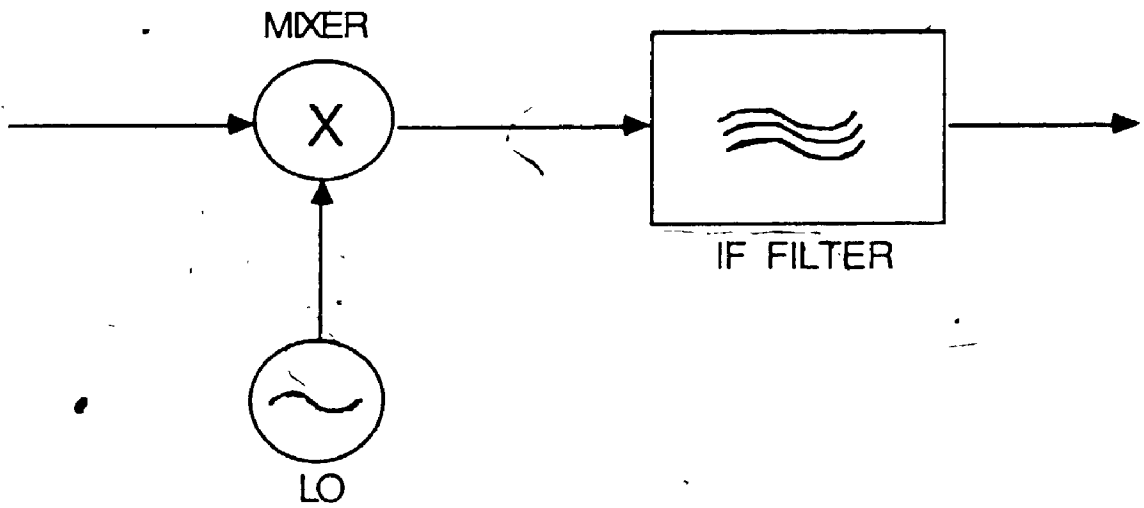


Figure 3.10: Basic superheterodyne receiver conversion stage.

certain performance parameters such as: (1) noise figure, (2) dynamic range, (3) intermodulation products, and (4) image-rejection. The requirement to analyze input signal levels as low as -126 dBm in a dense signal environment, where the occurrence of simultaneous input signals can create intermodulation products in the nonlinear RF-IF stages of the receiver, has led to the design of a low-noise front-end with a high spur-free dynamic range. Usually, the desire for a high dynamic range is often not compatible with the simultaneous requirement for low noise figure. The reason for this is that high-intercept receivers use RF-IF amplifier stages and double-balanced mixers having high 1 dB compression points. Generally speaking, these components also have high noise figure values. A low noise figure receiver, on the other hand, requires components with low noise figure and/or high gain. Therefore, the achievement of a low-noise figure and a high dynamic range front-end dictates a careful selection and placement of the RF-IF gain and mixer stages.

Another feature which must be highlighted in the design of this front-end receiver is the use of a double mixer downconversion stage with a filter in order to block out the image noise. This unwanted input occurs at the mirror image frequency of the desired signal with respect to the local oscillator, and mixes with the LO to appear at the same IF frequency as that of the desired signal [31]. The image signal is illustrated in Figure 3.11. If the LO steps or sweeps in frequency it becomes very difficult to determine whether the detected signal is on the high side or low side of the LO frequency. To effectively block out the image noise in the receiver front-end, a mixer downconverts an

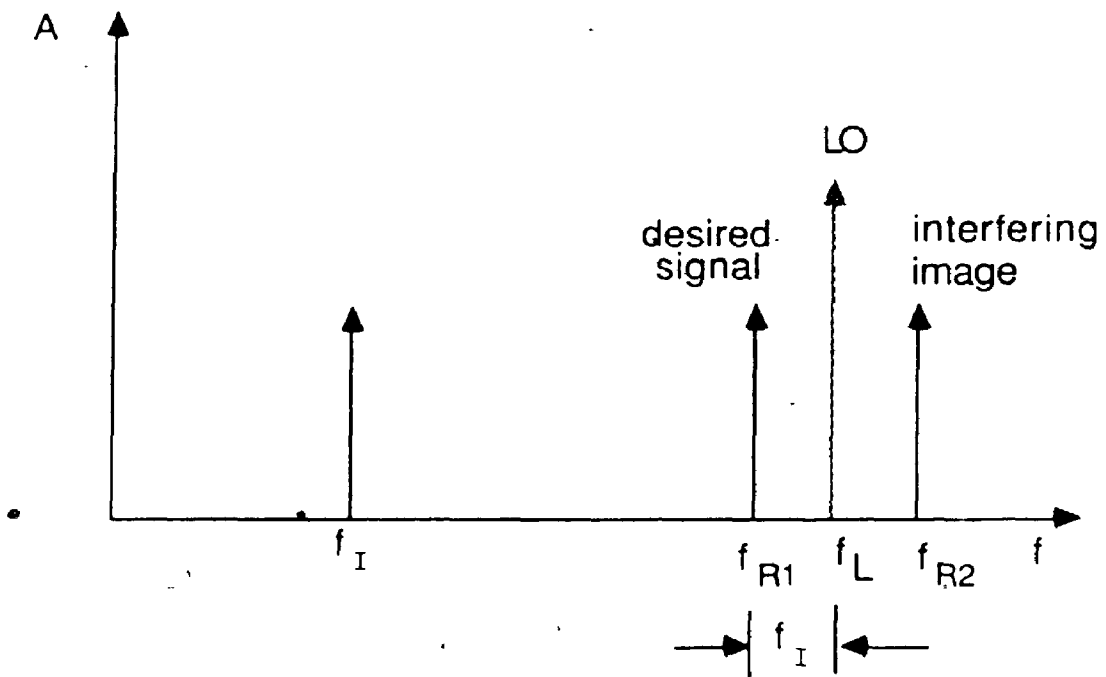


Figure 3.11: Desired signal competing with interfering image at IF frequency.

input-signal (between 3.2 and 4.2 GHz) to a first IF frequency of 1000 MHz and a second mixer downconverts the 1000 MHz signal to a final IF of 160 MHz.

3.3.2.1 Front-End Design

The block diagram of the receiver front-end is depicted in Figure 3.12. The 3.2 to 4.2 GHz input RF signals enter the receiver's downconversion stage through a wideband GaAsFET amplifier with a gain of 40 dB and a noise figure of 2.26 dB. This is followed by a fixed preselector bandpass filter which reduces the out-of-band frequency signals that could mix in the IF downconversion stages and create unwanted spurious responses. The filter is a five-section, Chebyshev design with 0.05 dB ripple. It has a 1 GHz 3 dB bandwidth centered at 3.7 GHz and covers the band extending from 3.2 GHz to 4.2 GHz. The signals are then routed to the RF port of a double-balanced mixer. The mixer has a 6.5 dB (typical) conversion loss and a 6.5 dB (typical) noise figure. The IF port feeds the downconverted 1000 MHz signals into a tunable BPF with 5% 3 dB bandwidth centered at 1000 MHz. The filter not only reduces the noise in the RF bandwidth to a much narrower IF bandwidth, but also provides attenuation of the local oscillator harmonics and to other mixing products generated outside the IF passband from the front-end of the receiver. The signals at the output of the filter are then amplified to recover some of the power loss incurred from both the first stage mixer and the subsequent stage mixer downconverter. The amplifier used has a low gain of 7.5 dB and a high intercept point of +28 dBm. The amplified signals are applied to the RF

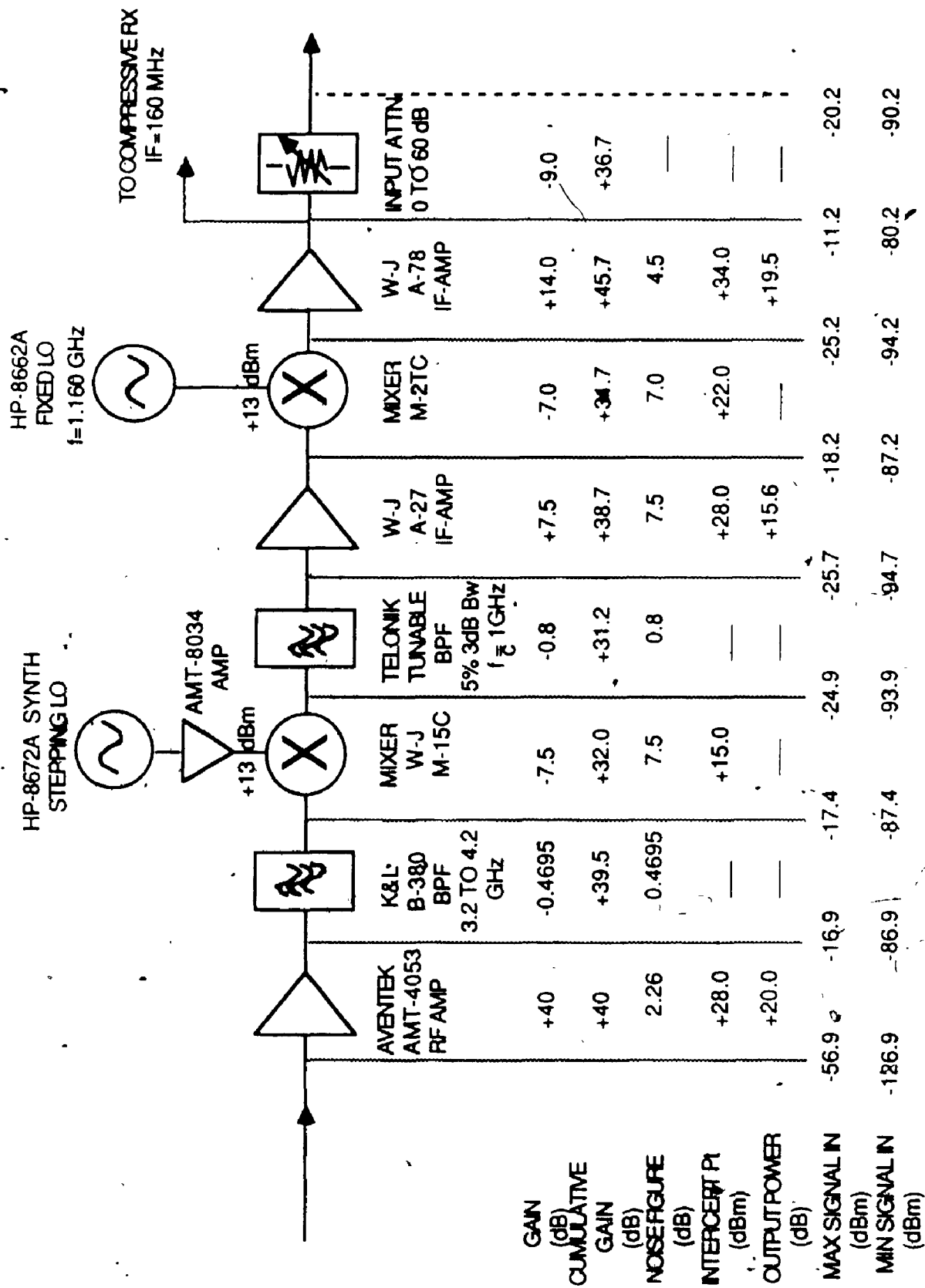


Figure 3.12: Front-end downconversion block diagram and signal flow budget.

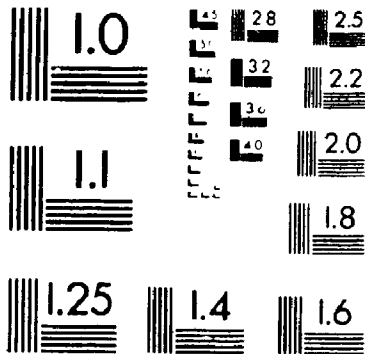
port of a hermetically-sealed double-balanced mixer. This mixer is a medium-class mixer which requires an LO drive level of +13 dBm at the LO port and which has a relatively high intercept point of +24 dBm in order to maintain a high dynamic range. Finally, the IF port of the second stage mixer feeds the downconverted 160 MHz signal to a power stage amplifier. This amplifier has a gain of +14 dB and a very high intercept point of 34 dBm which provide the necessary cascade output power to bring the low level signals within the dynamic range of the AS-520 microscan receiver. The signals, thus, proceed in the microscan receiver via the rear panel BNC input connector. The selectable input attenuation knob on the front-panel of the AS-520 is set to 9 dB in order to reduce the excess gain from the downconversion stage.

A small signal amplifier is placed at the LO input port of the first conversion mixer in order to provide the required LO drive level. The Class I mixer (1st downconverter mixer) uses a +7.5 dB gain amplifier to provide excess LO drive from a specified +7 dBm to +13 dBm for an additional 3 dB to 4 dB increase in the mixer intercept point. An improvement in two-tone third order intermodulation suppression is obtained by increasing the LO input level beyond the specified mixer LO drive level for class I mixers with low RF input signals (i.e., ≤ -20 dBm). This is the result of the mixer diodes operating for a shorter time in the highly nonlinear transition region [30]. The class II mixer (2nd downconverter), however, is driven at the specified LO drive level of +13 dBm without the use of an additional amplifier.

2

of/de

2



MICRO

The key to the performance of this design is the careful distribution of low gain amplifiers between the double-balanced mixers and appropriate filters to achieve a low-noise figure and high-dynamic range front-end. A detailed signal flow budget with component noise figures, gains, losses, and intercept points are included in Figure 3.12 to illustrate this point. Figure 3.13 shows a photograph of the front-end downconversion stage.

3.3.2.2 LO Synthesizer

The front-end downconversion stage utilizes the Hewlett-Packard 8672A synthesized signal generator as a stepping LO for the first stage mixer. The LO is required to hop 50 (i.e. 1×10^9 Hz / 20×10^6 Hz) steps having 20 MHz separation for full coverage of the 1 GHz bandwidth, as shown in Figure 3.14. The RF band is divided into 20 MHz sub-bands to match the input bandwidth of the AS-520 receiver. The second stage mixer, on the other hand, uses the HP-8662A synthesized sweeping generator to provide a fixed LO frequency at 1160 MHz.

Synthesizers are used since they provide very stable frequencies with very little phase noise. Stability is an important criterion in this application since it determines the accuracy by which the AS-520 receiver can measure the input signal. The AS-520 microscan receiver can resolve, in frequency, signals spaced 30 KHz apart. Therefore, in order to measure a signal at 3.7 GHz with 30 KHz of accuracy, the LO frequency stability must be better than 8.1×10^{-6} (i.e. 30×30^3 Hz / 3.7×10^9 Hz). If both LOs do not provide this order of accuracy, their frequency inaccuracy will be translated to the IF bandwidth and contaminate the input to the microscan receiver [2,32].

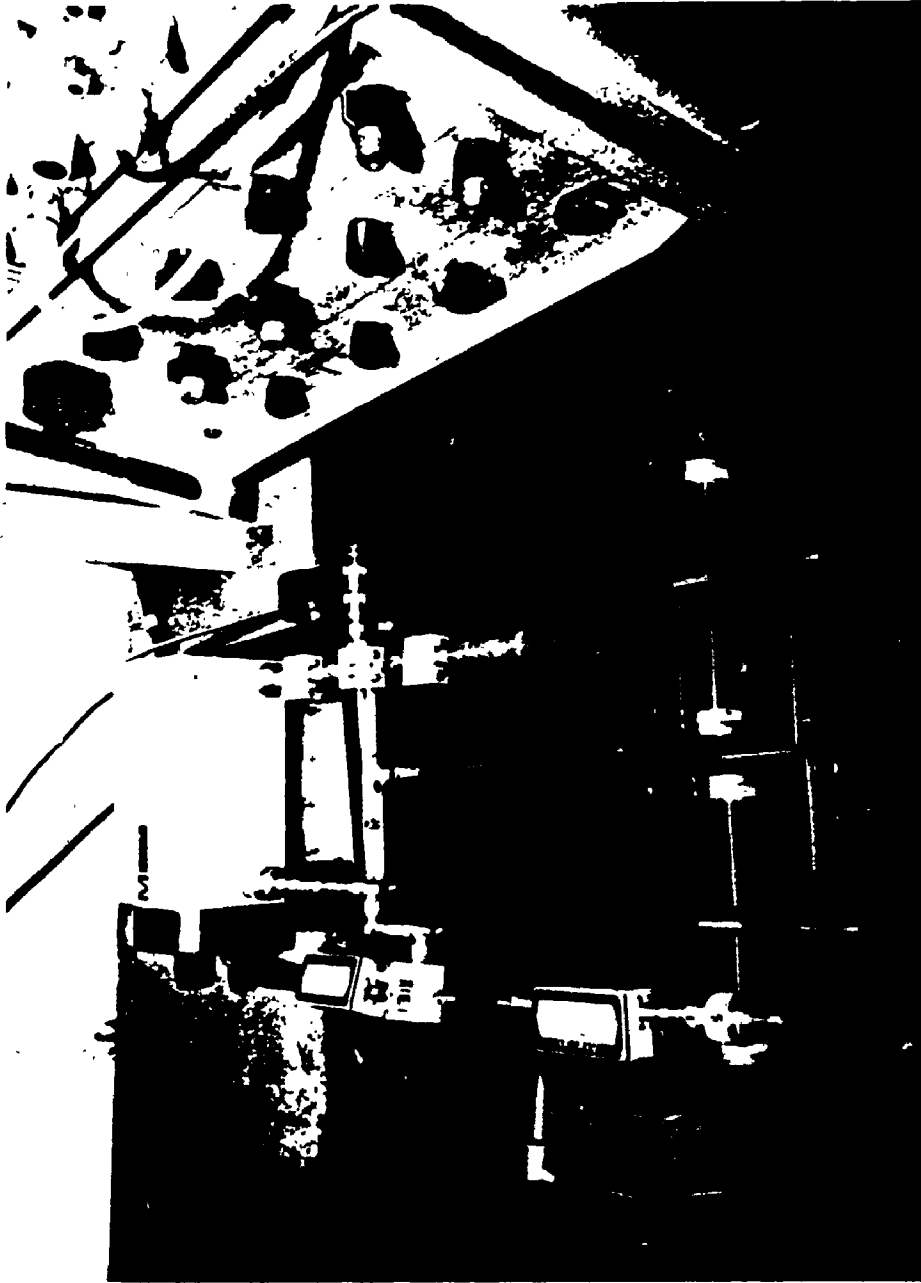


Figure 3.13: Front-end downconversion stage.

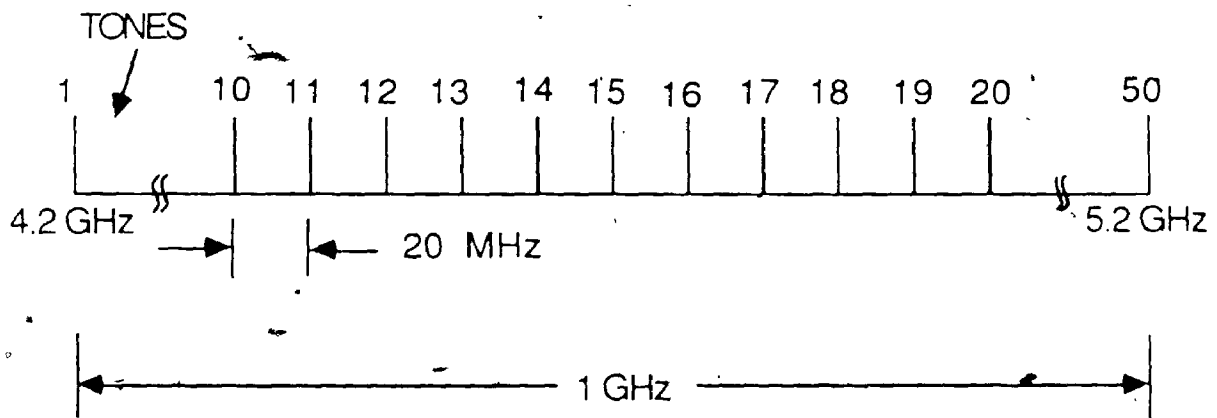


Figure 3.14: LO tone allocation.

Voltage controlled oscillators (VCO) exist which can provide a frequency stability of 10^{-6} or better but they have often inherent problems which make them less attractive. These problems include such things as poor close-in phase-noise, uncontrollable frequency drift due to temperature variations and load pulling, post-tuning drift, and settling time which are not found in a frequency synthesizer [2]. Most low cost, compact frequency synthesizers avoid most of these problems by using a method called indirect synthesis. The indirect method derives its frequency stability by using a feedback system whereby a VCO is phaselocked (PLL) to a very stable reference source [32].

A block diagram of a basic phaselocked synthesizer is shown in Figure 3.15. The reference oscillator frequency f_r is divided by N and the VCO frequency f_0 is divided by M . The two are then compared in a phase detector. The condition to have phaselock is $f_r/N = f_0/M$ so the output frequency is locked to a rational fraction of the reference. By changing the integers M and N , the output frequency f_0 also changes. This method offers a mean for generating a large number of highly accurate output frequencies at low cost [32]. A major drawback in using this technique is that frequency switching time is relatively slow. This switching time depends on fast acquisition of the correct lock frequency, however, speed of acquisition is limited by the loop bandwidth of the PLL. Thus, the slow switching time of the stepping LO will limit the processing speed of the entire receiving system.

It takes approximately 250 usec for the AS-520 microscan receiver to analyze a 20 MHz input bandwidth. Consequently, if the synthesizer has zero switching time, the entire 1 GHz RF bandwidth can be scanned in

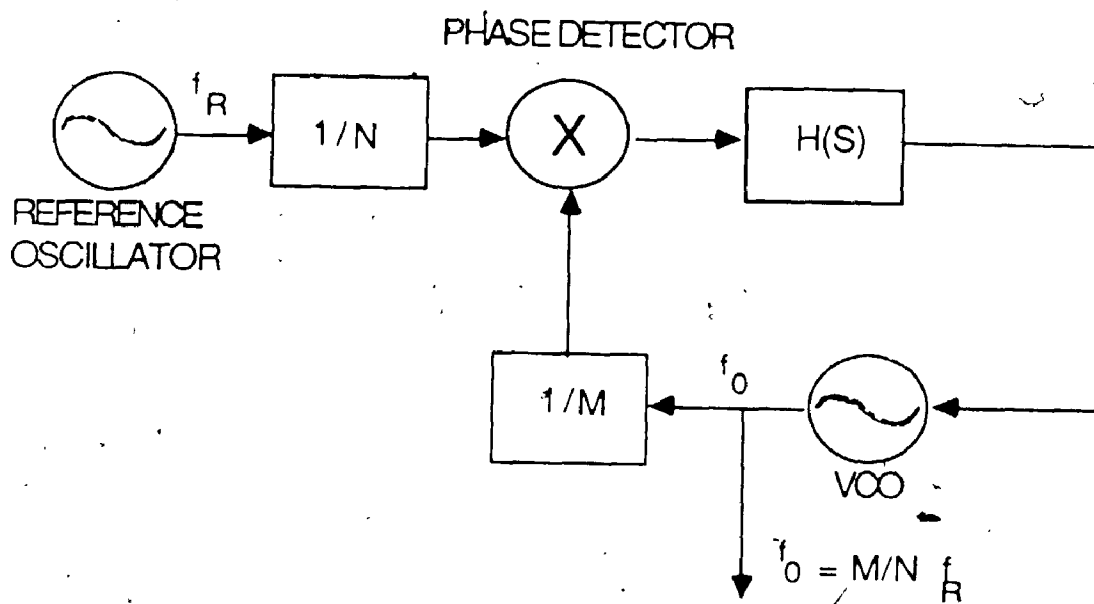


Figure 3.15: Basic phase-locked synthesizer.

12.50 msec. However, the HP8672A has a non-zero switching time slightly less than 15 msec. Therefore, the scan time for full band coverage is increased to 762.50 msec. This degrades the processing speed of the receiving system to approximately 3.4 (i.e. $(10.5 \text{ msec}/762.5 \text{ msec} \times 250)$) times that of an ordinary spectrum analyzer. Consequently, it requires a pulse duration of 762.75 msec or greater (i.e. scan period + filter/integration time = $762.50 \text{ msec} + 0.250 \text{ msec}$) to intercept pulses anywhere within the 1 GHz bandwidth with 100% POI. Fast frequency hopping is, however, possible by using a direct synthesis method which is not limited by the bandwidth of the PLL. Unfortunately a synthesizer based on this technique was not available for this thesis.

The HP8672A was selected for the stepping LO since it can deliver precise microwave signals over the 2.0 to 18.0 GHz frequency range. It features excellent spectral purity using an indirect synthesis method which phase-locks a YIG-tuned oscillator to a 10 MHz quartz crystal reference. This results in excellent long term stability (frequency drift $< 5 \times 10^{-10}$ per day). The phase locking responses are also optimized to allow the synthesizer to exhibit the lowest possible single-sideband phase noise. If the LO exhibited poor sideband-noise response, this would limit the usable dynamic range and selectivity of the receiver [37]. The HP8672A provides full programmability of all front-panel functions. The frequency range, step size, and output level of the signals can be remotely accessed via the HP-IB. This added feature was essential for a continuous scan of the 1 GHz band. For more information on the specifications of the HP8672A and the HP8662A refer to Appendix B.

3.3.2.3 Noise Figure and Dynamic Range Calculations

Two of the most important calculations in receiver design are the noise figure and dynamic range calculations. The former determines the sensitivity of the receiver while the latter determines the range at which the input signal level can be measured free of distortion and spurious products.

The overall noise figure for a cascaded network is given by equation (2.7) as:

$$F_T = F_1 + \frac{F_2 - 1}{G_1} + \frac{F_3 - 1}{G_1 G_2} + \dots$$

Using typical values for the components in the downconversion stage yields:

$$\begin{aligned}
 F_T &= 1.659 + \frac{0.11416}{1 \times 10^4} + \frac{4.6234}{(1 \times 10^4)(0.897)} + \\
 &\quad \frac{0.202}{(1 \times 10^4)(0.897)(0.177)} + \frac{4.6234}{(1 \times 10^4)(0.897)(0.177)(0.832)} \\
 &\quad + \frac{4.012}{(1 \times 10^4)(0.897)(0.177)(0.832)(5.6234)} + \\
 &\quad + \frac{1.818}{(1 \times 10^4)(0.897)(0.177)(0.832)(5.623)(0.199)} \\
 &= 1.6883
 \end{aligned}$$

The result can be expressed in dB as:

$$NF = 10 \log_{10} (1.6883) = 2.27 \text{ dB}$$

The above calculation does not include the AS-520 receiver noise figure. However, receiver sensitivity is normally established by the noise figure of the first few components at the front-end of the receiver. The sensitivity of the receiver is calculated from equation (2.3) as:

$$N_0 = KTB$$

Using our bandwidth and noise figure values, gives:

$$\begin{aligned} &= -174 \text{ dBm} + 10 \log_{10} (30 \times 10^3) + 2.27 \text{ dB} \\ &= -126.9 \text{ dBm} \end{aligned}$$

The MDS is also taken at the noise level. The overall gain of the system is calculated at 36.9 dB. Therefore the available noise power at the output of the system is equal to -90 dBm (i.e. -126.9 dBm + 36.9 dB) which corresponds to the lower end of the AS-520 receiver dynamic range. The threshold is set according to Section 3.3.1.5 at -76.9 dBm (i.e. -90 dBm + 13.1 dB) for a false alarm rate of 1 FA/sec.

The dynamic range calculation involves the receiver's simultaneous signal handling capability. To evaluate the front-end SFDR the total front-end 3rd order intercept point must be known. The total 3rd order intercept point of a cascaded network can be calculated from equation (2.20) as:

$$\frac{1}{P_{31,T}} = \sum_{i=1}^7 (P_{31,i} G_{(i+1,n)})^{-1}$$

Again using our downconverter values, provides:

$$\begin{aligned} \frac{1}{P_{31,T}} &= [(630)(0.897)]^{-1} + [(8 \times 10^9)(0.178)]^{-1} + [(63.24)(0.832)]^{-1} \\ &+ [(8 \times 10^9)(5.623)]^{-1} + [(630)(0.199)]^{-1} + [(158.48)(25.11)]^{-1} \\ &+ [2511.89]^{-1} \\ &= 0.04838 \end{aligned}$$

The total 3rd order intercept point $P_{31,T}$ can be written in dBm as:

$$\begin{aligned} P_{31,T} &= 10 \log_{10} \left(\frac{1}{0.04838} \right) \\ &= 15.31 \text{ dBm} \end{aligned}$$

This value gives the worst case performance assuming a perfect 50 ohm system. The SFDR can now be obtained from equation (2.19) as:

$$\begin{aligned} \text{SFDR} &= \frac{2}{3} (P_{31,T} - \text{G-threshold}) \\ &= \frac{2}{3} (15.31 \text{ dBm} - 36.9 \text{ dB} - (-126.9 \text{ dBm} + 13.1 \text{ dB})) \\ &= 61.5 \text{ dB} \end{aligned}$$

The AS-520 could not be included in the above calculation due to lack of information on some of its components. However, the manufacturer of the AS-520 has specified that spurious products generated by the mixers and SAW dispersive filters are suppressed 45 dB below the desired response. This value is much lower than the calculated SFDR of the front-end. Therefore, the front-end should not compromise the AS-520 receiver's spur-free range.

3.3.3 Controller

A Hewlett-Packard series 200 microprocessor controller is utilized to automate the entire system. The controller uses a Basic 2.1 extended software program to command the HP-8672A frequency synthesizer to "hop" in predetermined frequency steps and generate a time pulse, each hop, to be used as an external trigger to the AS-520 microscan receiver.

An illustration of the timing sequence for the various operations in the system is shown in Figure 3.16. An input trigger pulse to the HP8672A frequency synthesizer is repeated every 250 μ sec. It takes approximately 15 msec of switching time for the frequency synthesizer to output a new valid CW tone of frequency f_n . Each tone is spaced 20 MHz apart from the previous one (i.e. $f_n - f_{n-1} = 20$ MHz). Once a CW tone f_n is valid, a trigger pulse n is sent to the AS-520 microscan receiver to begin processing a new input bandwidth. For continuous operation, the step scan cycle may repeat itself with the touch of a softkey. Every operation is accessed by software. The commands for the sequential hopping, the delays, and the trigger pulse to the microscan receiver are all incorporated in the software program. A copy of the program can be found in Appendix C.

The program is very general and enables the user to select the frequency range of interest anywhere from 2 to 18 GHz. The start frequency, stop frequency, step size, and amplitude setting of the HP8672A can be tailored to meet the user's needs. To generate delays via software, the microprocessor has an interrupt service routine that can generate delays precise to 1 msec from its internal time clock. Shorter delays can be obtained by performing known arithmetical

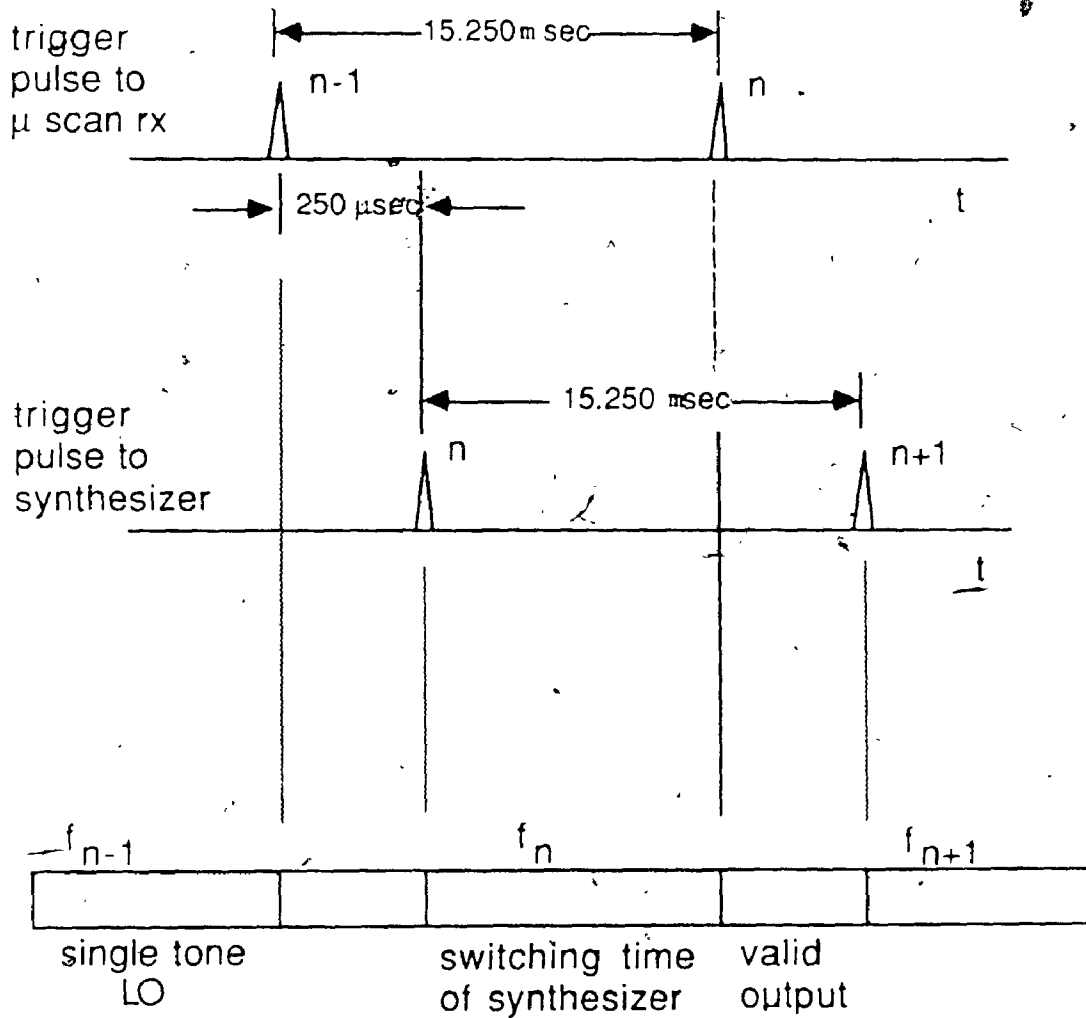


Figure 3.16: Timing sequence for HP-8672A frequency synthesizer, AS-520 trigger pulse, and LO single tone output.

operations which take up a specific amount of time to complete. A simple program was devised to calculate the time required to perform various arithmetical operations in order to choose the one suited for our needs. The 250 μ sec delay before the generation of a new LO tone is devised using this scheme. The external trigger pulse to the AS-520 microscan receiver is generated in an unusual manner.

Since the AS-520 receiver does not comply with the HP-IB protocol, a simple interface connection could not be used. Normally, devices that do not comply with the ANSI/IEE 488 standards can be still be accessed by an HP microprocessor through a General Purpose Interface Bus (GPIB) input-output card. However, this interface card was not available for the project. Therefore, after conducting certain tests with a data bus analyzer, it was decided to make use of the data available (DAV) line to generate the pulse. This line is normally used as one of the management lines for the HP-IB. Figure 3.17 illustrates the connection between the HP microprocessor and the AS-520 receiver. A cable physically connects to the DAV line on the 50 pin connector of the HP-IB input-output port of the controller and runs it to the BNC input connector of the external scan trigger (back panel) of the AS-520 receiver. An inverter is placed before the input to the external trigger because the HP-IB protocol lines use negative logic. The AS-520 receiver requires a pulse of amplitude greater than +1 volt and a width greater than 1 μ sec into a 1 kilohm input impedance in order to trigger the microscan receiver.

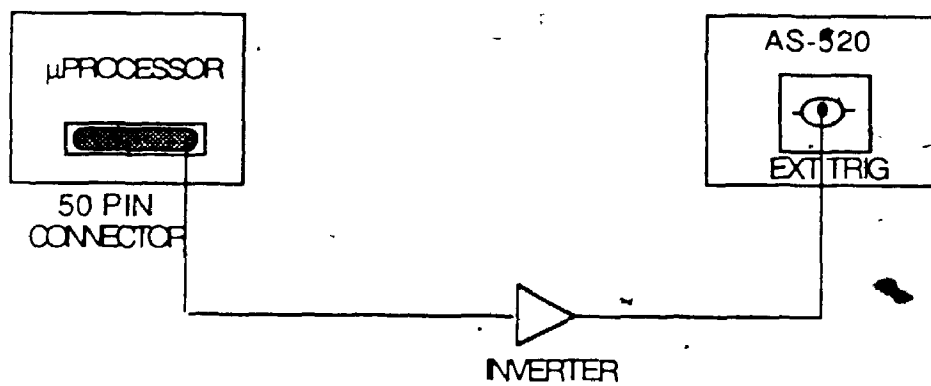


Figure 3.17: Cable connection between the HP microprocessor and the AS-520 receiver.

3.4 SUMMARY

The practical design of a wideband microwave surveillance system has been investigated. The entire system was divided into three sections: the microscan receiver, the downconversion stage, and the controller. These were examined individually in order to satisfy the system requirements.

As was described, a microscan receiver can extend its fine frequency measurement capability to the microwave region by synchronizing it with a front-end frequency stepping receiver. The system described is fully automated with the use of a microprocessor, and thus is capable of continuous coverage over a 1 GHz bandwidth.

Chapter 4

EXPERIMENTAL RESULTS

4.1 INTRODUCTION

The wideband microwave surveillance system of Chapter 3 was assembled and tested under laboratory conditions. The receiver performance was evaluated over the whole frequency range of interest. The AS-520 microscan receiver was first tested in order to provide insight to the system's overall performance. Important parameters were examined to verify that they are in accordance with the manufacturer's specifications. Overall system parameters were subsequently evaluated and compared with theoretical values. Included in the measurements were the sensitivity, frequency accuracy, frequency resolution, dynamic range and pulse width.

4.2 MICROSCAN RECEIVER MEASUREMENTS

In this section measurements on some important performance parameters of the AS-520 microscan receiver are presented. In specific, topics covered are the amplitude response of the output pulse, the pulse width at the -3 dB point, and the sidelobe suppression.

The amplitude response of the receiver derives from the slope of the output to input power relation of the logarithmic amplifier. The output of the log amplifier was discussed in Chapter 2 and can be written as:

$$V = m \log P_i$$

The measurement of the AS-520 log amplifier transfer curve is plotted in Figure 4.1. Here, the operating RF frequency was 160 MHz. As can be seen, the slope of the curve is linear for values of RF input power between -70 dBm to -20 dBm and corresponds to a value of 25 mV/dB. For input powers above -20 dBm the output voltage undergoes compression. Also, as the input decreases below -70 dBm the slope of the transfer curve changes to 10 mV/dB. Since distortion occurs at both the upper and lower ends of the operating range, most system measurements were taken in the linear region of operation. The ratio of the maximum permissible input power of -20 dBm to the minimum discernible output was found to be about 70 dB. This agrees with the manufacturer's specifications of noise-limited dynamic range.

The output pulse spectrum from the receiver is a weighted Fourier transform of the input signal. A weighting filter similar to the Hanning window with $\alpha=2.0$ is used to taper the sidelobe levels. The close-in sidelobe suppression was measured as well as the 3 dB pulse width for different CW tone input frequencies within the 20 MHz IF bandwidth of the receiver and the results are listed in Table 4.1. The measured 3 dB width was multiplied by the scaling factor $\mu=0.1$ MHz/ μ sec to give the proper frequency value. The theoretical 3 dB width is calculated by:

$$f_{3dB} = \frac{k}{T} \quad (4.1)$$

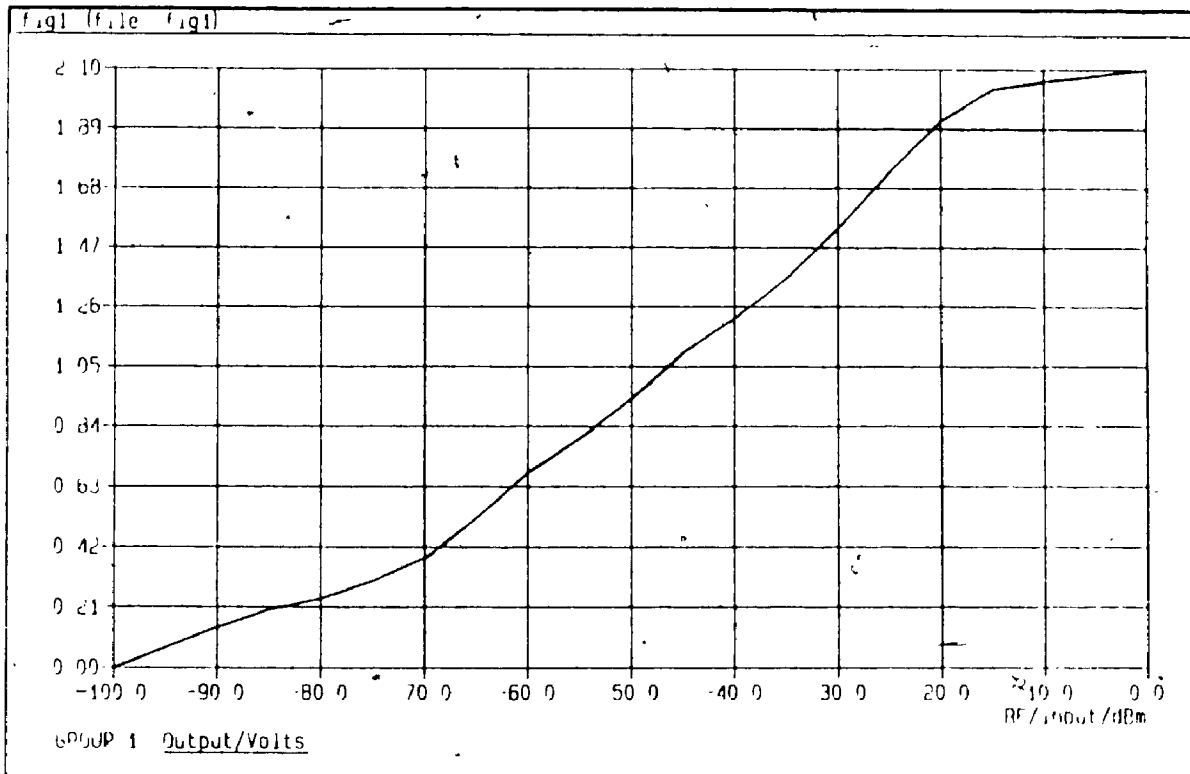


Figure 4.1: Output voltage versus input RF power for the AS-520 microscan receiver.

Table 4.1: Values of Sidelobe Suppression and 3 dB Width for the Output Pulses of the AS-520 Receiver at Different IF Frequencies.

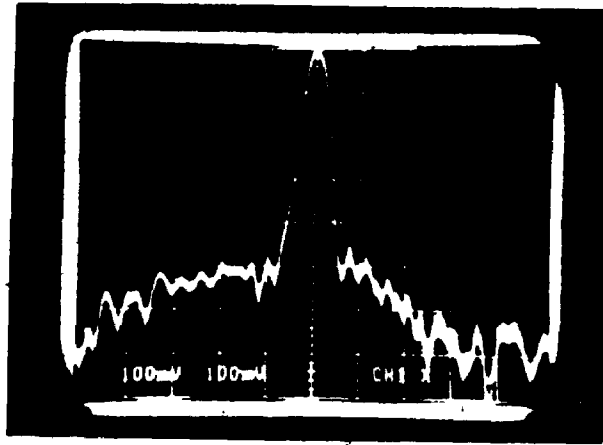
Frequency MHz	Close-In Sidelobe Suppression dB		3 dB Width KHz	
	Measured	Theoretical $\alpha = 2.0$	Measured	Theoretical $\alpha = 2.0$
152	35.0	32.0	30	28.8
154	36.0	32.0	29	28.8
156	32.0	32.0	52	28.8
158	32.0	32.0	42	28.8
159	32.0	32.0	41	28.8
160	32.0	32.0	35	28.8
162	35.2	32.0	30	28.8
164	28.8	32.0	29	28.8
166	35.2	32.0	52	28.8
168	35.2	32.0	48	28.8
169	35.2	32.0	53	28.8

where $k = 1.44$ for a Hanning window with $\beta = 2.0$, from Harris [26], and T is the filter integration time of 50 sec.

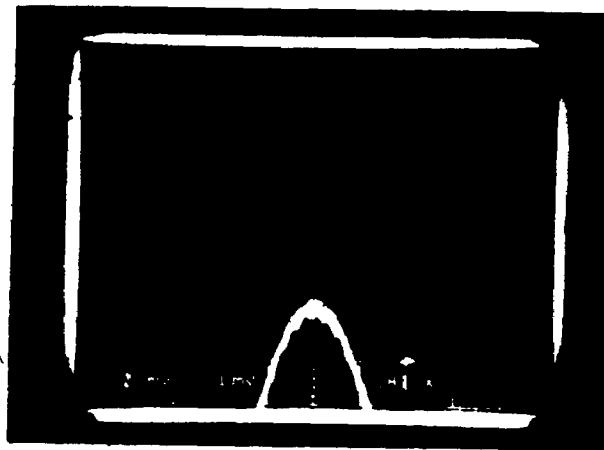
Both the output pulse spectrum and the 3 dB pulse width are displayed in Figure 4.2. The output pulse spectrum was found to be unsymmetrical; the sidelobe roll-off in dB/octave being much smaller on one side of the peak than on the other. Although the sidelobes remained relatively constant and in good agreement with the theoretical value, the 3 dB width varied widely and irregularly across the IF bandwidth. Only in the best case did the measured 3 dB width approach the theoretical value of 28.8 KHz, and on average was much closer to 40 KHz. In the worst case, the 3 dB width was larger by about 23 KHz. Moreover, the manufacturer claimed a constant 3 dB width of 28 KHz for any input frequency. The much wider than expected pulse width is thought to be related to the phase slope mismatches between the sweeping local oscillators and the dispersive delay filters in the twin multiplexed delay lines inside the receiver. In addition, the weighting filter is suspected of not having an ideal $\cos^2(x)$ shape, thereby leading to the unsymmetrical pulse spectrum.

The result of the unsymmetrical pulse shape and the varying pulse width affects both the instantaneous dynamic range and the simultaneous signal resolution of the whole system. This will be discussed in the next section.*

* It should be noted that the video threshold level was later raised to 0.1 dB above the previously set level of -76.9 dBm in order to conform with the average measured 40 KHz pulse width for a constant false alarm rate of 1 FA/sec.



(a)



(b)

Figure 4.2: (a) Output pulse spectrum of a CW tone (x-axis: 1 $\mu\text{sec}/\text{div}$, y-axis: 8 dB/div).
 (b) An expanded view of (a) at the 3 dB pulse width (x-axis: 0.2 $\mu\text{sec}/\text{div}$).

4.3 RECEIVER SYSTEM EVALUATION

4.3.1 Introduction

The system performance was measured for the range of frequencies between 3.2 GHz and 4.2 GHz and the results are reported in this section. The receiver measurements include sensitivity, frequency accuracy, frequency resolution, linear dynamic range, instantaneous dynamic range, two-tone spur free dynamic range and pulse width.

4.3.2 Basic Measurement Set-Up

Figure 4.3 illustrates the basic experimental set-up used to measure and evaluate most of the system performance parameters. Some experiments made use of the whole set-up while others only used a portion of it. The set-up consisted basically of two signal generators combined through a power divider at the front-end of the receiver. Most measurements were conducted with input CW tones. An oscilloscope was used to monitor the output pulses from the receiving system. A spectrum analyzer and a frequency counter were also employed in various experiments to monitor the IF signal at the output of the downconversion stage. In addition, a noise figure meter was utilized for determining receiver sensitivity and a pulse generator was employed for conducting pulse width measurements.

The testing of the wide band receiver was conducted manually at predetermined frequencies across the 1 GHz band with the final results giving only the best case, worse case, and average value of the sampling points measured. A thorough characterization of the receiver would have

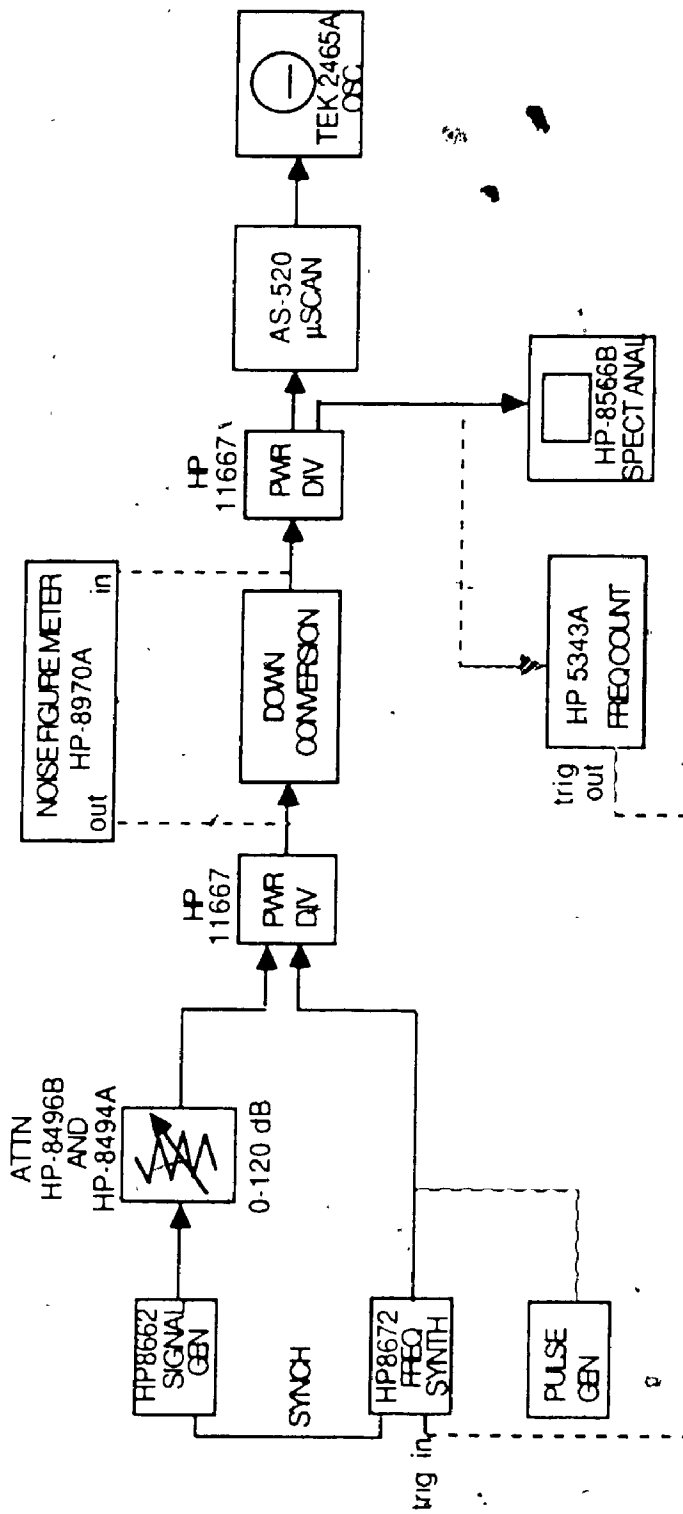


Figure 4.3: Basic experimental set-up.

required the examination of every resolution cell (both in frequency and in amplitude) across the 1 GHz bandwidth. However, such a task would be unmanageable without the use of automatic testing equipment. Unfortunately, the AS-520 receiver has only an analog output which renders it incompatible with most automatic testing equipment.

4.3.3 Sensitivity

The first test was conducted to determine the MDS level of the receiving system. A noise figure meter and noise source were used to measure the noise figure and gain of the system. The measurements were taken at the output of the downconversion stage and the results plotted at uniformly spaced RF frequencies across the 1 GHz bandwidth as shown in Figure 4.4. The measured gain curve has an average gain of 46.6 dB and a gain flatness of ± 2 dB about its mean value. This closely agrees with the theoretical gain value of 45.7 dB cited in Chapter 3. The measured noise figure curve also displays some ripples but this is to be expected since noise figure is inversely proportional to gain. The mean noise figure value measured is 2.97 dB; a difference of only 0.5 dB from the calculated theoretical value of 2.27 dB. In addition, the gain and noise figure were also measured at both the lower and upper edge of the 20 MHz band centered about the previously measured frequencies. It was found that the gain remained virtually constant within a 20 MHz band and that the noise figure varied no more than a few fractions of a dB. The experimental value for sensitivity was calculated at -126.3 dBm for $B=30$ KHz, $T=290^{\circ}\text{K}$, and $NF=2.97$ dB. This value corresponds rather nicely with the theoretical value for MDS of -126.9 dBm as calculated in Chapter 3. The experimental value for MDS is somewhat of a best case

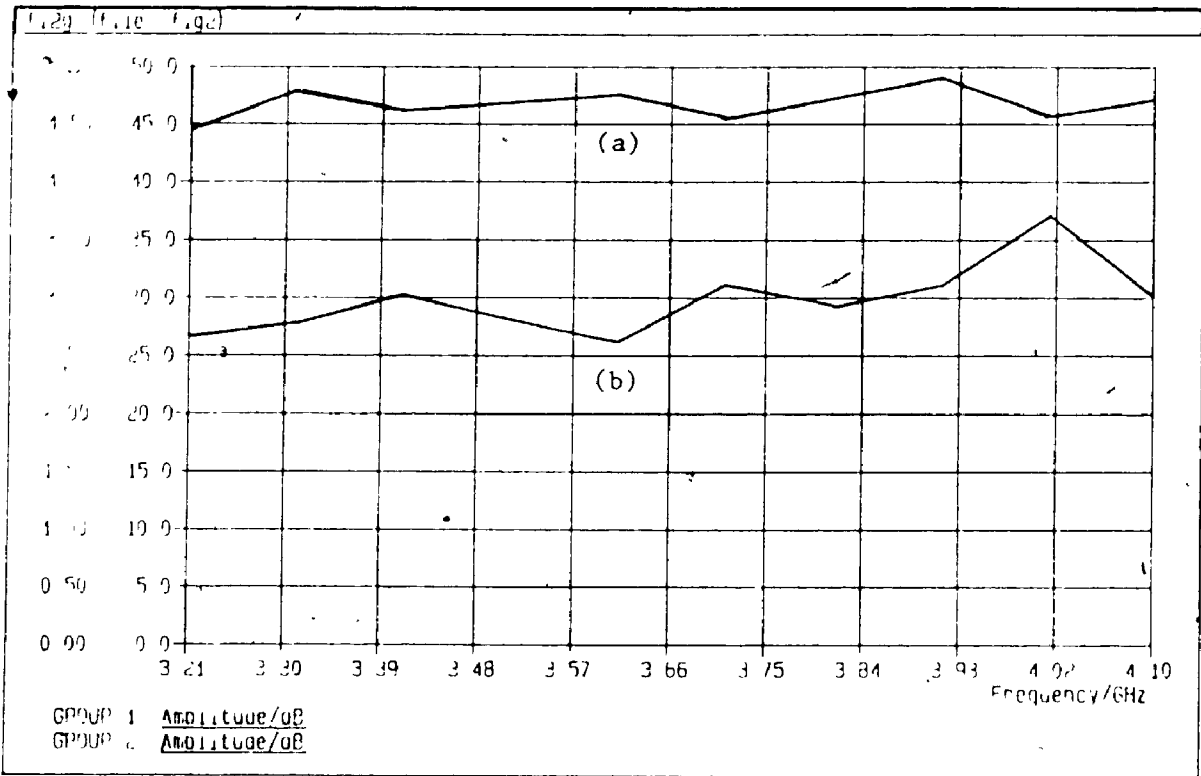


Figure 4.4: (a) System noise figure and (b) gain versus RF frequency.

value, considering that the measured value for the 3 dB resolution bandwidth, as reported in Section 4.2, was closer to 40 KHz than it was to 30 KHz. In addition, a degradation in receiver sensitivity equal to 2 to 3 dB resulted from cable losses. By taking into account the above, a realistic value for receiver sensitivity can be estimated to be -123 dBm.

4.3.4 Frequency Accuracy

The system frequency accuracy was measured at two locations in the signal path and compared with a known reference input signal. The RF input signal used was a synthesized source, and was initially calibrated with a microwave frequency counter for accurate frequency readings. The output IF frequency from the downconversion stage was then measured with the frequency counter, while simultaneously, the time at which the pulse emerged from the receiver was measured with an oscilloscope. The error frequency for the wideband receiver is plotted for different RF input frequencies in Figure 4.5. The error frequency is defined as the difference between the output and input frequencies. If the receiver performance was perfect, this error frequency would always be zero.

The results obtained showed that the frequency accuracy of the system is dominated by the AS-520 microscan receiver. The measured offset was, at times, as far as ± 90 KHz from the reference signal, while, at other times, no errors were recorded. The mean offset across the entire frequency range of interest was found to be ± 26 KHz (excluding the display). The manufacturer claimed an accuracy of ± 10 KHz (excluding the display). This large discrepancy in error is thought

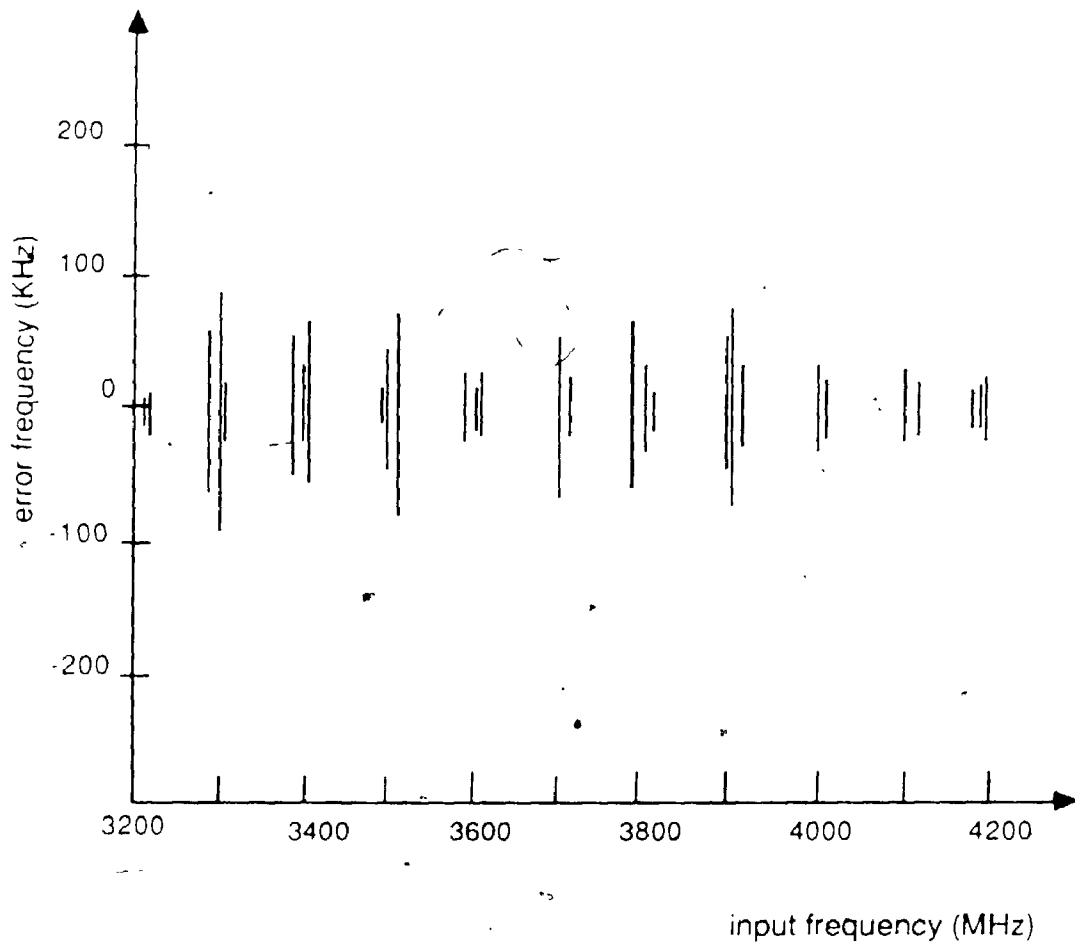


Figure 4.5: Error frequency versus input frequency.

to be linked to the aging of the sweeping local oscillators inside the AS-520, and to the random misalignments of the primary timing signals which trigger the SLOs and the generator of the display gates.

The errors introduced by the frequency translation alone are very small and are on the order of 3.73 parts in 10^8 across the entire 1 GHz bandwidth. This slight error is probably a result of the long term stability of the two synthesized LO sources in the downconversion stage and for all intents and purposes could be considered negligible in comparison to the frequency errors caused by the microscan receiver alone.

4.3.5 Frequency Resolution

The system's ability to distinguish between two simultaneous CW tones close in frequency was determined. These measurements were conducted on the AS-520 receiver alone since it determines the width of the pulses emerging from the system as discussed in Section 4.2.1. Two CW signals of the same amplitude were first widely separated in frequency. One of the tones was then progressively moved closer to the other until the receiver could no longer differentiate between the two. The results were taken at the lower and upper side of different fixed tone frequencies within the 20 MHz IF input bandwidth of the receiver and are listed in Table 4.2.

The average signal resolution reported within the 20 MHz IF bandwidth is about 40 KHz. The best case and worse case values are both 35 KHz and 50 KHz respectively. The measurements indicated that the 150 to 155 MHz and the 160 to 165 MHz bands had the best signal resolution

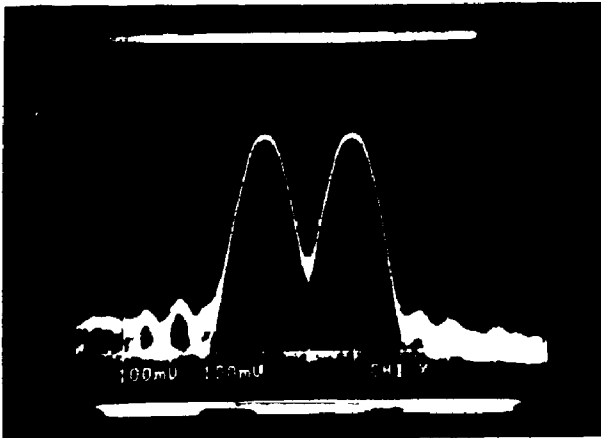
8

**Table 4.2: Frequency Resolution Measurement of the
150-170 MHz IF Input Band**

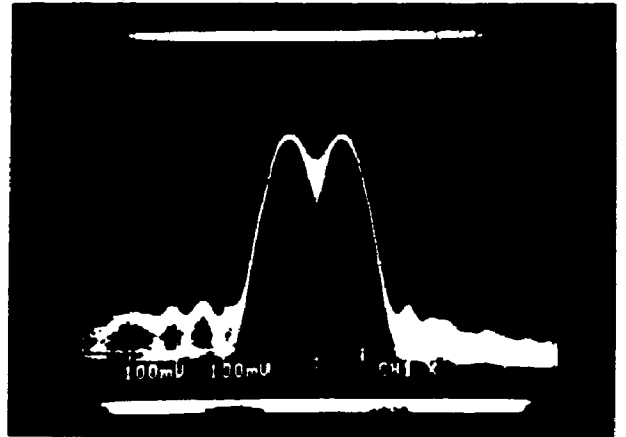
Fixed Frequency (MHz)	Min Resolution Upper Skirt (KHz)	Min Resolution Lower Skirt (KHz)
151	40	39
152	35	35
153	35	35
154	35	35
155	36	36
156	47	45
157	45	45
158	45	45
159	40	40
160	38	38
161	35	35
162	35	35
163	37	38
164	36	36
165	40	40
166	50	50
167	45	45
168	47	47
169	46	46

capability while the 155 to 160 MHz and the 165 to 170 MHz bands had the worst. However, the manufacturer's claim of minimum resolution of 28 KHz was not achieved. This outcome is strongly related to the observations made previously for the 3 dB width measurement in Section 4.2.1. The results support the earlier statement that one of the receiver arms which processes the affected bands has a larger phase mismatch between its sweeping local oscillator and dispersive delay filter, than the other. This results in a broadening of the compressed pulses and, hence, a degradation in resolution capability. From the tabulated results there are no significant differences in the minimum resolution capability of the receiver on either side of the stationary input signal.

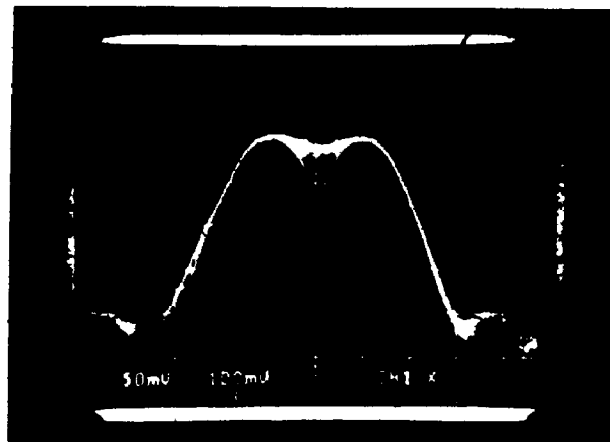
Figure 4.6 illustrates the minimum signal resolution for simultaneous input signals. Here, both input signals have power levels of -40 dBm; while one approaches the upper side of the other, stationary at 166 MHz. Figure 4.6(a) illustrates the two tones separated by 100 KHz; Figure 4.6(b) illustrates the tones separated by 60 KHz. Figure 4.6(c) shows the tones at the minimum signal resolution of 50 KHz. It should be noted that the noise filling the valley above the crossover point is due to the coherent summation of the spectral components weighted through the Hanning window at a given frequency.



(a)



(b)



(c)

Figure 4.6: Simultaneous signal resolution at
(a) 100 KHz separation,
(b) 60 KHz separation, (x-axis: 0.5 μ sec/div) and
(c) 50 KHz minimum separation (x-axis: 0.25 μ sec/div).

4.3.6 Dynamic Range

4.3.6.1 Linear Dynamic Range

The amplitude range where the wideband receiver correctly reads all frequencies was established using one signal generator and precision attenuators at the input to the system. The output was monitored on the oscilloscope as the input level was increased in 1 dB steps. The results are tabulated in Tables 4.3 and 4.4. The first set of readings was taken at several frequencies within the 20 MHz band centered at 3210 MHz in order to characterize the dynamic range of one individual band. Other bands are assumed to have similar values. The second set of data was taken at the center frequency of 20 MHz bands spaced 100 MHz apart from each other in order to cover the frequency range of the receiver. The linear dynamic range was previously defined as the difference between the 1 dB compression point and a specified threshold above the noise level for a constant false alarm rate. However, in this section, the lower limit of dynamic range is taken at the MDS level (equal to the noise floor) for a more accurate comparison with the value of dynamic range specified by the manufacturer of the AS-520 microscan receiver.

The measured results revealed that for both sets of data the linear dynamic range is not a sensitive function of frequency. The value obtained was typically 70 dB. This closely corresponds to the noise-limited dynamic range of the AS-520 receiver. The measured data also suggests that the downconversion stage has a linear dynamic range greater than or equal to the AS-520 microscan receiver, otherwise the measured 1 dB compression point would have been lower. This large

**Table 4.3: Linear Dynamic Range of the Receiving System Taken
at Selected Frequencies in the 3200 to 3220 MHz Band.**

RF (MHz)	IF (MHz)	Sensitivity (dBm)	1 dB Comp. Pt. (dBm)	Dynamic Range (dB)
3200	150	-123	-53	70
3206	156	-123	-54	69
3208	158	-123	-51	72
3209	159	-123	-53	70
3210	160	-123	-52	71
3215	165	-123	-50	73
3220	170	-123	-54	69

**Table 4.4, Linear Dynamic Range of the Receiving System
Taken at Frequencies Spaced 100 MHz From Each
Other in the Frequency Range Between 3.2 to 4.2 GHz.**

RF (MHz)	IF (MHz)	Sensitivity (dBm)	1 dB Comp. Pt. (dBm)	Dynamic Range (dB)
3310	160	-123	-53	70
3410	160	-123	-53	70
3510	160	-123	-50	73
3610	160	-123	-53	70
3710	160	-123	-53	70
3810	160	-123	-53	70
3910	160	-123	-53	70
4010	160	-123	-52	71
4110	160	-123	-51	72

dynamic range was verified with a spectrum analyzer at an input frequency of 3210 MHz, for which a linear dynamic range greater than or equal to 80 dB was measured. Figure 4.7 illustrates the linear dynamic range of the downconversion stage at an input frequency of 3210 MHz.

4.3.6.2 Instantaneous Dynamic Range

The maximum amplitude separation for which the receiver can handle both a strong signal and a weak signal correctly was evaluated. This test was conducted using two signal generators and an oscilloscope to monitor the output. A fixed input signal was set at a relatively strong level, while another (separated from the first by more than twice the signal frequency resolution of the receiver) was decreased in 1 dB steps using precision attenuators until it was barely discernible on the oscilloscope. This level for the weaker signal was measured at selected frequencies above and below the stationary strong signal, and the data was recorded. These steps were repeated for the upper, lower, and center frequencies of the first 20 MHz bandwidth inside the 3.2 to 4.2 GHz band. Similar measurements were then performed at the center frequencies of 20 MHz bands, separated by 100 MHz spacings, across the full 1 GHz bandwidth.

The results revealed that in both sets of measurements, for a frequency separation of approximately 80 KHz, the maximum amplitude separation is typically 28.3 dB on the upper side of the strong signal and 26.2 dB on the lower side. Again, the different results on each side of the strong signal was anticipated due to the unsymmetrical pulse spectrum. In addition, these values are slightly below the 30 dB amplitude separation specified by the manufacturer of the AS-520.

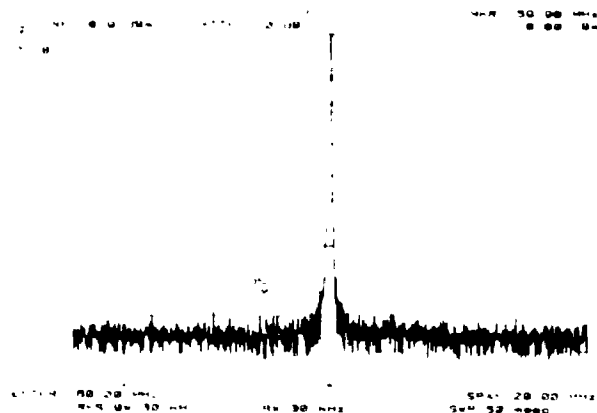


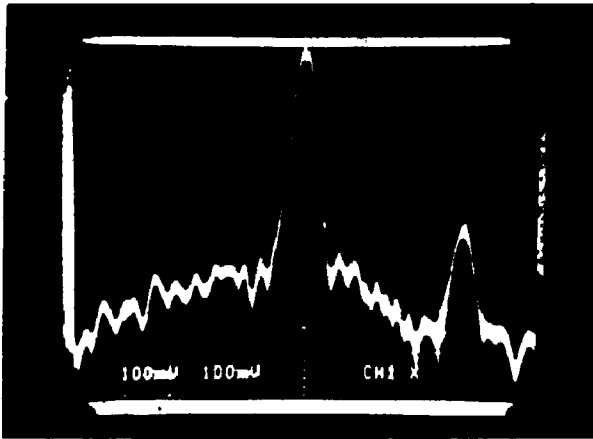
Figure 4.7: Downconversion stage linear dynamic range for CW tone at 3210 MHz.

However, this too was not surprising with the larger than expected 3 dB pulse width. The best case and worse case values for the upper side of the strong signal are 33 dB and 12 dB respectively. Best case and worst case values for the lower side are 29 dB and 30 dB respectively. The instantaneous dynamic range on the lower side of the strong signal is consistently worse than that of the upper side for offsets as large as 300 KHz. Also, a slight degradation occurs at the upper edge of the measured 20 MHz bandwidth as well as the higher frequencies in the 3.2 to 4.3 GHz band.

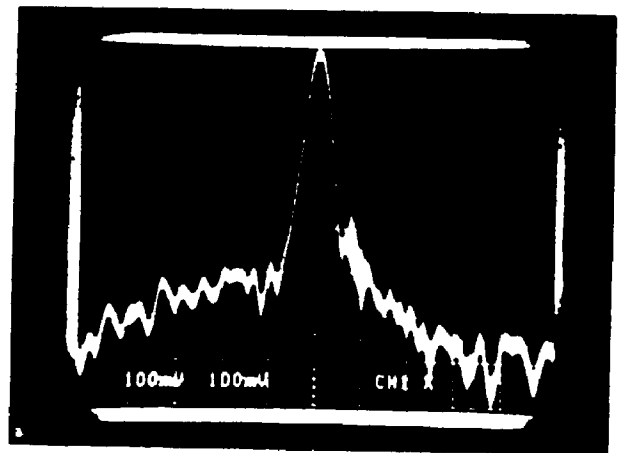
Figure 4.8 illustrates the instantaneous dynamic range measurement. The strong signal frequency was at 3212 MHz with an input power of -20 dBm. Figure 4.8(a) illustrates a weaker signal 30 dB down at 355 KHz offset from the stronger signal, while Figure 4.8(b) illustrates the weaker signal (still 30 dB down) almost indistinguishable at 80 KHz offset.

4.3.6.3 Two-Tone Spur Free Dynamic Range

For this test, two signals of equal amplitude, separated by more than two frequency resolutions of the receiver, were combined in a passive power combiner at the input of the system. Third order intermodulation suppression was measured at both the down conversion point, and at the output stage of the system using a spectrum analyzer and an oscilloscope respectively. Three sets of measurements were conducted in the 3.2 to 4.2 GHz band. The first set was performed in the frequency band extending from 3200 to 3220 MHz and consisted of maintaining a constant frequency separation between the two input signals while changing the absolute frequency. A second set of data was



(a)



(b)

Figure 4.8: Instantaneous dynamic range for a strong CW tone at 3212 MHz with -20 dBm input power.
 (a) Weak signal 30 dB down at 355 KHz offset.
 (b) Maximum amplitude separation of 30 dB at 80 KHz offset (x-axis: 1 μsec/div., y-axis: 8 dB/div.).

also taken inside the 3200 to 3220 MHz band by changing the frequency separation between the input signals. Lastly, the third set of data was obtained at frequencies spaced 100 MHz apart across the 3200 to 4200 MHz band with constant frequency separation between the input signals.

Some of the results obtained for the three sets of measurements are shown in Figure 4.9 for the downconversion stage. The CW tones had an input power of -43 dBm. The value for the third order suppression is clearly indicated by the delta marker in each of the figures. The third order intercept point was computed from the third order suppression as follows:

$$P_{31} = P_i + \frac{S}{2} \quad (4.2)$$

where P_i is the input signal power and S is the third order suppression. The typical third order intercept point value obtained from all the sampled data points is 19.92 dBm. This value compares relatively well with the previously calculated intercept point of 15.31 dBm, considering the theoretical value is for a worst case performance in a perfect 50 ohm system. The two-tone spur-free dynamic range was then calculated using equation (2.19). The results obtained using the experimental values of $P_{31,T}$, G , and threshold equals to:

$$\begin{aligned} \text{SFDR} &= \frac{2}{3} (P_{31,T} - G - \text{threshold}) \\ &= \frac{2}{3} (19.92 \text{ dBm} - 33.2 \text{ dB} - (-123 \text{ dBm} + 13.2 \text{ dB})) \\ &= 64.3 \text{ dB} \end{aligned}$$

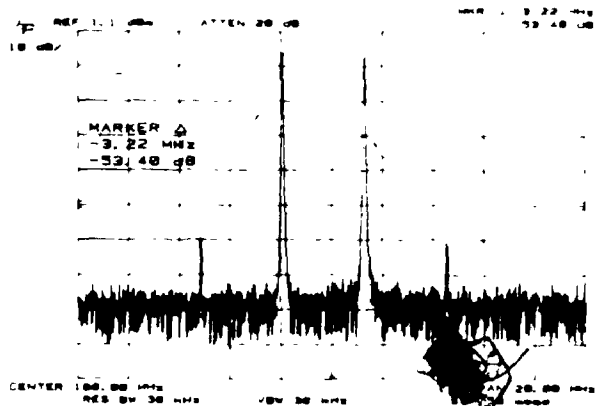
This value is approximately 3 dB greater than the calculated theoretical value obtained for the cascaded components in Chapter 3.

Similarly, the same sets of measurements were taken for the entire system at the output of the oscilloscopes with the results displayed in Figure 4.10. The typical third order intercept point obtained from the measured data point was -0.23 dB, while the SFDR was calculated to be 50.9 dB. Clearly, the higher level of spurious products are generated by the AS-520 microscan receiver and not the downconversion stage. However, the usable SFDR is not the limiting factor, here. The clutter level generated by the AS-520 receiver is far more limiting, as far as system dynamic range is concerned, for it always appears approximately 45 dB below the peak signal.

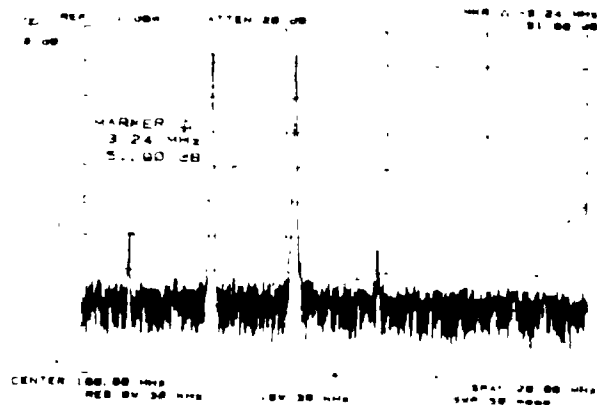
4.3.7 Pulse Width

The relative sensitivity of the receiver for different input pulse widths was determined. The input pulse width was varied using a pulse generator while the output was monitored on the oscilloscope.

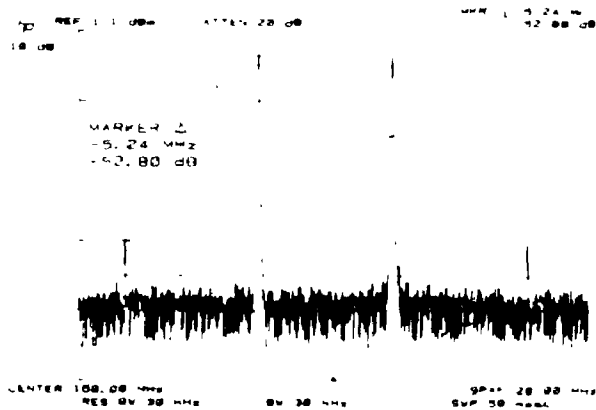
The relative sensitivity degradation of the receiver for pulses narrower than the filter integration time ($T \leq 50 \mu\text{sec}$) is evident in Figure 4.11. The measurements were taken at 160 MHz with an input power of -36 dBm. Figure 4.11(a) illustrates the output spectrum for a pulse duration of 200 μsec . No sensitivity degradation is noticeable at this point, however the base of the pulse is wider. This is the result of certain pulses being only partially intercepted during the 210 μsec scan period of the receiver.



(a)



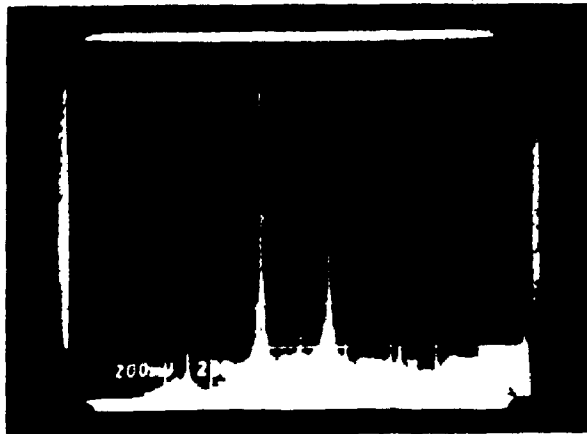
(b)



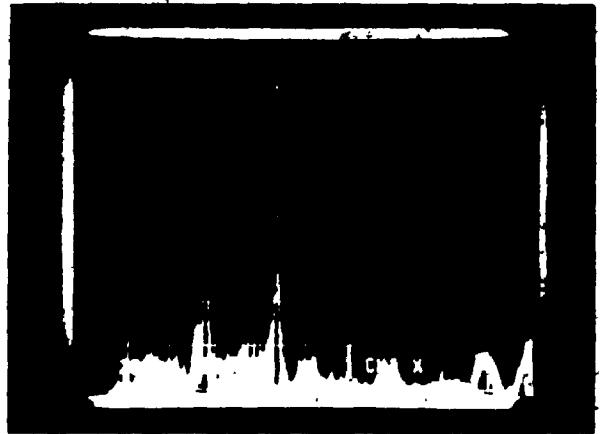
(c)

Figure 4.9: Two-tone 3rd order suppression of the downconversion stage inside the 3200 to 3220 MHz band for CW inputs of -43 dBm.

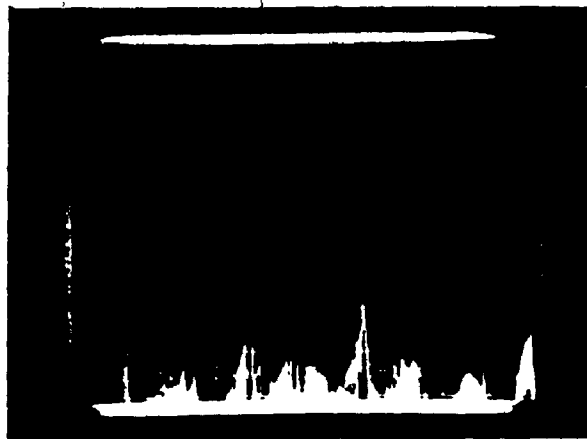
- (a) $f_1 = 3208.068$ MHz, $f_2 = 3211.320$ MHz, and 3rd order suppression = 53.40 dB;
- (b) $f_1 = 3208.38$ MHz, $f_2 = 3205.068$ MHz, and 3rd order suppression = 51.90 dB;
- (c) $f_1 = 3207.068$ MHz, $f_2 = 3212.34$ MHz, and 3rd order suppression = 52.80 dB.



(a)



(b)



(c)

Figure 4.10: Two-tone 3rd order suppression of the system inside the 3200 to 3220 MHz band for CW inputs of -43 dBm.

(a) $f_1 = 3208.068$ MHz, $f_2 = 3211.320$ MHz,
suppression = 38 dB;

(b) $f_1 = 3205.068$ MHz, $f_2 = 3208.380$ MHz,
suppression = 37 dB;

(c) $f_1 = 3207.068$ MHz, $f_2 = 3212.340$ MHz,
suppression = 38 dB.

(x-axis: 20 μ sec/div.; y-axis: 6.3 dB/div.)

Figure 4.11(b) illustrates the output spectrum for an input pulse duration of 20 μ sec. At this point sensitivity degradation results in a 3.2 dB drop in amplitude. The base of the pulse remains essentially the same as in (a).

Figure 4.11(c) illustrates the output pulse for an input pulse width of 2 μ sec. The shape of the pulse closely resembles the $\sin x/x$ pattern having a mainlobe with a number of adjacent nulls and sidelobes. The spreading of the pulse energy in the sidelobes results in a sensitivity degradation of 23 dB relative to the input.

Figure 4.11(d) illustrates the output pulse for an input pulse width of 0.2 μ sec. A severe sensitivity degradation occurs with the pulse energy completely spread throughout many adjacent frequency resolution cells, with the output pulse response being 45 dB below the input.

The input pulse width versus the relative sensitivity degradation is plotted in Figure 4.12 for a gated CW pulse at 160 MHz with an input power of -36 dBm. The slope of the curve reveals a 20 dB per pulsewidth-decade sensitivity degradation for pulses narrower than the filter integration time of 50 μ sec. This occurs as a result of a combination of compression ratio loss and conservation of energy as discussed in Chapter 2 under Section 2.3.4. Consequently, the wideband surveillance system can only faithfully process pulses that are greater than the filter integration time of 50 μ sec.

```

100 LOCAL 719
110 BEEP 2000,.5
120 PRINT TABXY(30,15),"END OF ROUTINE"
130 TOP
140 END
150
160 ..... SUB NO. 1 .....
170
180 SUB Check
190 BEEP 1000,.5
200 BEEP 500,.5
210 OUTPUT 21"K":
220 PRINTER IS "I
230 PRINT TABXY(4,10),"INSTRUMENT MALFUNCTION--CHECK SET UP"
240 PRINT TABXY(5,13),"GPIB CABLE CONNECTED ?"
250 PRINT TABXY(6,14),"CHECK IF PROPER ADDRESS?"
260 PRINT TABXY(7,15),"IS POWER SWITCH ON?"
270 PRINT TABXY(8,18),"PRESS RST/RUN KEY & TRY AGAIN"
280 PAUSE
290 OUTPUT 21"K":
300 SUBEND
310
320 ..... SUB NO. 2 .....
330
340 SUB Prog
350 PRINT TABXY(28,1),"FREQUENCY HOPPING PROGRAM"
360 PRINT TABXY(14,4),"DEVICE USED          MODEL          BUS ADDR "
370 PRINT TABXY(14,6),"FREQ. SYNTH          HP 8672A          19 "
380 PRINT TABXY(17,10),"THIS PROGRAM ENABLES THE FREQ. SYNTH TO HOP"
390 PRINT TABXY(17,12),"PREDETERMINED STEPS ANYWHERE FROM 1 GHZ TO "
400 PRINT TABXY(17,14),"18 GHZ & GENERATE A TIME PULSE AT EACH HOP"
410 PRINT TABXY(17,16),"TO BE USED AS AN EXTERNAL TRIGGER TO A RX"
420 PRINT USING "/"
430 SUBEND
440
450 .....

```

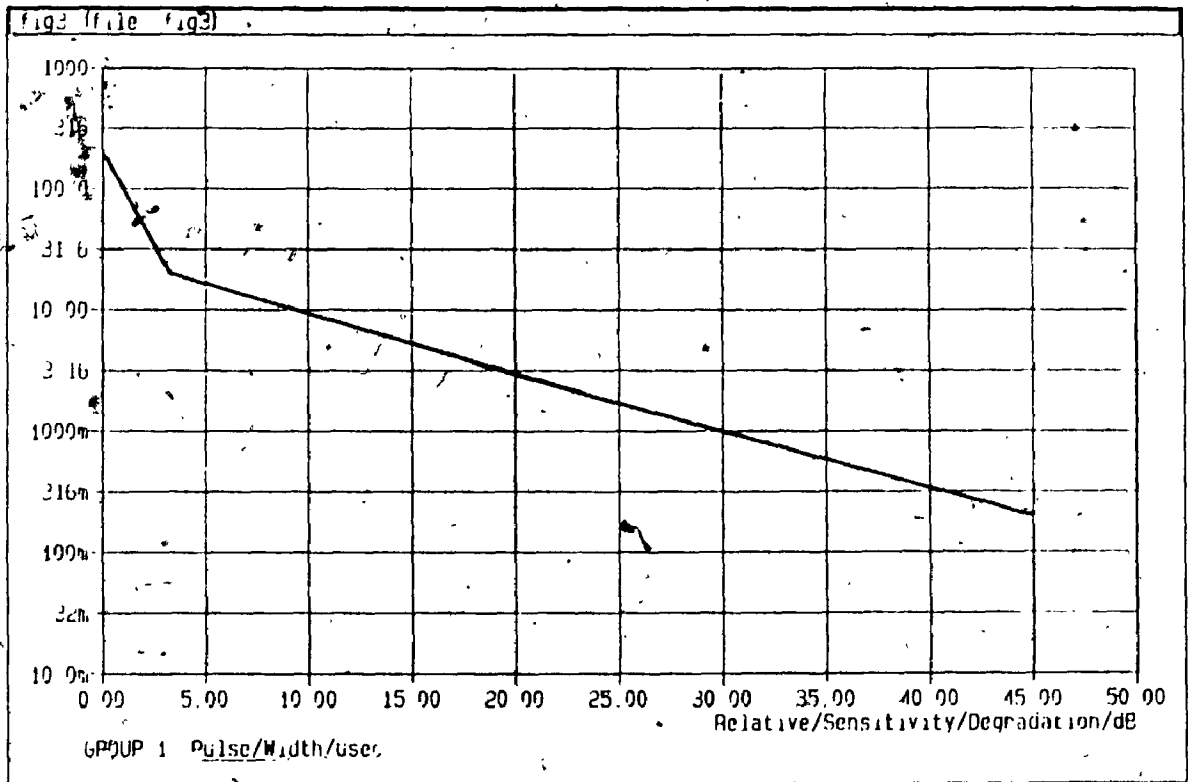


Figure 4.12: Pulse width versus relative sensitivity degradation.

Chapter 5

CONCLUSIONS

5.1 SYSTEM EVALUATION

A wideband microwave surveillance system for identifying pulsed and CW signals in a 1 GHz bandwidth has been conceived, assembled and demonstrated. The marriage of both a superheterodyne and a microscan receiver offers a viable solution for performing wideband signal analysis. The system performance was essentially in good agreement with the theoretical predictions. The receiver was shown to be capable of scanning a 1 GHz bandwidth in 762.5 msec, while providing real-time analog processing on signal levels as low as -123 dBm for a frequency separation of 40 KHz and an accuracy of ± 26 KHz. Its high processing speed, low power consumption, low cost, small size, and light weight definitely makes it an attractive candidate as a portable surveillance system for various applications.

Although, this receiver is a powerful measurement system some of its performance characteristics would have to be upgraded before it could actually be employed to identify undesired noise signals in a communication link. For instance, improved phase matching between the SLOs and the SAW dispersive filters would have to be introduced in order to produce frequency resolution cells on the order of 30 KHz for a closer match with the communication channel spacings. The sidelobe level of -32 dB and the clutter level of -45 dB would have to be

improved for better simultaneous signal dynamic range performance. This implies that better windowing be incorporated in the SAW filters. It would also be considered advantageous to have an AGC circuit to control the amount of power going into the system in order to avoid premature saturation or even damage to the receiver. An AGC would also maintain the noise level relatively constant and, hence, stabilize the false alarm rate. It would be deemed essential to improve the existing POI of the receiver by using a more rapid stepping LO such as a direct frequency synthesizer. The POI for frequency agile signals could also be improved considerably by increasing the TBP of the system with a wider instantaneous bandwidth (i.e. search window). Large TBPs are now achievable using RAC filtered technology. State-of-the-art microscan intercept receivers are now approaching TBPs on the order of 2000 with 80 dB linear dynamic range and a 100% POI using this technique. Despite some of its limitations, the present system is not precluded from performing in applications where it requires less fine-grain signal analysis.

5.2 FUTURE STUDIES

It is recommended that some future efforts be devoted to the implementation of fast-hopping. This would not only increase the system throughput but would improve the POI on short duration pulse signals immensely. Some work should also be devoted to developing a means for digitizing the analog output from the microscan receiver to extract such information as frequency, amplitude, and time of arrival on a pulse-by-pulse basis. The digitization of information is of paramount importance for processing large quantities of data coming from a system operating

in a dense signal environment. Finally, valuable knowledge could be gained on the real performance of this system by conducting field trial experiments.

REFERENCES

- [1] Skolnik, M.I., Introduction to Radar Systems, 2nd Edition, McGraw-Hill, New York, 1980.
- [2] Tsui, J.B-Y., Microwave Receivers and Related Components, Air Force Avionics Laboratory, Wright-Patterson Air Force Base, Ohio, 1983.
- [3] Zeimer, R.E. and Tranter, W.H., Principles of Communication Systems: Modulation and Noise, 2nd Edition, Houghton Mifflin Company, Boston, 1985.
- [4] Miller, R.P., "Understanding Receiving System Design Parameters", Microwave Journal, Vol.28, No.2, pp.175-177, February 1985.
- [5] Cheadle, D.L., "Performance Parameters Cascading Rule", Watkins-Johnson Co., Tech. Notes, Vol.6, No.1, January/February 1979.
- [6] McDowell, R.K., "High Dynamic Range Receiving Parameters", Watkins-Johnson Co., Tech. Notes, Vol.7, No.2, March/April 1980.
- [7] Cheadle, D.L., "Cascadable Amplifiers", Application Note, Watkins-Johnson Co., 1981.
- [8] Donaldson, G.J., "Competitive Receiver Technologies", Watkins-Johnson Co., Tech. Notes, Vol.11, No.4, July/August 1984.
- [9] Harper, T., "High Probability of Intercept Receivers", Watkins-Johnson Co., Tech. Notes, Vol.2, No.4, July/August 1975.
- [10] Jack, M., Grant, P.M. and Collins, J.H., "The Theory, Design and Applications of Surface Acoustic Wave Fourier-Transform Processors", Proceedings of the IEEE, Vol.68, No.4, pp.450-468, April 1980.
- [11] Otto, O.W., "The Chirp Transform Signal Processor", in Proc. IEEE Ultrasonics Symposium (76 CHL120-5S0), pp.365-370, 1976.
- [12] Bristol, T.W., "Review of Spectrum Analysis With SAW Chirp Transform and Filter Banks", IEE Conference Proceeding #180, pp.226-231, September 1979.
- [13] Klauder, J.R., Price, A.C., Darlington, S. and Albersheim, W.I., "The Theory and Design of Chirp Radars", The Bell System Technical Journal, Vol.39, No.4, pp.745-808, July 1960.
- [14] Schmid, H.F., "Microscan Receivers Boost Intercept Probability", Defense Electronics, pp.205-214, October 1986.

- [15] Harrington, J.B. and Nelson, R.B., "Compressive Intercept Receiver Uses SAW Devices", Microwave Journal, pp.57-62, September 1977.
- [16] Maines, J.D. and Paige, E., "Surface-Acoustic-Wave Devices for Signal Processing Applications", Proc. of the IEEE, Vol.64, No.5, pp.639-651, May 1976.
- [17] Jack, M.A. et al., "Real Network Analyzers Based On SAW Chirp Transform Processors", Proc. of IEEE Ultrasonic Symposium (76 CHI120-5SU), pp.376-381, 1976.
- [18] Bridle, L. and Haykin, S., "A Study of SAW Based Fourier Transformers - Part 1: An Executive Summary", CRL Internal Report Series CRL-108, February 1983.
- [19] Bridle, L. and Haykin, S., "A Study of SAW Based Fourier Transformers - Part II: The SAW Fourier Transformer", CRL Internal Report Series CRL-108, February 1983.
- [20] Williamson, R.C., "Wideband SAW Fourier Transform Design and Application", IEE Conference Proceeding #180, pp.237-243, September 1979.
- [21] Jack, M.A. and Collins, J.H., "Fast Fourier Transform Processor Based on the SAW Chirp Transform Algorithm", in Proc. IEEE Ultrasonic Symposium (78 CH1344-1SU), pp.533-548, 1978.
- [22] Arsenault, D.R. and Dolat, U.S., "Compact Multiple Channel SAW Sliding Window Spectrum Analyzer", in Proc. IEEE Ultrasonic Symposium, pp.220-225, 1981.
- [23] Lardat, C., "Improved SAW Chirp Spectrum Analyser With 80 dB Dynamic Range", in Proc. IEEE Ultrasonic Symposium (78 CH1344-ISU), pp.518-521, 1978.
- [24] Butson, C., Lucas, W.J. and Thompson, G.T., "Theoretical Assessment of the Use of Pulse Compression in a Panoramic Receiver", Proc. of the IEE, Vol.113, No.5, pp.725-739, May 1966.
- [25] Taub, J., "Microwave and Millimeter-Wave Technology Aids EW System Design", Military Microwaves, pp.233-262, 1984.
- [26] Harris, F.J., "On the Use of Windows for Harmonic Analysis With Discrete Fourier Transform", in Proc. of the IEEE, Vol.66, No.1, pp.51-83, January 1978.
- [27] Bharj, J.S. and Rushton, J.F., "17/12 GHz Low Noise Receiver for UNISAT TV DBS Satellite", Microwave Journal, Vol.28, No.10, pp.143-146, October 1985.
- [28] Hundley, R.E., Estabrook, P. and Crescenzi, E.J., "Small Low Gain Amplifiers for Front-End Designs", Application Note, Watkins-Johnson Co., 1980/1981.

- [29] Henderson, B.C., "Mixers - Part 1: Characteristics and Performance", Watkins-Johnson Co., Tech. Notes, Vol.8, No.2, March/April 1981.
- [30] Cheadle, D., "Selecting Mixers For Best Intermod Performance - Part I and II", Application Note, Watkins-Johnson Co., 1980/1981.
- [31] Henderson, B.C. and Cook, J.A., "Image-Reject and Single-Sideband Mixers", Watkins-Johnson Co., Tech. Notes, Vol.12, No.3, May/June 1985.
- [32] Gardner, F.M., Phaselock Techniques, 2nd Edition, Wiley-Interscience, New York, 1979.
- [33] ARGO Systems Inc., "Model AS-520 IF Compressive Receiver", Prod. Spec., November 1978.
- [34] Hewlett-Packard Co., Prod. Cat., 1986 Edition New Products.
- [35] Daniels, W.D., Churchman, M. and Kyle, R., "Compressive Receiver Technology", Microwave Journal, Vol.29, No.4, pp.175-185, April 1986.
- [36] Haykin, S., Communications Systems, John Wiley & Sons, New York, 1978.
- [37] Dexter, C.E., "Digitally Controlled VHF/UHF Receiver Design", Watkins-Johnson Co., Tech. Notes, Vol.7, No.3, May/June 1980.
- [38] Hatcher, B.R., "EW Acquisition Systems ... Probability of Intercept and Intercept Time", Watkins-Johnson Co., Tech. Notes, Vol.3, No.3, May/June 1976.

APPENDIX A

ARGOS AS-520 MICROSCAN RECEIVER SPECIFICATIONS

Table of Specifications

FREQUENCY COVERAGE	155 MHz to 165 MHz and 150 MHz to 170 MHz
SCAN RATE	4.7 KHz for 20 MHz coverage 9.1 KHz for 10 MHz coverage
RESOLUTION BANDWIDTH	28 KHz typical at -3 dB points 80 KHz typical at -30 dB points
FREQ. ACCURACY (EXCLUDING DISPLAY)	<u>+10 KHz</u>
DYNAMIC RANGE	
FULL SCALE INPUT	<u>-20 dBm post attenuator</u>
FULL SCALE TO MINIMUM DETECTABLE SIGNAL RATIO	>60 dB for 50 percent detection and 1 FA/sec
CLOSE-IN SIDELobe SUPPRESSION	<u>>30 dB</u>
CLUTTER SUPPRESSION	<u>>45 dB</u>
AMPLITUDE VARIATION	<u>+1.5 dB</u>

FRONT PANEL CONTROL

IF ATTENUATOR

0 to 60 dB in 1 dB and 10 dB steps

BANDWIDTH

10 MHz, 20 MHz

SCAN TRIG

Internal, External

FREQUENCY MARKERS

Crystal derived tones at 150, 155, 160, 165, 170 MHz energized at 0.025, 0.25, 2.5, or 25 percent of scans with off position

DISPLAY SELECT

PAN

Panoramic (Amplitude versus Frequency)

PAN/EXP PAN

Split screen display with normal panoramic on upper half and expanded panoramic on lower half

PAN/RASTER

Split screen display with normal panoramic on upper half and raster on lower half

PAN/EXP RASTER

Split screen display with normal panoramic on upper half and expanded raster on lower half.

DISPLAY CONTROLS

RASTER

Selects 10, 20, 40, or 80 lines

EXPAND WIDTH

Selects 10 percent or 20 percent of scanned bandwidth to be expanded.

EXPAND POSITION

Positions area to be expanded

RASTER TRIG

Internal, External, Internal adjustable with front panel potentiometer

Z-AXIS CONTROLS

THRESHOLD

Sets level at which thresholding occurs

INTENSITY

Adjusts level of Z-Axis voltage

AUDIO

SELECT AM, FM and OFF positions with volume control

POSITION Coarse and fine control of demodulation gate

OUTPUT 600 ohm phone jack

POWER

ON/OFF Pushbutton with light

REAR PANEL

INPUTS

IF 150 MHz to 170 MHz; $\leq 2.0:1$ VSWR

SCAN TRIG Requires $\geq +1$ volt pulse into 1 Kiloohm for external triggering

RASTER TRIG Requires $\geq +1$ volt pulse into 1 Kiloohm for external triggering

DISPLAY OUTPUT

VERT -1V to +1V video into 50 ohms

HORIZ +1 volt to -1 volt ramp into 50 ohms

Z-AXIS 0 to +1 Volt into 50 ohms

VISICORDER OUTPUT

HORIZ +3 volt to -3.volt ramp into 1 Kiloohm

Z-AXIS TTL with high drive capability

AUX OUTPUT

VIDEO 0 volt to +1 volt video into 50 ohms

THRESHOLDED VIDEO TTL with high drive capability

DATA FRAME

TTL with high drive capability.
Brackets the valid output video;
PW=100 μ sec for 10 MHz coverage
and 200 μ sec for 20 MHz coverage.

1 MHz CLK

TTL with high drive
capability. Synchronized
to internal timing clocks.

TTL INVERTER

TTL input and TTL output with
high drive capability

PACKAGING

SIZE

8" x 19" x 20" (H,W,D)

WEIGHT

45 lbs.

POWER

VOLTAGE

107 to 127 VAC

FREQUENCY

47 to 440 Hz

CURRENT

1.0 AMPS

APPENDIX B

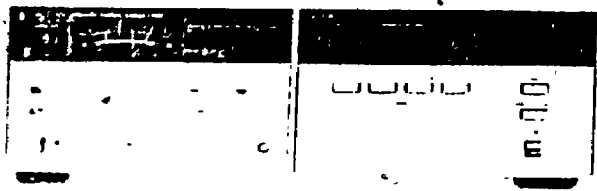
HP8672A AND HP8662A SIGNAL GENERATOR SPECIFICATIONS

SIGNAL GENERATORS

545



... frequency range
... phase noise



HP 8672A

HP 8672A, 8673B Specifications

(HP 8672A and 8673B specifications are identical except for additional HP 8673B specifications in *italics* type.)

Frequency range: 20-180 GHz (18-99997 GHz overrange)

20-260 GHz; 126.5 GHz overrange

Frequency bands: Band 1, 20-6.2 GHz; 20-6.6 GHz;

Band 2, 6.2-12.4 GHz; 6.6-12.4 GHz;

Band 3, 12.4-18.0 GHz; 12.3-18.6 GHz;

Band 4, 18.6-26.0 GHz

Frequency resolution: 1 kHz in Band 1, 2 kHz in Band 2, 3 kHz in Band 3, 4 kHz in Band 4

Time base: 100 MHz (±0.1%), day aging rate) or external 10 MHz

Frequency switching time: 15 ms to 20 ms to be within specified resolution in all bands.

Single-sideband phase noise (1 Hz BW, CW mode):

F _c	Offset from F _c			
	10 Hz	100 Hz	1 kHz	10 kHz
E	70 dBc	78 dBc	86 dBc	110 dBc
F	64 dBc	72 dBc	80 dBc	104 dBc
G	60 dBc	68 dBc	76 dBc	100 dBc
H	58 dBc	65 dBc	74 dBc	98 dBc

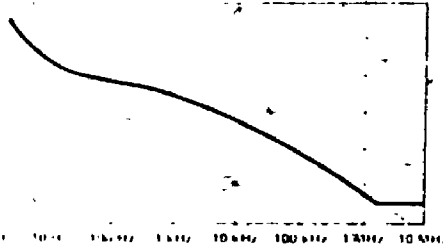


Figure 2. Typical HP 8672A & 8673B single-sideband phase noise performance using the internal standard, Band 1.

Harmonics (up to maximum frequency, output level meter readings 0 dB on 0 dBm range and below): -25 dBc, -40 dBc

Sub-harmonics and multiples thereof: -40 dBc, Bands 1, 3, 4; -45 dBc, Band 2

Spurious (CW and AM modes):

Non-harmonically related: -70 dBc, Band 1; -64 dBc, Band 2; -60 dBc, Band 3; -55 dBc, Band 4

Power line related and fan rotation related within 5 Hz below line frequency and multiples thereof:

Offset from F _c	Offset from F _c	
	300 Hz to 1 kHz	1 kHz
300 Hz	-60 dBc	-65 dBc
1 kHz	-55 dBc	-59 dBc
3 kHz	-50 dBc	-55 dBc
10 kHz	-45 dBc	-50 dBc

Output Characteristics

Output level (+15°C to +35°C): +3 to -120 dBm;

+8 to -100 dBm up to 18 GHz; +4 to -100 dBm up to 22 GHz; 0 to -100 dBm up to 26 GHz.

Flatness (0 dBm range, +15°C to +35°C): ±0.75 dB through Band 1, ±1.0 dB through Band 2, ±1.25 dB through Band 3, ±1.75 dB through Band 4.

Remote programming output level resolution: 1.0 dB; 0.1 dB

Source impedance: 50 ohms nominal.

Pulse Modulation (HP 8673B)

ON/OFF ratio: >80 dB

Rise/fall times: <35 ns

Minimum-leveled pulse width: <100 ns

Pulse repetition frequency: dc-1 MHz.

Maximum peak power: same as in CW mode

Peak level accuracy (relative to CW, +15°C to +35°C): ±1.5 dB.

Pulse modulation input requirements: normal mode, positive-true TTL levels, complement mode, negative-true TTL levels

Video feedthrough: typically <-50 dBc

Video input to 100 MHz

Rates (3 dB BW, 30% depth): 10 Hz-100 kHz; 10 Hz-50 kHz

(Option 008), 20 Hz-100 kHz

Sensitivity: 30%/V, 100%/V ranges. Max. input 1 V peak into 600 Ω

Peak deviation (max.): the smaller of 10 MHz or f_{mod} × 5, Band 1;

10 MHz or f_{mod} × 10, Band 2; 10 MHz or f_{mod} × 15, Band 3;

10 MHz or f_{mod} × 20, Band 4

Sensitivity: 30, 100, 300 kHz/V and 1, 3, 10 MHz/V ranges

Max. input 1 V peak into 50 Ω

Rates (3 dB BW typical): 30, 100 kHz/V ranges 50 Hz to 10 MHz;

300 kHz/V and 1, 3, 10 MHz/V ranges 1 kHz to 10 MHz

Video input to 100 MHz (HP 8673B)

Sweep function: start/stop or ΔF (span) sweep.

Sweep modes: manual, auto, or single sweep

Step size: maximum of 9999 frequency points per sweep, minimum

step size equals frequency resolution

Dwell time: set from 1 to 255 μs per frequency.

Markers: 5 independent, settable frequency markers

Sweep outputs: 0 to +10 V ramp start to stop; 1 V/GHz ramp (18 V maximum), Z-axis blanking/markers, tone marker, penlift.

Remote Programming

All functions HP-IB programmable except line switch. The HP 8673B can output over the interface frequency and output level settings, error/malfunction codes, and operational status codes.

Interface functions:

HP 8673B: SHI, AHI, T5, TE0, L3, LE0, SRI, RLI, PPI, DCI, DTI, CO, EI

HP 8672A: SHI, AHI, T6, TE0, L4, LE0, SRI, RLO, PP2, DCI, DT0, CO, EI

General

Operating temperature range: 0°C to +55°C.

Power: 100, 120, 220, 240 V, +5%, -10%, 48-66 Hz; 400 VA max.

Weight: net, 27 kg (60 lb), 29 kg (64 lb). Shipping, 32.5 kg (72 lb), 34.5 kg (76 lb).

Size: 133 mm H x 425 mm W x 603 mm D (5.25" x 16.75" x 23.75").

Ordering Information

HP 8673B Synthesized Signal Generator

HP 8672A Synthesized Signal Generator

Option 001: Delete RF output attenuator

Option 002: Delete reference oscillator

Option 003: Operation at 400 Hz line

Option 004: Rear panel RF output

Option 005: Rear panel RF output without RF

attenuator

Option 006: Chassis slide kit

Option 008: +8 dBm (+7 dBrms) output level

Option 907: Front panel handle kit

Option 908: Rack mounting flange kit

Option 909: Front panel handle kit plus rack mounting

flange kit

Option 910: Extra operating and service manual

HP 11712A Support kit (for HP 8672A)

HP 11726A Support kit (for HP 8673B)

App-B2

SIGNAL GENERATORS

Synthesized Signal Generators

Models 8662A, 8663A (cont.)

HP 8662A Specifications

Frequency

Range: 10 kHz to 1280 MHz (1279.9999998 MHz).

Resolution: 0.1 Hz (0.2 Hz above 640 MHz).

Accuracy and stability: same as reference oscillator.

Internal reference oscillator: 10 MHz quartz oscillator. Aging rate $< 5 \times 10^{-10}$ /day after 10 day warm-up (typically 24 hrs in normal operating environment).

Spectral Purity

Residual SSB Phase Noise In 1 Hz BW ($320 \leq f_c < 640$ MHz)

Offset from Carrier				
10 Hz	100 Hz	1 kHz	10 kHz	100 kHz
-100 dBc	-112 dBc	-121 dBc	-131 dBc	-132 dBc

SSB broadband noise floor in 1 Hz BW at 3 MHz offset from carrier: < -146 dBc for f_c between 120 and 640 MHz at output levels above +10 dBm.

Spurious Signals

	Frequency Range (MHz)				
	0.01 to 120	120 to 160	160 to 320	320 to 640	640 to 1280
Spurious non-harmonically related ^{1,2}	-90 dBc	-100 dBc	-96 dBc	-90 dBc	-84 dBc
Sub-harmonically related ($\frac{1}{2}, \frac{3}{2}$, etc.)	none	none	none	none	-75 ³ dBc
Power line (60Hz) related or microphonically generated (within 300 Hz) ⁴	-90 dBc	-85 dBc	-80 dBc	-75 dBc	-70 dBc
Harmonics	< -30 dBc				

Output

Level range: +13 to -139.9 dBm (1V to 0.023 μ V_{rms} into 50 Ω).

Resolution: 0.1 dB.

Absolute level accuracy (+15° to +45°C): ± 1 dB between +13 and -120 dBm, ± 3 dB between -120 and -130 dBm.

BWR: typically from 1.5 to 1.8 depending on output level and frequency.

Reverse power protection: typically up to 30W or ± 8 Vdc.

Amplitude Modulation

Depth: 0 to 95% at output levels of +8 dBm and below (+10 dBm in uncorrected mode). AM available above these output levels but not specified.

Resolution: 1%, 10 to 95% AM; 0.1%, 0 to 9.9% AM.

Incidental PM (at 30% AM): 0.15-640 MHz, < 0.12 radian peak; 640-1280 MHz, < 0.09 radian peak.

Incidental FM (at 30% AM): 0.15-640 MHz, $< 0.12 \times f_{mod}$; 640-1280 MHz, $< 0.09 \times f_{mod}$.

Indicated accuracy: $\pm 5\%$ of reading $\pm 1\%$ AM. Applies for rates given in table below, internal or external mode, for depths $\leq 90\%$.

Rates and Distortion with Internal or External Modulating Signal

Frequency range	AM rate	AM Distortion		
		0-30% AM	30-70% AM	70-90% AM
0.15-1 MHz	dc-1.5 kHz	2%	4%	5.75%
1-10 MHz	dc-5 kHz	2%	4%	5.75%
10-1280 MHz	dc-10 kHz	2%	4%	5.75%

Frequency Modulation

FM rates (1 dB bandwidth): external ac, 20 Hz to 100 kHz; external dc, dc to 100 kHz.

FM deviation: from 25 to 200 kHz depending on carrier frequency. Indicated FM accuracy: $\pm 8\%$ of reading plus 10 Hz (30 Hz to 20 kHz).

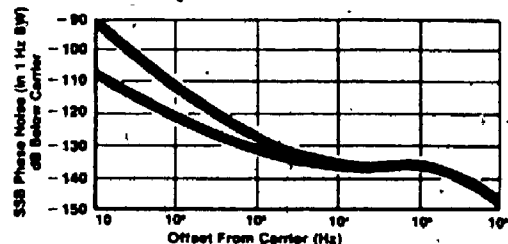
FM resolution: 100 Hz for deviations < 10 kHz, 1 kHz for deviations ≥ 10 kHz.

Incidental AM (AM sidebands at 1 kHz rate and 20 kHz deviation): < -72 dBc, $f_c < 640$ MHz; < -65 dBc, $f_c \geq 640$ MHz.

FM distortion: $< 1.7\%$ for rates < 20 kHz, $< 1\%$ for rates < 1 kHz. Center frequency accuracy and long term stability in AC mode: same as CW mode.

Supplemental Characteristics

Typical Absolute and Residual SSB Phase Noise, 630 MHz Carrier.



Frequency switching speed:⁶ From 420 μ sec to 12.5 msec, depending on the programming mode.

HP 8663A Specifications

The HP 8663A signal generator is related to the HP 8662A in both concept and structure. The HP 8662A concept of an extremely low phase noise signal source incorporating signal generator modulation capabilities and output characteristics is carried even further by the HP 8663A. While maintaining high spectral purity, the HP 8663A offers increased frequency range to 2560 MHz, increased output level to +16 dBm, and the addition of phase and pulse modulation. The result is a highly flexible and powerful signal generator that utilizes and extends the proven circuitry of the HP 8662A. Thus, the HP 8662A and HP 8663A share many of the same specifications as shown below:

Frequency

Range: 100 kHz to 2560 MHz (2559.9999996 MHz)

Resolution: 0.1 Hz ($f_c < 640$ MHz)

0.2 Hz ($640 \text{ MHz} \leq f_c < 1280$ MHz)

0.4 Hz ($f_c \geq 1280$ MHz)

Accuracy, stability, and internal reference oscillator: identical to HP 8662A.

¹In the remote mode it is possible to have microprocessor clock related spurious signals spaced 3 MHz apart at an absolute level of typically less than -145 dBm.
²Spurious signals can be up to 3 dB higher in the dc FM mode.
³Not specified for carrier frequencies above 640 MHz.
⁴At a 60 Hz line frequency, power line or microphonically related spurious signals may be up to 3 dB higher and appear at offsets as high as 1 kHz from the carrier.
⁵Due to automatic leveling loop bandwidth changes, brief (30 msec) level inaccuracies may occur when switching through 160 kHz and 1 MHz HP output frequencies.

APPENDIX C

PROGRAM LISTING FOR FREQUENCY HOPPING

A

10
20
30
40
50
60
70
80
90
100
110
120
130
140
150
160
170
180
190
200
210
220
230
240
250
260
270
280
290
300
310
320
330
340
350
360
370
380
390
400
410
420
430
440
450
460
470
480
490
500
510
520
530
540
550
560
570
580
590

FREQUENCY HOPPING USING HP 8672A

WRITTEN BY ANDRE VARIN

USING THE HP 8672A FREQUENCY SYNTHESIZER
THIS PROGRAM ENABLES TO HOP FREQUENCIES
IN PREDETERMINED STEPS ANYWHERE FROM
2 GHZ TO 18 GHZ & GENERATE A TIME PULSE
AT EACH HOP TO BE USED AS AN EXTERNAL
TRIGGER TO A COMPRESSIVE RECEIVER

MAIN PROGRAM

DECLARATION OF VARIABLES

REAL F1,F2,F3,A,Z,X,Y

ON TIMEOUT 7,3 CALL Check

CALL Frog

PRINTER IS 1

ICRT IS THE PRINTER

INPUT "ENTER START FREQ. IN MHZ",F1

IREJECT FREQ. < 2 GHZ

IF (F1 < 2000) OR (F1 > 18600) THEN 290

PRINT "START FREQUENCY":F1;"MHZ"

PRINT "

INPUT "ENTER STOP FREQUENCY IN MHZ",F2

IREJECT F1 GHZ > FREQ. > 18 GHZ

IF (F2 < F1) OR (F2 > 18600) THEN 330

PRINT "STOP FREQUENCY":F2;"MHZ"

PRINT "

INPUT "ENTER STEP SIZE IN MHZ",F3

PRINT "STEP SIZE":F3;"MHZ"

PRINT "

INPUT "ENTER SIGNAL OUTPUT LEVEL",A

IF (A < -120) OR (A > 3) THEN 400

PRINT "SIGNAL LEVEL":A;"dBm"

PRINT "

PRINT "PRESS CONT. KEY TO CONTINUE PROGRAM "

PAUSE

IWAITS FOR CONT. KEY

OUTPUT 2;"K";

ICLR SCREEN

Range=INT(ABS(MIN(A/10,11)))

IAMPLITUDE SETTING

Vernier=-10+Range-A

IVERNIER SETTING

IMAGE "K",B,B,"0",D

IFORMATING

OUTPUT 719 USING 490;48+Range,51+Vernier,1

IOUTPUT AMPLITUDE SETTING

PI*1.E+53

IVALUES TO GEN. 245us WAIT

X=1.

FOR F=F1 TO F2 STEP F3

ILOOP TO HOP FREQ.

OUTPUT 719 USING "A,BZ,6A";"P",1000*F,"J0"

WAIT .015

I15 ms DELAY FOR SETTLING

TRIGGER 8

IOUTPUT A PULSE ON DAV

Z=Y-X

IEND OF HP18

2=Y-X

IWAIT APPROX. 245 us

NEXT F

```

600 LOCAL 719
610 BEEP 2000,.5
620 PRINT TABXY(30,15),"END OF ROUTINE"
630 TOP
640 END*
650
660 ..... SUB NO. 1 .....
670
680 SUB Check
690 BEEP 1000,.5
700 BEEP 500,.5
710 OUTPUT 2,"F";
720 PRINTER JS T
730 PRINT TABXY(4,10),"INSTRUMENT MALFUNCTION--CHECK SET UP"
740 PRINT TABXY(5,13),"GPIB CABLE CONNECTED ?"
750 PRINT TABXY(6,14),"CHECK IF PROPER ADDRESS?"
760 PRINT TABXY(7,15),"IS POWER SWITCH ON?"
770 PRINT TABXY(8,18),"PRESS RST/RUN KEY & TRY AGAIN"
780 PAUSE
790 OUTPUT 2,"F";
800 UREND
810
820 ..... SUB NO. 2 .....
830
840 SUB Prog
850 PRINT TABXY(28,1),"FREQUENCY HOPPING PROGRAM"
860 PRINT TABXY(14,4),"DEVICE USED          MODEL          BUS ADDR "
870 PRINT TABXY(14,6),"FREQ. SYNTH          HP 8672A          19 "
880 PRINT TABXY(17,10),"THIS PROGRAM ENABLES THE FREQ. SYNTH TO HOP"
890 PRINT TABXY(17,12),"PREDETERMINED STEPS ANYWHERE FROM 1 GHZ TO "
900 PRINT TABXY(17,14),"18 GHZ & GENERATE A TIME PULSE AT EACH HOP"
910 PRINT TABXY(17,16),"TO BE USED AS AN EXTERNAL TRIGGER TO A RX"
920 PRINT USING "?";
930 SUBEND
940
950 .....

```

END

22.06.88

FIN